Université de Lille 1 SCIENCES ET TECHNOLOGIES

THESE

Délivrée par

L'Université Lille 1 Sciences et Technologies

Ecole Doctorale Sciences pour l'Ingénieur

Discipline : Micro-Nanosystèmes et capteurs

Laboratoire : Institut d'électronique, de microélectronique et de nanotechnologie

DIPLOME DE DOCTORAT

(Arrêté du 7 août 2006)

Soutenue publiquement le 06 octobre 2017

Par

M. Mathieu DANOY

Development of a physiologically-relevant in-vitro microfluidic model for monitoring of pancreatic cancer cells interactions with the liver

Jury :

Vincent SENEZ, directeur de thèse

Dominique COLLARD, codirecteur de thèse

Yasuyuki SAKAI, invité

Atsushi MIYAJIMA, rapporteur

Cécile LEGALLAIS, rapporteur

Fabrice SONCIN, examinateur

Teru OKITSU, examinateur

“センスは時代を先駆ける。

技術はその後について来るんだ”

ジョヴァンニ・バッチスタ・カプロニ、「風立ちぬ」

“Inspiration unlocks the future. Technology will catch up”

Giovanni Battista Caproni, The Wind Rises

Table of Contents

List of Figures

Abstract

English

The cancer metastatic process and its understanding have been a major topic of interest for researchers in the past. Using *in-vitro* models in both standard culture conditions and in microfluidic devices, we investigated the feasibility of such models in the representation of the physiological *in-vivo* situation.

We developed a hierarchical coculture model in PDMS plates, composed of hepatocytes, pericytes and endothelial cells. In different culture conditions, the influence of the different cells composing the model on the adhesion of cancer cells and promyeloblastic cells was investigated. Cross-talk between the different types of cells in the model was highlighted as a change in the cells' secretion and phenotypes was observed. The coculture of the three types of cells also exhibited to a certain extent a regulation of an inflammation voluntarily provoked by stimulation with an inflammatory cytokine. This yet to be reported mechanism was observed on both the endothelial cells' phenotype and on the adhesion of cancer cells and promyeloblastic cells.

To reproduce the in-vivo blood flow and shear stress to which the endothelial cells and the adhering cells are subjected, the model was then transferred into a microfluidic biochip. The device was composed of three channels, separated by micropillars and which could be filled independently one from another. Pericytes embedded in a hydrogel, hepatocytes, endothelial cells and finally pancreatic cancer cells could be inserted successively to reproduce the in-vivo hierarchical situation. Cells in the three channels were found to be viable and the hepatocytes to produce albumin though the culture. Stabilin-1, a common liver endothelial

marker, as well as ICAM-1, a marker related to cellular adhesion and to inflammation were found to be expressed. By performing a control experiment with only endothelial cells, gel and pancreatic cancer cells, the influence of the presence of hepatocytes and pericytes was investigated. It was found that pancreatic cancer cells were attracted by the cells in other channels while they migrated to low flow and high shear stress areas when hepatocytes and endothelial cells were not present.

The established models lay the bases for more complex and relevant systems that could complement their in-vivo counterparts in the drug discovery process.

Résumé

Français

Titre en français : Développement de modèles in-vitro microfluidique d'intérêt physiologique pour le suivi des interactions entre les cellules cancéreuses pancréatiques et le foie.

Le développement d'un cancer dans un tissu se caractérise par la croissance incontrôlée de cellules mutées. La mutation de ces cellules peut quelques fois s'expliquer par l'hérédité ou par une exposition à un environnement spécifique ou peut quelques fois ne pas s'expliquer du tout. Une fois le cancer développé dans son organe d'origine, son site primaire, il peut avoir accès à la circulation sanguine par le procédé communément appelé angiogenèse. Dans la circulation sanguine, les cellules cancéreuses vont ainsi être disséminée dans le reste du corps en suivant le principe de « la graine et du sol ». En effet, des profils de dissémination des cellules cancéreuses peuvent être observés. Ainsi, le cancer du sein a tendance à métastaser dans le cerveau ou aux os alors que le cancer du poumon aura aussi tendance à métastaser dans le foie. Il est cependant intéressant de remarquer que nombre de cancers ont tendance à métastaser dans le foie et que le traitement devient très difficile une fois le foie atteint.

Afin de trouver et tester de nouveaux traitements, un procédé, passant par des tests pré-cliniques sur animaux, puis des tests cliniques sur humains a été défini. Cependant, le problème éthique posé par l'usage intensif d'animaux ainsi que le manque d'efficacité du procédé ont motivé le développement de nouveaux modèles *in-vitro* d'étude pour la migration des cellules cancéreuses. Ces modèles posent cependant toujours un certain nombre de problème qui doivent être résolus avant leur utilisation systématique par l'industrie. Ils sont en effet incomplets et ne représentent qu'une situation donnée où beaucoup de variables sont ignorées.

De plus, ils restent souvent assez difficile d'accès étant donné que l'opérateur doit être formé à son utilisation.

Néanmoins, depuis plusieurs dizaines d'années, de nombreux efforts ont été fait dans la mise en œuvre de ces modèles et dans leur perfectionnement. Les premiers modèles d'étude 2D ont simplement cherchés à comprendre le mécanisme d'adhésion des cellules cancéreuses sur d'autres couches de cellules ou la façon dont les cellules cancéreuses migrent après qu'une partie d'entre elles aient été grattées du substrat de culture. Des systèmes plus complexes, dont font parties les chambres dites de Boyden, étudient la migration de cellules à travers une membrane, qui peut elle aussi être couverte d'un autre type cellulaire, d'une chambre de culture à une autre. Le mécanisme étudie lors de ce phénomène est plus communément appelé la chimiotaxie. Cependant, le corps humain et les tissus sont des environnements en trois dimensions, souvent riches en matrices extracellulaires et où les cellules possèdent des voisins dans chaque direction. Dans l'optique de la reproduction de cet environnement, des modèles de migration de cellules dans des gels ou des études dans des sphéroïdes ont été menées. La complexité croissante de ces modèles a fourni des résultats très encourageants dans le domaine des modèles *in-vitro* mais, manque toujours d'une caractéristique fondamentale du corps humain, la circulation sanguine.

Le désir de reproduire l'effet de la circulation sanguine sur les cellules ainsi que le développement des nanotechnologies a poussé le développement des dispositifs micro fluidiques en tant que réponse. Ces nouveaux outils permettent en effet de reproduire au mieux les tailles présentes dans le corps humain ainsi que les flux et les contraintes de cisaillement auxquels sont soumises les cellules. Les effets de ceux-ci sur les cellules endothéliales ont par exemple ainsi pu être facilement observes notamment en termes d'orientation, de morphologie et solidité des jonctions intercellulaires. La migration de cellules provoquée par des gradients de facteurs de croissance précisément contrôlés a aussi pu être observée et des modèles

complexes de réseaux vasculaires dans des gels ont pu être formes. Cependant, l'environnement cellulaire et physique de la migration des cellules cancéreuses reste toujours assez mal représenté. Dans le premier cas, il est possible d'inclure de plus en plus de types cellulaires dans les cultures et d'augmenter étape par étape la complexité du modèle. Dans le second, l'environnement riche en matrice extracellulaire peut être reproduit de manière de plus en plus précise et la reproduction de conditions de culture dynamiques peut être faite de par l'utilisation de système microfluidiques. Dans cette thèse, nous avons choisi de combiner les deux approches qui ne l'ont été pour l'instant que dans de rares cas.

Dans un premier temps, nous avons réalisé un modèle de coculture hiérarchique en puits visant à reproduire la microvasculature du foie. Ce modèle, inspiré de la structure *in-vivo* du foie, est composé d'hépatocytes, de péricytes et de cellules endothéliales. Les hépatocytes sont les cellules qui composent la majorité du foie. Leur rôle est divers mais peuvent être notés la synthèse de nombreuses protéines ou la détoxification comme fonctions majeures. Les péricytes sont des cellules que l'on trouve le long de la microvasculature du foie. Ces cellules prennent souvent la forme d'étoiles dans le foie d'où le nom de cellules stellaires qui leur est parfois attribué. Elles sont impliquées de façon notable dans le stockage de la vitamine A quand elles sont dans leur état normal. Cependant, une fois activées suite à un dommage au foie ou à un état inflammatoire, elles produisent en quantité de la matrice extracellulaire et mènent à la cirrhose. Enfin, les cellules endothéliales sont celles qui composent les parois des vaisseaux sanguins et notamment de la microvasculature du foie. Dans celle-ci, ces cellules présentent un phénomène appelle la fenestration, des petites ouvertures permettant les échanges entre le sang circulant et les cellules du foie. L'état de ces cellules est primordial dans tout modèle d'interaction entre cellules cancéreuses et le foie car ce sont celles qui sont directement en contact avec les cellules cancéreuses lors de leur adhésion et leur migration.

Notre modèle est donc composé de trois différentes couches de cellules. Tout d'abord, les hépatocytes sont ensemencés de façon à former une unique couche dense. Ensuite, les péricytes sont incorporés en fine couche dans du collagène afin de reproduire l'espace de Disse présent *in-vivo*. Afin de ne pas être confronté au ménisque de gel formé par la tension de surface dans les puits de petite taille, une plaque spécifique avec une structure en forme de marche a été utilisée. De plus, ces plaques de culture produites spécialement pour ce projet possèdent un fond en PDMS (polydiméthylsiloxane) afin de faciliter l'oxygénation dans la culture et notamment afin de préserver la fonction des hépatocytes comme les recherches de notre groupe l'ont précédemment démontré. Enfin, les cellules endothéliales sont ensemencées en unique couche dense afin de ne laisser aucun trou. Après quelques jours de culture, les cellules cancéreuses du pancréas sont ajoutées et leur adhésion sur une durée limitée est évaluée. Afin d'évaluer l'influence de chaque type cellulaire composant le modèle, différentes conditions de culture, variant la présence ou l'absence de chaque type cellulaire ont été mises en œuvre. De plus, afin de juger de la nécessité de l'utilisation de plaques de culture avec un fond en PDMS, des contrôles dans des plaques de culture standards en polystyrène ont été fait.

Le test d'adhésion des cellules cancéreuses se faisant au jour 6 à compter du début de la culture des hépatocytes, il est important de vérifier de la bonne viabilité et fonction des cellules du modèle. Dans toutes les conditions de culture, les cellules endothéliales ont formé une couche complète ne laissant apparaitre aucun trou. Les péricytes ont quant à eux proliféré et ont adopté leur morphologie typique de cellules stellaires. Afin de vérifier la bonne fonction des hépatocytes, la mesure de l'albumine produite par ceux-ci est un très bon premier indicateur. Dans notre modèle, la concentration d'albumine détectée dans le milieu de culture s'est trouvée être plus importante après l'ajout des cellules endothéliales et accentuée par l'ajout de pericytes. Cela peut être interprété comme un effet positif de la présence des autres types cellulaires sur le maintien de la fonction hépatique. De plus, il est connu que les hépatocytes produisent en

quantité des facteurs de croissance pour cellules endothéliales vasculaires. Ces facteurs, détectés en culture d'hépatocytes seuls, ne l'ont plus été lors de la coculture avec les cellules endothéliales, indiquant une consommation probable des facteurs par ces dernières. Ces résultats illustrent bien que les différents types cellulaires inclus dans le modèle sont capables d'interagir entre eux et prouve la nécessité de modèle de culture plus complets.

Etant donné que l'objectif du modèle est d'étudier les interactions entre les cellules cancéreuses du pancréas et le foie, les cellules endothéliales, qui sont en contact direct avec les premières ont été en partie caractérisées. Diffèrent marqueurs endothéliaux relatifs à l'adhésion des cellules, à l'inflammation ou des marqueurs spécifiques à différentes cellules du foie ont été observés par immunomarquage. Les marqueurs relatifs à l'inflammation ont été trouvé moins exprimés dans le modèle de coculture complet que dans les autres conditions alors que la tendance inverse a été observée par un marqueur relatif aux cellules vasculaires du foie. Au niveau de l'adhésion des cellules cancéreuses, cela s'est traduit par une diminution de celle-ci en fonction de l'augmentation de la complexité du modèle. Globalement, cela peut être interprété par le fait que la coculture amène les cellules endothéliales à un état plus mature et moins inflammé et que, étant donné que l'adhésion des cellules cancéreuses est connue pour être très liée à l'inflammation des tissus, cela s'est traduit par une diminution de l'adhésion en coculture.

Afin de tester la robustesse du modèle à l'inflammation, différentes conditions de culture ont été soumises à une stimulation par une cytokine. Dans le cas de la culture de cellules endothéliales seules, la réponse inflammatoire s'est trouvée être importante. Dans le cas du système de coculture complet, la réponse du système s'est trouvée être plus faible en termes de marqueurs relatifs à l'inflammation. Cela s'est traduit en termes d'adhésion de cellules cancéreuses par une forte augmentation de celle-ci après stimulation en culture de cellules endothéliales seules mais par aucun changement après stimulation dans le modèle de coculture

complet. L'hypothèse principale pour expliquer ce phénomène est qu'en coculture d'hépatocytes et de péricytes, il est connu que la production de facteurs de croissance hépatocytaires est stimulée et que ces facteurs, ayant un effet anti-inflammatoire notable, ont affectés les cellules endothéliales pour autoréguler leur état inflammatoire. Les résultats de cette première partie de la thèse montrent l'importance de modèle de culture complets au niveau cellulaire et physique afin de reproduire le mieux possible des phénomènes observes *in-vivo*.

Dans la seconde partie de la thèse, le modèle précédemment établi a été transféré dans un système microfluidique pour la culture. Ce transfert a pour but de reproduire au mieux la situation physiologique de l'*in-vivo* en réduisant notamment la tailles de espaces de matrice extracellulaires et en incluant un flux reproduisant des valeurs de forces de cisaillements semblables à celles observées *in-vivo*. Le dispositif microfluidique, conçu en PDMS, se compose de trois canaux parallèles séparés par des micro-piliers. En utilisant la tension de surface, il est possible de remplir un des canaux indépendamment des autres. Ainsi, le canal du milieu a tout d'abord été rempli d'un hydrogel résistant, composé de collagène, d'acide hyaluronique et dans lequel des péricytes ont été ensemencé. Après durcissement de cet hydrogel, chacun des canaux du haut ou du bas peuvent être perfusés de manière indépendante et diffèrent types cellulaires peuvent y être ajoutés. Les hépatocytes ont ainsi ensuite été ajoutés dans le canal du bas et les cellules endothéliales dans le canal du haut. Une fois la coculture établie, le dispositif microfluidique a été perfusé à l'aide d'une pompe péristaltique connectée par des tubulures limitant l'adhésion de facteur de croissance et incluant un réservoir empêchant la formation de bulles dans le circuit.

Après six jours de culture, les cellules cancéreuses ont été insérées avec minutie dans le canal du haut, en contact avec les cellules endothéliales et leurs mouvements ont été monitorés sur quatre jours. Après dix jours de culture au total, la viabilité dans tous les canaux

a été évaluée par un marquage avec de la calcéine. Malgré la difficulté posée par les nombreux lavages nécessaires lors des marquages, les cellules dans chacun des canaux ont été marquées en tant que cellules viables. Afin d'évaluer le maintien de la fonction hépatique, la concentration d'albumine dans le système perfusé a été mesurée tout le long de l'expérience. Une concentration d'albumine a été détectée tout au long de la culture. Avant l'ajout des cellules cancéreuses, une diminution progressive de la production d'albumine dans le système a été détectée. Cependant, l'ajout de ces cellules a entrainé une forte augmentation de la production avant une nouvelle baisse progressive. Cela peut s'expliquer par les nombreuses interactions entre cellules du pancréas et du foie qui ont été reportées dans la littérature. Ces résultats n'ont cependant pas être reportés ou étudiés jusque lors avec des cellules cancéreuses pancréatiques.

L'influence de la présence des hépatocytes et des péricytes a été étudiée en variant les conditions de culture et en préparant des dispositifs de contrôle ne contenant que des cellules endothéliales, du gel et des cellules cancéreuses pancréatiques. Dans les dispositifs comportant le modèle de coculture complet, il a été observé que les cellules cancéreuses avaient tendance à migrer dans le canal du haut, vers l'interface avec le gel et donc vers les autres types cellulaires. Donc les dispositifs de contrôle, l'effet inverse a été observé alors que les cellules cancéreuses migraient vers le mur opposé où le flux est plus faible mais les forces de cisaillement plus fortes. Cela peut être explique par des effets de chimiotaxie connus pour les cellules cancéreuses et tout à fait en accord avec la théorie de Paget. En termes de marqueurs, les cellules endothéliales ont exprimé dans les deux conditions des marqueurs inflammatoires relatifs à l'adhésion autour des cellules cancéreuses en contact direct. Un marqueur spécifique du foie a aussi été détecté dans le modèle de coculture en accord avec les résultats de la partie un.

Les modèles établis lors de ces travaux de thèse posent les bases pour de nouveaux modèles d'études des interactions entre le foie et les cellules cancéreuses encore plus complexes. Une fois ces modèles assez complets et satisfaisants des critères de l'industrie, ils pourront être utilises en complément de l'*in-vivo* lors des procèdes de test de nouvelles drogues et permettront d'obtenir des résultats moins couteux, plus rapides et plus efficaces.

Chapter 1

General Introduction

1.1 The Origins of Cancer Metastasis

1.1.1 Development of the Cancer in the Primary Site.

Cancer is a disease which can be characterized by the fast proliferation rate of mutated cells in healthy tissues [1]. Foulds *et al.* described the tumor (i.e. abnormal growth of tissues) progression as the irreversible change of one or more of the characteristics of a group of cells which leads to the development of a tumor in a primary site. They described this change as a phenomenon which can be triggered by chemical exposure, infectious agents, hormonal stimulation or even spontaneously. The phenomenon is also known to be subjected to a certain age dependency, following tendencies which vary in the different organs in which the tumor develops [2].

Types of cancer in the body vary widely but can be defined by six alterations in the cell physiology [3,4]. Hanahan *et al.* described the set of abilities that the cancer cells acquire during their development (Fig. 1-1). In details, cancer cells should be able to produce their own growth signaling to become independent from the surrounding environment. The cells will also need to evade the antigrowth signals which are usually produced in healthy tissues, to free themselves from the programmed cell apoptosis and to be able to reproduce themselves indefinitely. Finally, the cells, or aggregates of cancer cells will be required to develop their own vasculature to be alimented in oxygen and nutrients by the process that is called angiogenesis. This last phenomenon is also the trigger to cancer cells invasion and to metastasis which will allow the colonization of close and distant tissues.

1.1.2 Implications of the Development of Cancer

Cancer has been a major subject of interest for many years because of the high number of death related to it and as it remains the second cause of death in the United States [5]. Especially, the probability to develop an invasive cancer has been established to 1 in 2 for males and 1 in 3 for females (Fig. 1-2) enforcing the global interest in the disease.

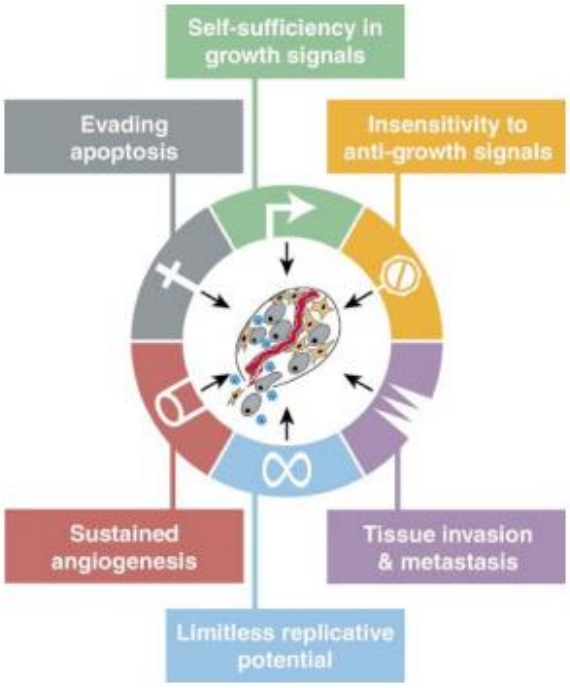

Fig. 1-1: The Hallmarks of Cancer [3].

While the occurrence of cancer did, in certain cases remain stable and in other cases, progress, the survival rate did, in general, raise drastically due to the evolution of the different treatments and surgical possibilities for patients. However, some cancers remain extremely deadly, especially for the ones, such as pancreatic cancer, which have tendencies to develop in distant sites in a process called metastasis.

1.1.3 Migration of Cancer Cells through the Metastasis Process

The metastatic process can be detailed in different steps that will lead to the growth of a secondary tumor in close or distant tissues [6-8]. Briefly, due the development of the vascularization network of the primary tumor during angiogenesis, the cancer cells have access to the bloodstream (In the process is called "Intravasation") and can reach distant sites in a very inefficient manner [9] as most of the cell are destroyed in circulation. Once a secondary site is reached, the cancer cell will be able, under certain circumstances, to migrate into the tissues (In the process called "Extravasation") and to form a secondary tumor which, in turn, will develop its own vascular network (Fig. 1-3).

		BIRTH TO 49	50 TO 59	60 TO 69	≥70	BIRTH TO DEATH
All sites†	Male	3.4 (1 in 29)	6.7 (1 in 15)	15.1 (1 in 7)	36.0 (1 in 3)	43.3 (1 in 2)
	Female	5.4 (1 in 19)	6.0 (1 in 17)	10.0 (1 in 10)	26.4 (1 in 4)	37.8 (1 in 3)
Breast	Female	1.9 (1 in 53)	2.3 (1 in 44)	3.5 (1 in 29)	6.7 (1 in 15)	12.3 (1 in 8)
Colorectum	Male	0.3 (1 in 300)	0.7 (1 in 148)	1.3 (1 in 80)	3.9 (1 in 26)	4.8 (1 in 21)
	Female	0.3 (1 in 326)	0.5 (1 in 193)	0.9 (1 in 112)	3.5 (1 in 28)	4.5 (1 in 22)
Kidney & renal pelvis	Male	0.2 (1 in 468)	0.3 (1 in 292)	0.6 (1 in 157)	1.3 (1 in 76)	2.0 (1 in 49)
	Female	0.1 (1 in 752)	0.2 (1 in 586)	0.3 (1 in 321)	0.7 (1 in 134)	1.2 (1 in 84)
Leukemia	Male	0.2 (1 in 419)	0.2 (1 in 598)	0.4 (1 in 271)	1.3 (1 in 75)	1.7 (1 in 59)
	Female	0.2 (1 in 516)	0.1 (1 in 968)	0.2 (1 in 464)	0.9 (1 in 117)	1.2 (1 in 84)
Lung & bronchus	Male	0.2 (1 in 578)	0.7 (1 in 140)	2.0 (1 in 49)	6.6 (1 in 15)	7.4 (1 in 13)
	Female	0.2 (1 in 541)	0.6 (1 in 173)	1.6 (1 in 64)	4.9 (1 in 20)	6.2 (1 in 16)
Melanoma of the skin‡	Male	0.3 (1 in 294)	0.4 (1 in 240)	0.8 (1 in 129)	2.1 (1 in 47)	3.0 (1 in 34)
	Female	0.5 (1 in 207)	0.3 (1 in 323)	0.4 (1 in 246)	0.9 (1 in 112)	1.9 (1 in 53)
Non-Hodgkin lymphoma	Male	0.3 (1 in 366)	0.3 (1 in 347)	0.6 (1 in 173)	1.8 (1 in 55)	2.4 (1 in 42)
	Female	0.2 (1 in 543)	0.2 (1 in 483)	0.4 (1 in 233)	1.4 (1 in 72)	1.9 (1 in 52)
Prostate	Male	0.3 (1 in 304)	2.3 (1 in 44)	6.3 (1 in 16)	10.9 (1 in 9)	15.0 (1 in 7)
Thyroid	Male	0.2 (1 in 585)	0.1 (1 in 827)	0.2 (1 in 653)	0.2 (1 in 464)	0.6 (1 in 174)
	Female	0.7 (1 in 135)	0.3 (1 in 288)	0.3 (1 in 306)	0.4 (1 in 263)	1.7 (1 in 60)
Uterine cervix	Female	0.3 (1 in 358)	0.1 (1 in 840)	0.1 (1 in 842)	0.2 (1 in 565)	0.6 (1 in 154)
Uterine corpus	Female	0.3 (1 in 367)	0.6 (1 in 170)	0.9 (1 in 109)	1.3 (1 in 76)	2.7 (1 in 37)

*For people free of cancer at beginning of age interval.

†All sites excludes basal cell and squamous cell skin cancers and in situ cancers except urinary bladder.

‡Probabilities are for whites.

Fig. 1-2: Probability (%) of development of an invasive cancer in the United States between 2009 and 2011 sorted by age and sex [5].

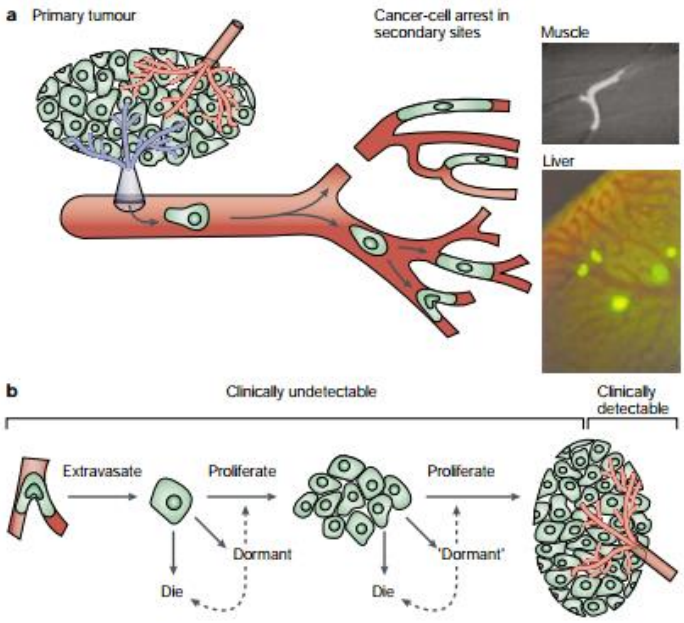

Fig. 1-3: The metastatic process from the primary site to the secondary site [8].

1.1.4 Metastatic Distribution Patterns

Several theories have been elaborated regarding the repartition of cancer metastasis in the different secondary sites observed in-vivo [10]. The first theory is effective in most cases for metastasis which could be found close to the primary tumor site. It is supposed that the cancer cells, after exiting the primary site, will, due to their size and mechanical properties, stop in the first capillary bed which is encountered. In such cases, the cell would be blocked in vessels of small size and cause an embolus.

However, some metastasis in distant sites cannot be explained with the latter theory. Stephen Paget hypothesized, after *in-vivo* observations, the theory of the "Soil and Seed" [11] which details that the properties and characteristics of the primary tumor and the microenvironment of the secondary site are determinant in the distribution of the metastasis in the body. Indeed, while it was hypothesized that the cancer cells would migrate after causing an embolus in the first capillary bed encountered, *in-vivo* experiments on animals showed that,

in some cases, there was no trace of embolus close to secondary sites of metastasis [12]. Moreover, some tissues such as the heart, the kidneys, the intestine and the muscles which account for a great part of the blood output in the body, are not found to be common sites of metastasis and are rarely colonized [10].

The site specific and non-blood flow dependent colonization of metastasis in the body has been explained since Paget's hypothesis [13]. The interactions between the endothelial cells of the secondary site and the cancer cells have been defined by the fact that the cell-surface receptors of the endothelial cells in each organ are different and that the cancer cells respond to local growth factors which are able to stimulate their migration into the tissues.

This hypothesis, made from *in-vivo* observations, could be verified, in some cases, in *in-vitro* models [14]. Auerbach *et al.* have shown that the adhesion of several types of cancer cells on endothelial cells extracted from different sites exhibited in most cases, the same patterns observed previously. This proves that without even taking in account the different growth factors produced by the cells in the vicinity of the endothelial cells, the cell specific cell-surface markers expressed would explain, in most cases, the distribution of the metastasis in non-random sites.

Since then, number of molecules have been analyzed and their correlation with organ-specific metastasis has been defined [15]. Metastasis specific to the liver, the brain, the bones, and other major sites have been partially eluded but the complexity of the phenomenon and the discrepancies of the data obtained by different groups have not lead to the identification of specific targets for therapy. However, as the liver is one of the most common distant site for metastasis which cannot be explained by the pattern of blood flow in the body (Fig. 1-4), it has been a therapeutic focus for many years and many trials have been performed.

Type of cancer	Common primary site	Common distant site(s) of metastases
Clear cell carcinoma	Kidney	Bone, liver, thyroid
Cutaneous malignant melanoma	Skin	Brain, liver, bowel
Ocular malignant melanoma	Eye	Liver
Small cell carcinoma	Lung	Brain, liver, bone
Prostatic adenocarcinoma	Prostate	Bone
Testicular carcinoma	Testis	Liver
Neuroblastoma	Mediastinum, abdomen	Liver, adrenal
Follicular adenocarcinoma	Thyroid	Bone
Breast adenocarcinoma	Breast	Bone, brain, adrenal
Kruckenberg adenocarcinoma	Gastrointestinal	Ovary, liver
Bladder carcinoma	Urinary bladder	Bone, liver, brain

Fig. 1-4: Examples of metastatic pattern which cannot be explained by the pattern of blood flow in the body [10].

Historically, therapies toward cancer metastasis includes resection (i.e. the surgical removal of an organ, in this case, host of the tumor), radiation therapy and chemotherapy. However, in the case of the liver, results from resection have been quite mixed and unsuccessful [16]. The survey performed by Foster indicated that, because there are much difficulties to perform the resection of parts of the liver, the mortality during the operation remained at 11%. Moreover, the survival rate after 5 years was found to be close to zero, strongly putting in perspective the usefulness of the operation. The lack of therapeutic success and the continuing high mortality rate of the primary cancers that metastases in the liver have led to the development of new strategies either acting directly on the adhesion of the cells in the vasculature or on their migration into the tissues.

1.2 Main Issues in Assays for Cancer Metastasis

The increase of regulations toward animal experiments has made the research for an alternative and by extension, the development of *in-vitro* assays, a hot topic for the past few years. Indeed, in addition to stricter guidelines in terms of protocol approval and of formation of the individuals performing the experiment, the rule of the "3R" has been set for example in Japan [17]. This rule compels the researchers to find alternative methods (Replacement) to their experiments on animals, to reduce the number of animals used (Reduction) and to reduce the pain inflicted to them (Refinement).

While the development of *in-vitro* models is strongly encouraged by this rule, both *in-vivo* and *in-vitro* methods have their advantages and inconvenient. The simplicity of *in-vitro* models allows to decrease the number of variables and the fluctuations in the results [7]. However, those models do, by definition, not represent the exact *in-vivo* situation and need to be compared in *in-vivo* situation while limiting the use of animals. The skills required to perform *in-vitro* assays are also different from those of their main targeted users, the clinicians and they are still laborious to completely characterize. *In-vivo* studies then appear as a "gold standard" for assays of cancer metastasis but they also have their limits. For example, assays for drug screening should be designed for a human patient. Many trials which have been led from the animal stage to the human trial stage have been seen to fail as the behavior of the species are generally different. Ethics concerns regarding animal experiments might also be raised regarding *in-vivo* assays. Moreover, and more importantly, *in-vivo* assays do give a general information on the final output of an assay. The metastasis might or might not have occurred but the specific reason remains unknown [7]. This is due to the lack of technic, allowing a direct real-time *in-vivo* observation of the phenomenon and which would permit to conclude on the specific mechanism involved in the assay.

1.3 Current Strategies in Cancer Metastasis

1.3.1 Previous research on *in-vivo* models

1.3.1.1 Choice of the animal model

Murine models have been extensively used for *in-vivo* metastasis assays and have been challenged in only a few cases by companion animal models [18,19]. The use of rat and mouse for *in-vivo* experiments is indeed favored by a relatively low cost, the high degree of development of the assays, the possibility to genetically engineer mice and the lower ethical concern of experimenting on those small animals [18]. However, while being a primary source of information regarding cancer metastasis, those models, often issued from inbred population and raised in environmentally-controlled laboratories, may not be the most representative models for cancer in the human which, unlike in murine species, appears spontaneously and is affected by the environmental exposure of the patient [19].

Companion animals (dogs and cats), may give an alternative to murine models and have already been used in preclinical trials [20]. The advantages of pets as a model are numerous. As companions, they are often exposed to the same environment, source of carcinogenesis, as their owner and, for example, the exposure of the later to asbestos has been related to the occurrence of cancer in their pet animals [21]. Those models are also obtained from natural outbreeds (in opposition with murine models), are subjected to spontaneous metastasis as it is the case in human, exhibit higher incidence rates of cancer than humans, allowing studies over large population and with a rate of progression higher than in humans [18]. Finally, in terms of size, they are more comparable to human and similarities in genes responsible for cancer have been found in canine models and humans [22]. However, the use of these models is often limited by the lack of reagents, such as antibodies available for analysis [19] and ethical concerns. While both murine and companion animal models provide different set of information regarding

cancer progression, it is important to note that one model is not to be taken as better than the other and that different models are able to answer different questions regarding the same phenomenon.

1.3.1.2 Syngeneic & Xenograft models

Murine models can be devised in two distinct categories, syngeneic or xenograft. Syngeneic models refer mostly to assays involving cancer cells of the same genetic background as the host [18]. Most of these models are designed by using murine models, with the disadvantages previously described. However, as both the cancer cells and the host are of the same origin, interactions between the cells and the tumor microenvironment can be studied in detail. Especially in those models, the influence of proteins added to the extracellular space [23] or of the modification of the tumor environment [24] have been studied and the possibility to stimulate metastasis shown. More interestingly, those models have also been used to test the effects of different tumor-inducing chemicals [25]. While the same oncogenes were found in the tumor, different mutations of the cells were noticed in each case. In this case, the model allowed to understand that in response to different exposures, different pathways of mutations were activated but tumors containing the same oncogenes could be finally formed, highlighting the diversity of initiating agents for the cancer cascade. The tumors formed by chemical exposure can, in most cases, be transplanted in other animals after extraction [26]. The character of the cells can be preserved up to several transplantations, allowing to perform several assays with cells of the same origin, behavior and genetic expression and reducing drastically the lack of reproducibility in *in-vivo* assays.

Xenograft models correspond to the transplantation of human tumor cells in immuno-deficient mice. The animal host must be immuno-depressed to prevent any rejection of the

transplanted tissue. This type of model is the most widely used nowadays by cancer researchers. Especially, the transplantation of human breast cell lines into different types of mice has been extensively characterized and the difference of progression in different mutations of mice allowed to understand more in details the immunobiology of breast cancer [27]. Those models allow to follow, for extended period, the progression of cancer in the host [28] and provide useful information on what might be the development of those cancers in human. As the mice used are immuno-deficient, the interactions between the immune system and the tumor cannot be studied. To solve this problem, models including both human immune cells and human tumor cells in an *in-vivo* model have been established [29]. However, those models using transplant of human cells still have limits. It has been suggested that in terms of angiogenesis and tumor growth, tumors that have been transplanted and tumor that developed spontaneously behave differently [30,31].

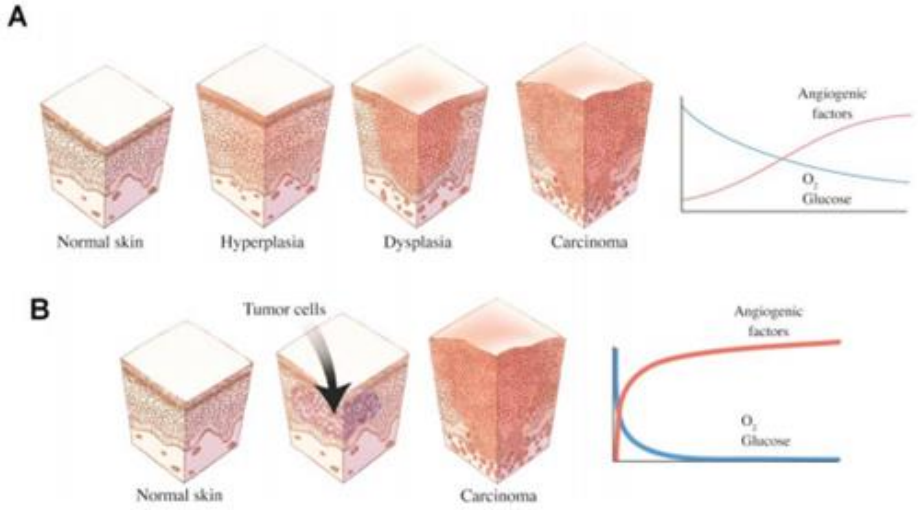

Fig. 1-5: Steps and effects in the development of (A) spontaneous cancer (B) transplanted cancer [30].

Xenograft are proposed to be less dependent on the regulation of angiogenesis in the host and their vascular network suggested to be rapidly developing independently of the host. In

opposition, tumors developed spontaneously are told to be following a long development over time and to extend their vascular network gradually during development, depending on the host tissue (Fig. 1-5).

1.3.1.3 Experimental & Spontaneous metastasis models

In addition, *in-vivo* metastatic models can be divided into two additional categories, experimental and spontaneous metastasis assays. Experimental metastasis models refer to assays in which the cancer cells are injected in the circulatory system of the animal model and let to metastasize following the soil and seed theory [18]. While the possibility to observe metastasis has been established with certain specific cell lines after intravenous injection, certain tumor cell lines that were supposed to be metastatic did not form any metastasis [32]. This method has also been shown to be dependent on the number of cells and by extension, lack of reproducibility [33]. Moreover, as the cells are directly injected into circulation, the first steps of metastasis, including intravasation are not modelized, making the models greatly differing for the actual situation. However, those models can still be used in drug screening with cell lines in which the metastatic potential has been already established [18].

Spontaneous metastasis is obtained from the transplantation of tumor cells in tissues. In the early stages of the metastatic research, the cells were often injected subcutaneously and the metastatic events were found to be rare. To reproduce the actual situation, the tumor cells were orthotopically transplanted (i.e. in the site corresponding to their origin) and more frequent metastatic events could be observed [18]. Especially, those models were shown to reflect clinical cancer very well and drug discovery could be made as a result of their use [34,35]. By performing an orthotropic transplantation, the influence of and interactions with the microenvironment can be reproduced and phenotypic changes in the transplanted cancer could

be observed. While the labor required for those models is relatively higher than for all the other models, they allow the obtention of quantifiable data with a higher reproducibility and relevancy [34]. Moreover, while models relying on injection often require a cell selection for the metastatic potential, the structure provided by the host organ in orthotropic transplantation allows the selection to be performed by the organ's microenvironment itself, as it is the case in the actual situation and only part of the transplanted cells, with a metastatic potential, will migrate [36]. Further proofs of the influence of the organ's microenvironment have been established as the same tumor cells were transplanted in different organs and as their characteristics were studied after recovery [37]. Finally, in orthotropic transplantation models, different agents have been shown to have an effect on the growth of the primary tumors, on the triggering of the metastatic events and on the global survival rate of the animal model [35].

1.3.1.4 *In-vivo* metastasis characterization & imaging

One of the important challenge of *in-vivo* assays is the possibility to quantify the metastatic potential of the tumor cells in different conditions. Usually, quantification and measurement of the size of the metastasis used to be performed after sacrifice of the animal host [38]. After retrieval, the tumor could also be analyzed in detail with different markers. For example, the influence of the presence of the transplanted tumor on the metastasis that resulted from it has been characterized [39]. After removal of the tumor, it was proved by staining that angiogenesis could occur in metastasis which was not the case when the original tumor was present (Fig 1-6).

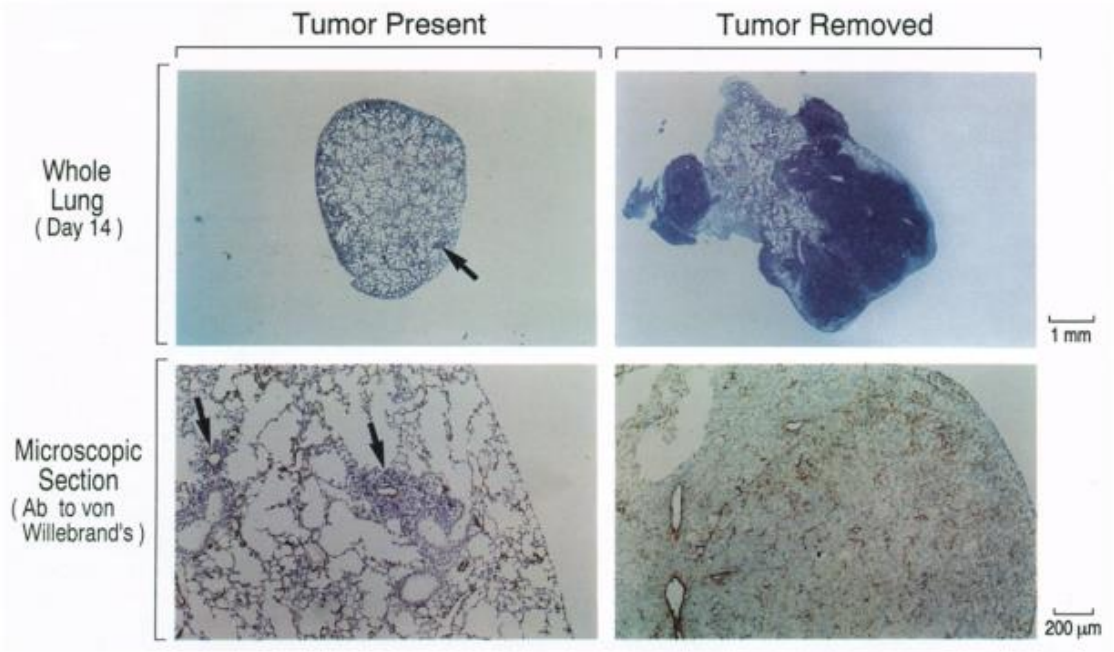

Fig. 1-6: Influence of the presence of the originally transplanted tumors on the growth of its metastasis and of the related angiogenesis (Blue staining: tumors, brown staining: new vessels) [39].

The necessity to monitor the metastatic progression in real-time has motivated the development of several imaging methods. A commonly used method for researchers that have access to the material usually available in hospital is the MRI (Magnetic Resonance Imaging). The method, performed in radiology uses magnetic fields and radio waves to perform an image of tissues, deep into the body and in cross-section. It has been possible to obtain images of tumors with a great level of details compared to post-retrieval analysis [40] but the single-cell level of detail is yet to be attained. In order to observe more in details the metastatic phenomenon, fluorescence technics have been developed in the past decades [41-43]. At first, fluorescent protein-expressing tumors were used to image the tumors in the whole body [42]. It was possible to observe metastasis to both organs and bones but levels of details were sufficient only in bones metastasis (Fig. 1-7).

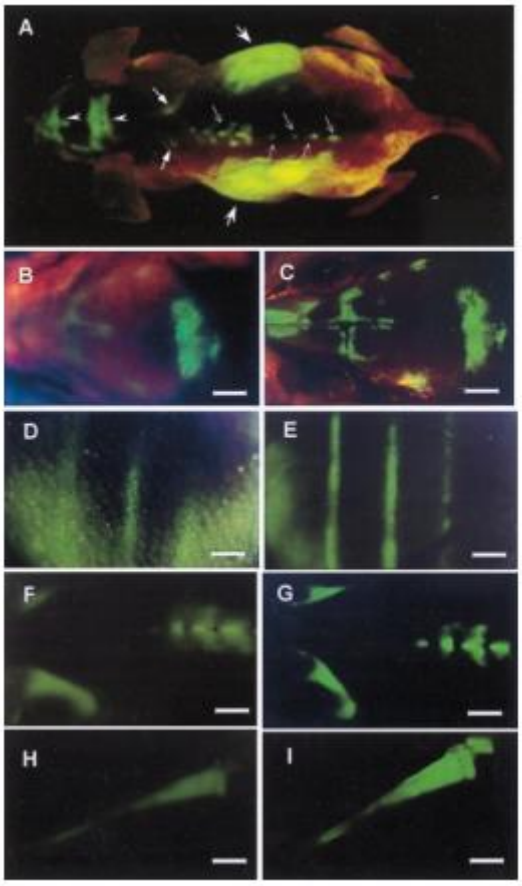

Fig. 1-7: Imaging of fluorescent protein-expressing cancer cells metastasis in mice. (A) Whole body image (B-I) Details of bones metastasis [42].

As each cell is modified with a fluorescent protein, it should be possible to observe each of them during imaging. While this is the case during the injection, after migration into tissues and a long period, the observation becomes more and more difficult (Fig. 1-8). A solution that has been developed in the recent years is to use quantum dots. They can be used for extended period and exhibit a very high stability [44]. However, a method to combine them with cancer cells without any interferences with the metastatic process has yet to be found and blocks the development of the method that could be the future of cancer metastasis real-time imaging.

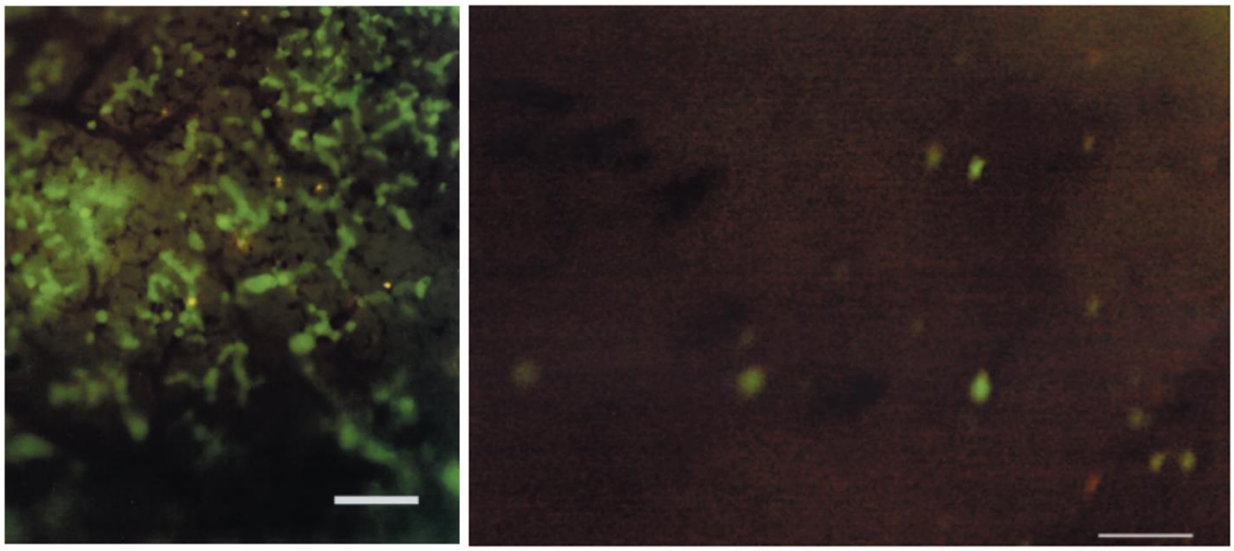

Fig. 1-8: (Left) Imaging of fluorescent protein-expressing cancer cells after injection in the adrenal gland, scale bar 100 μm. (Right) After colonization in the brain, scale bar 80 μm [43].

1.3.2 Previous research on *in-vitro* models

1.3.2.1 Generalities

As an alternative to *in-vivo* models, *in-vitro* models have been developed in the past decades for a various panel of applications. Because of their relative simplicity, *in-vitro* models do not provide all the information that are needed for a complete study of cancer adhesion and migration. However, because of their flexibility in many terms, they provide complementary information to their *in-vivo* counterpart. Especially, clinical observations that were made *in-vivo* by Paget [11], serving as a base for the "Soil and Seed" theory, could be mostly observed and confirmed in simple *in-vitro* models [45]. Indeed, cell surface antigens, specific to each endothelium, are hypothesized to play a strong part in the cancer cell adhesion. As long as the markers relative to cellular adhesion are still expressed in the *in-vitro* culture, specific interactions between cancer cells from a certain location and a specific endothelium can be simply studied and quantified, confirming *in-vivo* observations. Moreover, as *in-vitro* models

are often extremely simplified compared to their *in-vivo* counterparts, crosstalk between several specific types of cells can be studied and their influence on the microenvironment in which the cancer cells will grow, characterized. In such manner, the role of the crosstalk between hepatic stellate cells and hepatocytes in the progression of hepatocellular carcinoma could be studied [46]. Indeed, one of the strong point of *in-vitro* models is the possibility to study details. This can be done either by the simplification of the model compare to the *in-vivo* situation but also by enabling many microscopy options. In such manner, the effect of hypoxia in angiogenesis [47] or the transendothelial migration of tumors [48] could be clearly observed (Fig. 1-9). Those results, complementary to *in-vivo* observations, give valuable information on specific phenomenon which could never been observed *in-vivo*, but only hypothesized.

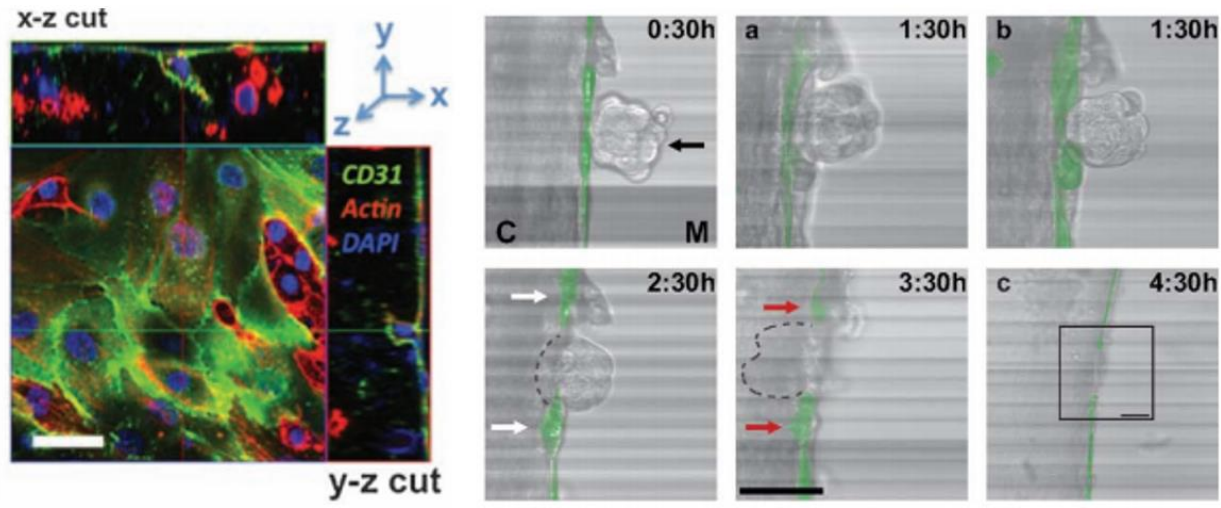

Fig. 1-9: (Left) Migration of endothelial cells (Green Staining) towards Tumors (Red staining) during angiogenesis and driven by hypoxia, scale bar 50 µm [47] (Right) Migration of bladder carcinoma (Arrow) through the endothelial barrier (Green staining), leaving the latter damaged, scale bar 50 µm [48].

The field of Bioengineering and *in-vitro* assays have been developing simultaneously in the past decades. By taking inspiration from the *in-vivo* situation, many solutions to observe and understand cancer cells migration have been designed over the past decades [49,50]. From basic 2D culture models, to 3D matrix experiments and microfluidic devices, those models are becoming more and more complex, and more than completing *in-vivo* experiments, aspire to replace them.

1.3.2.2 2D *in-vitro* assays

First trials regarding the interactions between cancer cells with endothelial layers have paved the way for a better understanding on how the cells adhere to and migrate through the endothelium. Indeed, at this point, the complete behavior of the cancer cells, when attaching to an endothelial monolayer was still unknown. Using microscopy, the complete physical mechanism of cancer cells adhesion and migration was elucidated, as illustrated in Fig. 1-10 [51]. Round cancer cells could be seen adhering, adopting a flat morphology and then migrating through the endothelial layer. Other methods such as radioactive labelling allowed to give the dynamic of attachment of the cancer cells to the monolayer [52] which is unknown in *in-vivo* conditions as the phenomenon cannot be easily quantified.

As adhesion is still a quite simple mechanism to understand, the interest of researchers rapidly shifted to the dynamic of migration of cancer cells. Many different models have been designed with specific aims and each of them give precious, defined information about the cancer cells and the reaction to its surrounding. The simplest migration assay is called the “Scratch assay” (Also called “Wound healing assay”) [53,54]. As its name indicates, this assay consists of scratching physically, part of a cell layer and, observing how the cells will migrate to cover the created hole (Fig. 1-11). While this assay is easy to perform, it gives basic information on the

cells, and has for example given evidences on the role integrins (Serie of receptors related to cell-cell interactions and cell-Extracellular matrix interactions) in their adhesion mechanism [53]. Moreover, this kind of assay is completely suitable for High Throughput Screening [54], one of the most important advantage of *in-vitro* models over *in-vivo* models.

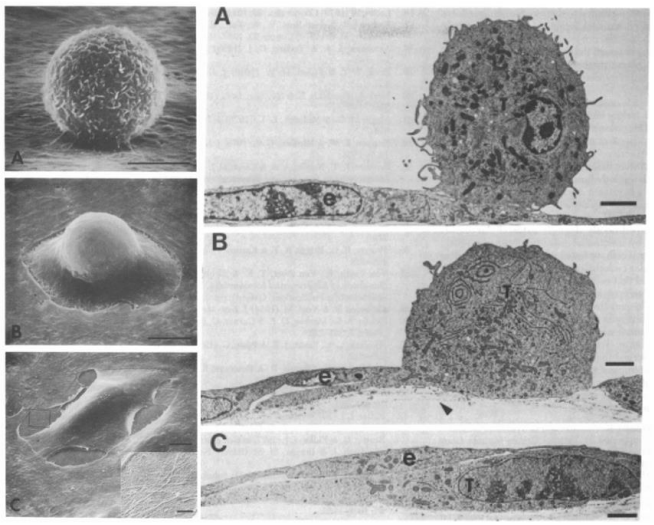

Fig. 1-10: (Left) Scanning Electron Microscopy images of the adhesion and migration of melanoma cells on endothelial cells, scale bar 5 μm (Right) Transmission Electron Microscopy images of the same phenomenon, scale bar 2 μm [51].

In an analog manner, the spreading of small circular monolayers of cells in response to cellular matrix with different treatments has been studied [55]. Indeed, cells react different in presence of growth factors or chemoattractants, they tend to migrate toward zone which are rich in them. This study, called chemotaxis, has for aim to understand why the cancer cells migrate from the blood vessels to an organ and the reasons of the cancer cells migration's specificity. The simplest model for this study is the chemotaxis chamber [56]. In these devices, the migration or the orientation of cells towards zone rich of chemoattractants, created by a

gradient, are observed. However, the previously described models are limited to the migration of cells on surfaces and do not, as it is the case *in-vivo*, represent the fact that the cells need to migrate through a layer during metastasis. This precise phenomenon has been widely studied by using filter-based assays also known as Boyden chamber assays.

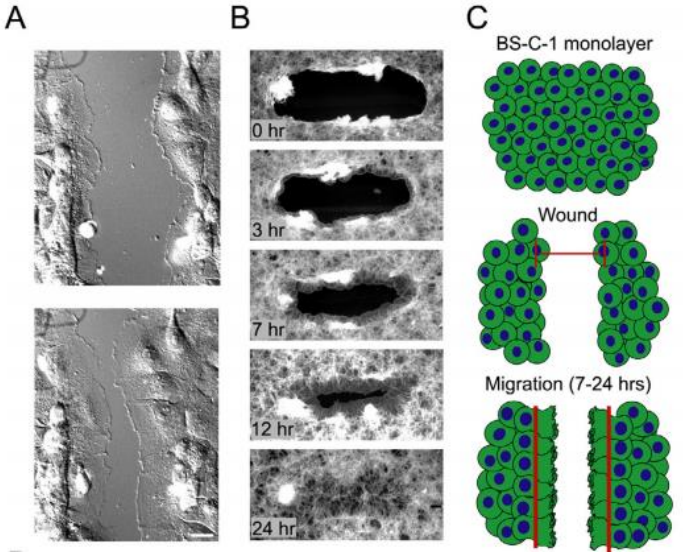

Fig. 1-11: (A) Time-lapse sequence of epithelial cells, covering the wound after the scratch assay was performed, scale bar 20 μm (B) Same phenomenon observe with actin staining, scale bar 100 μm (C) Process of a basic scratch assay [54].

Many variants of the Boyden chamber have been designed in the past decades. The simplest model consists of a filter/membrane bottom insert on top of a usual culture well. The migration of cells through the filter or membrane, often triggered by a chemoattractant is then quantified [57]. To model transendothelial migration of cells, variants of the chamber, where cells are seeded as a monolayer on the coated membrane were established (Fig.1-12) [58]. In these models, the different comportment of the migrating cells can be quantified, allowing to estimate its invasiveness in the studied conditions. In such manner, those models have been used to understand the reaction of the endothelial barrier to migrating tumor cells [59], to test

the effects of antibiotics [60] or to establish different migration stimulation protocols [61]. However, those models still suffer from a design weakness as they fail to represent the 3D microenvironment of the *in-vivo* microvasculature. Indeed, organs, such as the liver, are often rich in extracellular matrix and cells, migrating through the endothelium, also must cross this 3D matrix layer. The representation of this phenomenon has become a challenge in invasion assay and in the understanding of cellular migration.

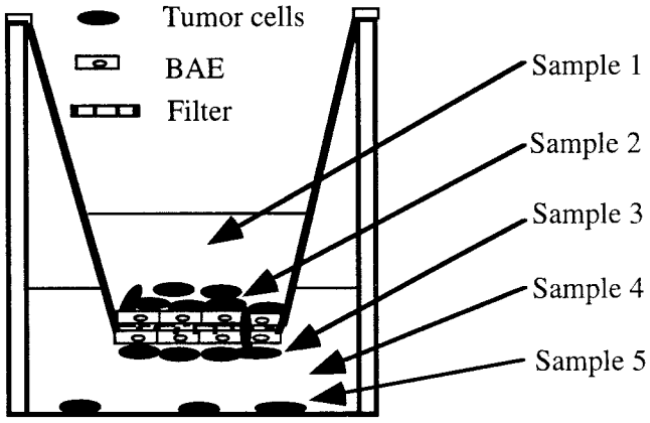

Fig. 1-12: In-vitro transendothelial migration assay in a Boyden chamber [58].

1.3.2.3 3D *in-vitro* assays

As a simple solution to this problem, layers of gel have been added to Boyden chamber assays to mimic the migration of cells through extracellular matrixes [62,63]. This modification of the Boyden chamber assay allowed to assess the metastatic potential of different type of cancer cells but more importantly to give their dynamic of migration in function of the matrix characteristics, highlighting the importance to mimic as close as possible the *in-vivo* situation. Indeed, while it could be expected, it is more difficult for cells to migration in highly concentrated matrixes. In order to reproduce the process that the cell has to go through during

intravasation or extravasation, the matrix need to have the same characteristics as the *in-vivo* one that it should represent.

More complex models have then been designed, modeling the migration of carcinoma cells [64]. The migration, normally triggered by the coculture with fibroblasts, could be there enhance or prevented chemically. Indeed, the importance of coculture when studying cancer cells migration has been shown (Fig. 1-13) [65]. This phenomenon can be easily explained by the presence of different chemoattractants, secreted by fibroblasts and diffusing on the matrix. Those models, derived from 2D and modified into 3D models by using different types of matrixes have been giving precious information on the migration of cancer cells and the different ways to trigger it. However, their use is not sufficient to explain all the cellular behavior of cancer. Naturally, cells, and especially cancer cells, tend to grow in aggregates, where cell to cell contact is much higher than in the previous 2D derived models.

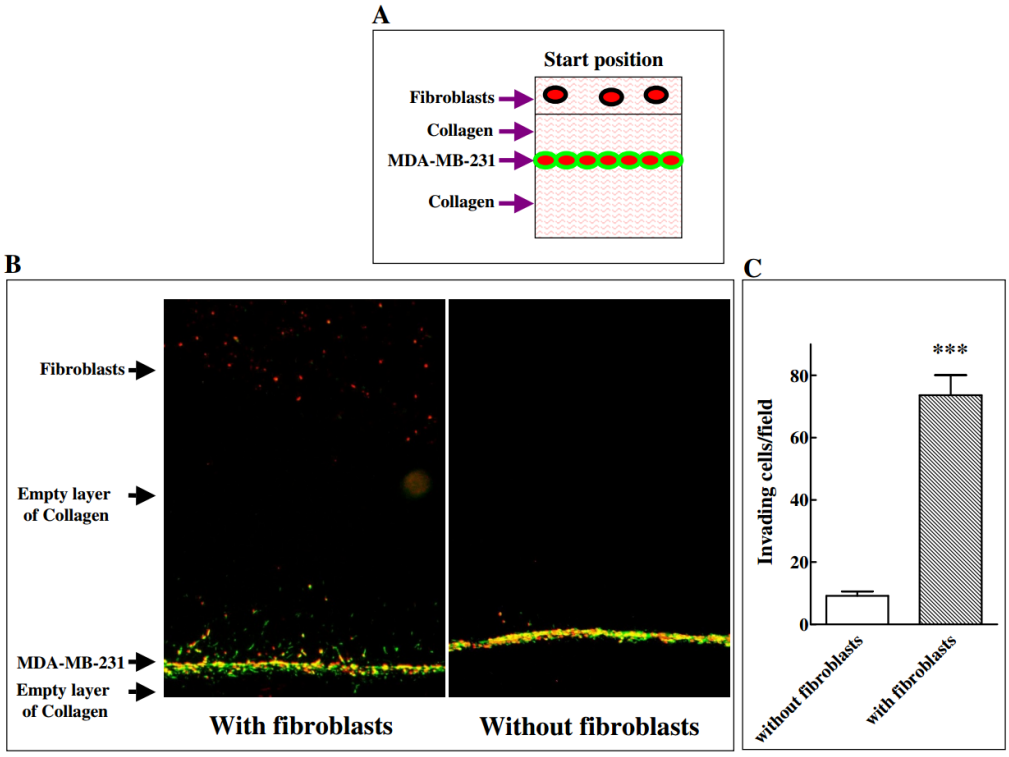

Fig. 1-13: Migration of breast cancer cells, triggered by coculture with fibroblasts [65].

In those study, models with higher cell to cell contact, spheroids are widely used. While the production of spheroids is usually done in suspension culture, they can be seeded after formation in usual tissue culture plates or embedded in gel. Then, the migration from the body of the spheroids to the environment can be observed [66,67]. More complex models can include different types of cells in the spheroids, mimicking the migration of cancer cells from the organ to the blood flow. Other solutions to study the interactions between tumors and the other cells present in their environment exist. One of them is the confrontation culture. In these models, tumor spheroids are put in contact with other cellular spheroids [68] and phenomenon like angiogenesis could be observed. However, the differences with the *in-vivo* situation are still important as all the cells of the organ are not present in the spheroids. Regarding that issue, tumor spheroids have been put in contact with samples obtained from biopsy [69] and invasion into the tissues could be observed.

As an ideal reproduction of the *in-vivo* environment in *in-vitro* situation is often still quite difficult, the use of membranes and explants from animal models is quite developed [70,71]. While those models give interesting insights on the behavior of cancer and solve one of the weakest point of *in-vivo* models, observation, they also retain some of their weaknesses. As ethics and the restriction of the interactions between human cancer cells and animal models are usually brought up, scientists have been looking for creative alternatives. Nanotechnologies, being developed intensively in the past decades started to get the interest of bioengineers. Nanofibers have been used to reproduce the *in-vivo* white matter [72] and physiologically-relevant events could be observed. However, as far as the model is limited by culture in plates, some of the *in-vivo* phenomenon could not be simulated or reproduced. Motivated by the development of bioMEMS, microfluidic models have recently made their apparition in bio-related topics and especially in models for cancer migration.

1.3.2.4 Microfluidic *in-vitro* assays

The development of microfluidic devices has been pushed by the integration of the technics issued from nanotechnologies in tools for medical applications. The relative degree of freedom provided by those technics allows to influence on parameters such as the shape, the number of channels and their size. To reproduce the migrative events observed in static culture, devices with multiple channels are often used. In those models, gradients of chemoattractants or coculture with different types of cells could be easily established. Indeed, the effect of chemical gradients in channels could be monitored [73.74]. In those simple devices, the effect of chemoattractants on cell migration, orientation and deformation could be demonstrated.

To further mimic *in-vivo* events, it is usually necessary to replicate more accurately the microenvironment of cells to allow *in-vitro* models to be more relevant. It is a known fact that there is a crosstalk between the different types of cells and that some cells tend to attract some others. In those models, coculture has been performed in conditions reproducing the microenvironment of cell migration by the use of gels and of gradients of chemoattractants formed by coculture [75] (Fig. 1-14). More specifically, regarding the study of cancer metastasis, intravasation events could be reproduced and observed in an *in-vitro* device [76]. In this case, the cancer cells were attracted and migrated toward the endothelial layer seeded in another channel. Additionally, regulation of the invasiveness of the cancer cells could be performed by stimulation with cytokines which are known to have this specific effect *in-vivo*. Other effects of coculture on cancer migration, which have been observed in static culture, could be reproduced in microdevices. For example, the importance of fibroblasts in metastatic events has been proved in a coculture device [77].

In the metastatic process, and more especially during extravasation, the cancer cells are interacting mostly with endothelial cells. However, those cells are submitted to a constant flow

and shear stress *in-vivo* which is not reproduce by *in-vitro* models in culture plates. By using microfluidic technologies, the reproduction of these parameters has been done very precisely. The effect of the flow on the orientation of endothelial cells could be observed and simple artificial capillaries could be formed [78]. While very few microfluidic models combine the reproduction of the specific microenvironment of cancer cells extravasation with a physiological blood flow, the most advanced models in the domain are to be attributed to Pr. Kamm's group from the MIT [76,79]. A complete vascular network has been reproduced and extravasation of cancer cells could be clearly observed in a physically-relevant microenvironment (Fig. 1-15).

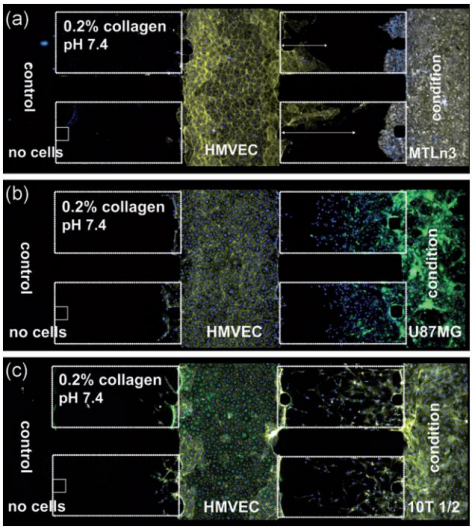

Fig. 1-14: The coculture of different types of cells induces different pattern of migration [75]. In controls, no migration of cells was specifically observed. Angiogenesis of the endothelial cells (HMVEC) was detected as the cells migrated toward the breast cancer cells (MTLn3). However, brain cancer cells (U87MG) and pericytes (10T1/2) were observed to migrated toward the endothelial cells by chemoattraction.

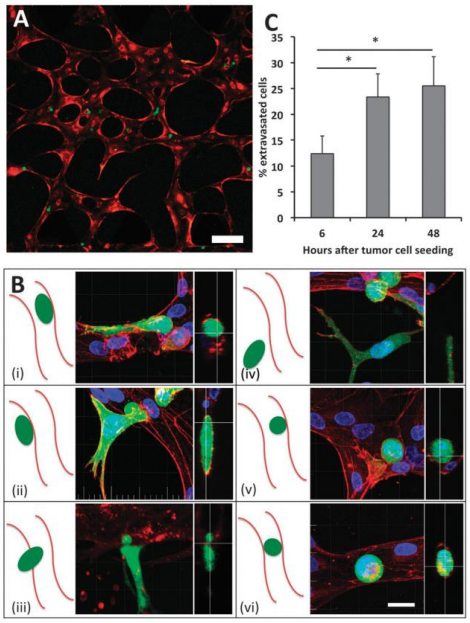

Fig. 1-15: (A) Formation of a microvascular network of endothelial cells. (B) Extravasation events observed in the same microvasculature. (C) Quantification of tumor cells migration [79].

1.4 Remaining Issues of the Current Models

As previously discussed, the use of *in-vivo* models in research related to cancer metastasis is currently subject to controversy. Indeed, it is difficult in those models to observe the intravasation and extravasation phenomena precisely due to the low resolution of the imaging solutions. Moreover, the use of all types of animals for experiments still raises ethical concerns, especially in the case of pet animal models. Those models, while probably giving the best insight on the metastasis phenomenon in the human, are also costly and require heavy maintenance. These issues have motivated the development of in-vitro models as a complement or even as an alternative. *In-vitro* models would allow to observe directly the metastasis related phenomena by live imaging, with a relatively easy handling compared to animal models.

However, as introduced earlier, *in-vitro* models often lack in terms of complexity compared to their *in-vivo* counterpart.

For the improvement of the current *in-vitro* models, different approaches have been taken. Coculture has been performed to observe the influence of certain cells on the migration of cancer cells. On another hand, the physical environment has been reproduced in microfluidic up to high levels of details. However, those approaches have been combined for the study of cancer cells extravasation in only a few cases. Especially, Pr. Kamm's group obtained impressive results by reproducing the extravasation events in a physically-relevant microenvironment by using a microfluidic biochip. Whereas this group still makes effort in that direction, their model still lacks in terms of physiologically-relevancy as many supportive cells, such as parenchymal cells are missing. Indeed, the closest representation of the complete *in-vivo* microenvironment is yet, the biggest issue in the representation of all *in-vivo* phenomenon by *in-vitro* models.

1.5 Objectives and Approach of the Thesis

In this study, we chose to focus on the extravasation of pancreatic cancer cells in the liver microvasculature. Pancreatic cancer still has kept a very low survival rate over the years, despite the evolution of treatments and has the highest probability to metastases in the liver through the vascular pathway [5]. With the objective of reproducing as close as possible the cellular microenvironment of tumor extravasation in the liver, we reproduced, in chapter 2, a static model of the hierarchical structure of the liver microvasculature. While coculture of different cell types, especially endothelial cells and pericytes, have already been performed recently, we chose to go further by coculturing three types of cell, hepatocytes, stellate cells and endothelial cells in custom designed PDMS bottom plate. In this model, significantly more

complete than previously proposed ones, the hierarchical structure of the liver was reproduced and the cells' function could be maintained as the oxygenation from the bottom of the plate was possible though the PDMS membrane. The coculture exhibited higher function of both hepatocytes and endothelial cells and the adhesion of pancreatic cancer cells could be linked to the complexity of the model. Inflammation in the model was also shown to be auto-regulated as it is the case *in-vivo*, proving that the model gives a better representation of the *in-vivo* physiological behavior of the liver and poses itself as a basic reference for the modelling of the interactions between adhering cells and the liver microvasculature.

In chapter 3, we included the model in a "cross-section-like" microfluidic device. Culture in dynamic conditions allowed to reproduce the blood flow with a shear stress in the range of the in-vivo's. The device consisted of three channels separated by micropillars and which could be filled independently. By using the experience obtained by establishing the model in static culture conditions, we built a physiologically-relevant model, distinct from the other works, were successively, pericytes embedded in gel, hepatocytes, endothelial cells and pancreatic cancer cells were added to the device. All the cells were found to be viable during culture and the function of hepatocytes, to be maintained over 10 days. Common markers for hepatic function or endothelial function and adhesion, both liver specific or inflammation-related were also found to be expressed. By varying the culture conditions, the influence of the presence of hepatocytes and pericytes on the migration of pancreatic cancer cells was investigated. In the presence of hepatocytes and pericytes, pancreatic cancer cells could be observed to be migrating toward the top channel-gel interface. When hepatocytes and pericytes were not present in the culture, the cancer cells were seen to migrate toward the wall where the flow is minimized and the shear stress is higher. While impressive models of the cancer cells extravasation have been established, reproducing a physically-relevant microenvironment, we here proposed an original, more physiologically-relevant model for the interactions between

the liver and adhering cancer cells. Although there is still much room for improvements, the produced models lead the path toward more complete and physiologically-relevant models of the interactions between cancer cells and the liver microvasculature.

References

[1] Foulds, L. (1954). The experimental study of tumor progression: a review. Cancer research, 14(5), 327-339.

[2] Balmain, A., Barrett, J. C., Moses, H., & Renan, M. J. (1993). How many mutations are required for tumorigenesis? Implications from human cancer data. Molecular carcinogenesis, 7(3), 139-146.

[3] Hanahan, D., & Weinberg, R. A. (2000). The hallmarks of cancer. cell, 100(1), 57-70.

[4] Hanahan, D., & Weinberg, R. A. (2011). Hallmarks of cancer: the next generation. cell, 144(5), 646-674.

[5] Siegel, R. L., Miller, K. D., & Jemal, A. (2015). Cancer statistics, 2015. CA: a cancer journal for clinicians, 65(1), 5-29.

[6] Woodhouse, E. C., Chuaqui, R. F., & Liotta, L. A. (1997). General mechanisms of metastasis. Cancer, 80(S8), 1529-1537.

[7] Welch, D. R. (1997). Technical considerations for studying cancer metastasis in vivo. Clinical & experimental metastasis, 15(3), 272-306.

[8] Chambers, A. F., Groom, A. C., & MacDonald, I. C. (2002). Metastasis: dissemination and growth of cancer cells in metastatic sites. Nature Reviews Cancer, 2(8), 563-572.

[9] Weiss, L. (1990). Metastatic inefficiency. Advances in cancer research, 54, 159-211.

[10] Nicolson, G. L. (1988). Organ specificity of tumor metastasis: role of preferential adhesion, invasion and growth of malignant cells at specific secondary sites. Cancer and Metastasis Reviews, 7(2), 143-188.

[11] Paget, S. (1889). The distribution of secondary growths in cancer of the breast. The Lancet, 133(3421), 571-573.

[12] Greene, H. S., & Harvey, E. K. (1964). The relationship between the dissemination of tumor cells and the distribution of metastases. Cancer research, 24(5), 799-811.

[13] Ribatti, D., Mangialardi, G., & Vacca, A. (2006). Stephen Paget and the 'seed and soil'theory of metastatic dissemination. Clinical and experimental medicine, 6(4), 145-149.

[14] Auerbach, R., Lu, W. C., Pardon, E., Gumkowski, F., Kaminska, G., & Kaminski, M. (1987). Specificity of adhesion between murine tumor cells and capillary endothelium: an in vitro correlate of preferential metastasis in vivo. Cancer Research, 47(6), 1492-1496.

[15] Fokas, E., Engenhart-Cabillic, R., Daniilidis, K., Rose, F., & An, H. X. (2007). Metastasis: the seed and soil theory gains identity. Cancer and Metastasis Reviews, 26(3-4), 705-715.

[16] Foster, J. H. (1978). Survival after liver resection for secondary tumors. The American Journal of Surgery, 135(3), 389-394.

[17] Kurosawa, T. M. (2007, August). Japanese regulation of laboratory animal care with 3Rs. In Proceedings of 6th World Congress on Alternatives & Animal Use in the Life Sciences (pp. 317-321).

[18] Khanna, C., & Hunter, K. (2005). Modeling metastasis in vivo. *Carcinogenesis*, *26*(3), 513-523.

[19] Vail, D. M., & Macewen, E. G. (2000). Spontaneously occurring tumors of companion animals as models for human cancer. *Cancer investigation*, *18*(8), 781-792.

[20] Khanna, C., & Vail, D. M. (2003). Targeting the lung: preclinical and comparative evaluation of anticancer aerosols in dogs with naturally occurring cancers. *Current cancer drug targets*, *3*(4), 265-273.

[21] Glickman, L. T., Domanski, L. M., Maguire, T. G., Dubielzig, R. R., & Churg, A. (1983). Mesothelioma in pet dogs associated with exposure of their owners to asbestos. *Environmental Research*, *32*(3), 305-313.

[22] Lingaas, F., Comstock, K. E., Kirkness, E. F., Sørensen, A., Aarskaug, T., Hitte, C., ... & Breen, M. (2003). A mutation in the canine BHD gene is associated with hereditary multifocal renal cystadenocarcinoma and nodular dermatofibrosis in the German Shepherd dog. *Human molecular genetics*, *12*(23), 3043-3053.

[23] Schmidt-Hansen, B., Klingelhöfer, J., Grum-Schwensen, B., Christensen, A., Andresen, S., Kruse, C., ... & Grigorian, M. (2004). Functional significance of metastasis-inducing S100A4 (Mts1) in tumor-stroma interplay. *Journal of Biological Chemistry*, *279*(23), 24498-24504.

[24] Dingemans, K. P., Zeeman-Boeschoten, I. M., Keep, R. F., & Das, P. K. (1993). Transplantation of colon carcinoma into granulation tissue induces an invasive morphotype. *International journal of cancer*, *54*(6), 1010-1016.

[25] Brown, K., Buchmann, A., & Balmain, A. (1990). Carcinogen-induced mutations in the mouse c-Ha-ras gene provide evidence of multiple pathways for tumor progression. *Proceedings of the National Academy of Sciences*, *87*(2), 538-542.

[26] Takayama, S. (1968). Induction of Transplantable Liver Tumors in DBF1 Mice After Oral Administration of N, N′-2, 7-Fluorenylenebisacetamide. *Journal of the National Cancer Institute*, *40*(3), 629-641.

[27] Clarke, R. (1996). Human breast cancer cell line xenografts as models of breast cancer—the immunobiologies of recipient mice and the characteristics of several tumorigenic cell lines. *Breast cancer research and treatment*, *39*(1), 69-86.

[28] Takizawa, Y., Saida, T., Tokuda, Y., Dohi, S., Wang, Y. L., Urano, K., ... & Ueyama, Y. (1997). New immunodeficient (nude-scid, beige-scid) mice as excellent recipients of human skin grafts containing intraepidermal neoplasms. *Archives of dermatological research*, *289*(4), 213-218.

[29] Mueller, B. M., & Reisfeld, R. A. (1991). Potential of the scid mouse as a host for human tumors. *Cancer and Metastasis Reviews*, *10*(3), 193-200.

[30] Sikder, H., Huso, D. L., Zhang, H., Wang, B., Ryu, B., Hwang, S. T., ... & Alani, R. M. (2003). Disruption of Id1 reveals major differences in angiogenesis between transplanted and autochthonous tumors. *Cancer cell*, *4*(4), 291-299.

[31] Alani, R. M., Silverthorn, C. F., & Orosz, K. (2004). Tumor angiogenesis in mice and men. *Cancer biology & therapy*, *3*(6), 498-500.

[32] Nagamachi, Y., Tani, M., Shimizu, K., Tsuda, H., Niitsu, Y., & Yokota, J. (1998). Orthotopic growth and metastasis of human non-small cell lung carcinoma cells injected into the pleural cavity of nude mice. *Cancer letters*, *127*(1), 203-209.

[33] Yamamoto, N., Yang, M., Jiang, P., Xu, M., Tsuchiya, H., Tomita, K., ... & Hoffman, R. M. (2003). Determination of clonality of metastasis by cell-specific color-coded fluorescent-protein imaging. *Cancer research*, *63*(22), 7785-7790.

[34] Killion, J. J., Radinsky, R., & Fidler, I. J. (1998). Orthotopic models are necessary to predict therapy of transplantable tumors in mice. *Cancer and Metastasis Reviews*, *17*(3), 279-284.

[35] Hoffman, R. M. (1999). Orthotopic metastatic mouse models for anticancer drug discovery and evaluation: a bridge to the clinic. *Investigational new drugs*, *17*(4), 343-360.

[36] AN, Zili, WANG, Xiaoen, GELLER, Jack, *et al*. Surgical orthotopic implantation allows high lung and lymph node metastatic expression of human prostate carcinoma cell line PC-3 in nude mice. *The Prostate*, 1998, vol. 34, no 3, p. 169-174.

[37] Fidler, I. J., Naito, S., & Pathak, S. (1990). Orthotopic implantation is essential for the selection, growth and metastasis of human real cell cancer in nude mice. *Cancer and Metastasis Reviews*, *9*(2), 149-165.

[38] Nierodzik, M. L. R., Kajumo, F., & Karpatkin, S. (1992). Effect of thrombin treatment of tumor cells on adhesion of tumor cells to platelets in vitro and tumor metastasis in vivo. *Cancer Research*, *52*(12), 3267-3272.

[39] O'Reilly, M. S., Holmgren, L., Shing, Y., Chen, C., Rosenthal, R. A., Moses, M., ... & Folkman, J. (1994). Angiostatin: a novel angiogenesis inhibitor that mediates the suppression of metastases by a Lewis lung carcinoma. *cell*, *79*(2), 315-328.

[40] Metz, S., Daldrup-Link, H. E., Richter, T., Räth, C., Ebert, W., Settles, M., ... & Piert, M. (2003). Detection and quantification of breast tumor necrosis with MR imaging: value of the necrosis-avid contrast agent Gadophrin-3. *Academic radiology*, *10*(5), 484-490.

[41] Jenkins, D. E., Oei, Y., Hornig, Y. S., Yu, S. F., Dusich, J., Purchio, T., & Contag, P. R. (2003). Bioluminescent imaging (BLI) to improve and refine traditional murine models of tumor growth and metastasis. *Clinical & experimental metastasis*, *20*(8), 733-744.

[42] Yang, M., Baranov, E., Jiang, P., Sun, F. X., Li, X. M., Li, L., ... & Shimada, H. (2000). Whole-body optical imaging of green fluorescent protein-expressing tumors and metastases. *Proceedings of the National Academy of Sciences*, *97*(3), 1206-1211.

[43] Hoffman, R. M. (2002). Green fluorescent protein imaging of tumour growth, metastasis, and angiogenesis in mouse models. *The lancet oncology*, *3*(9), 546-556.

[44] Ballou, B., Lagerholm, B. C., Ernst, L. A., Bruchez, M. P., & Waggoner, A. S. (2004). Noninvasive imaging of quantum dots in mice. *Bioconjugate chemistry*, *15*(1), 79-86.

[45] Auerbach, R., Lu, W. C., Pardon, E., Gumkowski, F., Kaminska, G., & Kaminski, M. (1987). Specificity of adhesion between murine tumor cells and capillary endothelium: an in vitro correlate of preferential metastasis in vivo. *Cancer Research*, *47*(6), 1492-1496.

[46] Coulouarn, C., Corlu, A., Glaise, D., Guénon, I., Thorgeirsson, S. S., & Clément, B. (2012). Hepatocyte–stellate cell cross-talk in the liver engenders a permissive inflammatory microenvironment that drives progression in hepatocellular carcinoma. *Cancer research*, *72*(10), 2533-2542.

[47] Verbridge, S. S., Choi, N. W., Zheng, Y., Brooks, D. J., Stroock, A. D., & Fischbach, C. (2010). Oxygen-controlled three-dimensional cultures to analyze tumor angiogenesis. *Tissue Engineering Part A*, *16*(7), 2133-2141.

[48] Brandt, B., Heyder, C., Gloria-Maercker, E., Hatzmann, W., Rötger, A., Kemming, D., Zanker, K., Entschalen, F., & Dittmar, T. (2005, October). 3D-extravasation model–selection of highly motile and metastatic cancer cells. In *Seminars in cancer biology* (Vol. 15, No. 5, pp. 387-395). Academic Press.

[49] Decaestecker, C., Debeir, O., Van Ham, P., & Kiss, R. (2007). Can anti-migratory drugs be screened in vitro? A review of 2D and 3D assays for the quantitative analysis of cell migration. *Medicinal research reviews*, *27*(2), 149-176.

[50] Zimmermann, M., Box, C., & Eccles, S. A. (2013). Two-dimensional vs. three-dimensional in vitro tumor migration and invasion assays. *Target Identification and Validation in Drug Discovery: Methods and Protocols*, 227-252.

[51] Kramer, R. H., & Nicolson, G. L. (1979). Interactions of tumor cells with vascular endothelial cell monolayers: a model for metastatic invasion. *Proceedings of the National Academy of Sciences*, *76*(11), 5704-5708.

[52] Nicolson, G. L. (1982). Metastatic tumor cell attachment and invasion assay utilizing vascular endothelial cell monolayers. *Journal of Histochemistry & Cytochemistry*, *30*(3), 214-220.

[53] Pinco, K. A., He, W., & Yang, J. T. (2002). α4β1 integrin regulates lamellipodia protrusion via a focal complex/focal adhesion-independent mechanism. *Molecular biology of the cell*, *13*(9), 3203-3217.

[54] Yarrow, J. C., Perlman, Z. E., Westwood, N. J., & Mitchison, T. J. (2004). A high-throughput cell migration assay using scratch wound healing, a comparison of image-based readout methods. *BMC biotechnology*, *4*(1), 21.

[55] Cai, G., Lian, J., Shapiro, S. S., & Beacham, D. A. (2000). Evaluation of endothelial cell migration with a novel in vitro assay system. *Methods in cell science*, *22*(2-3), 107-114.

[56] Muinonen-Martin, A. J., Veltman, D. M., Kalna, G., & Insall, R. H. (2010). An improved chamber for direct visualisation of chemotaxis. *PloS one*, *5*(12), e15309.

[57] Muir, D., Sukhu, L., Johnson, J., Lahorra, M. A., & Maria, B. L. (1993). Quantitative methods for scoring cell migration and invasion in filter-based assays. *Analytical biochemistry*, *215*(1), 104-109.

[58] Li, Y. H., & Zhu, C. (1999). A modified Boyden chamber assay for tumor cell transendothelial migration in vitro. *Clinical & experimental metastasis*, *17*(5), 423-429.

[59] Lewalle, J. M., Cataldo, D., Bajou, K., Lambert, C. A., & Foidart, J. M. (1998). Endothelial cell intracellular Ca concentration is increased upon breast tumor cell contact and mediates tumor cell transendothelial migration. *Clinical & experimental metastasis*, *16*(1), 21-29.

[60] Soeda, S., Honda, O., & Shimeno, H. (1996). Vascular endothelial cell monolayer formed on membrane filter potentiates the defense against tumor cell invasion by treatment with brefeldin A. *Cancer letters*, *108*(1), 49-54.

[61] Okada, T., Okuno, H., & Mitsui, Y. (1994). A novelin vitro assay system for transendothelial tumor cell invasion: significance of E-selectin and α3 integrin in the transendothelial invasion by HT1080 fibrosarcoma cells. *Clinical & experimental metastasis*, *12*(4), 305-314.

[62] Sieuwerts, A. M., Klijn, J. G., & Foekens, J. A. (1997). Assessment of the invasive potential of human gynecological tumor cell lines with the in vitro Boyden chamber assay: influences of the ability of cells to migrate through the filter membrane. *Clinical & experimental metastasis*, *15*(1), 53-62.

[63] Albini, A., Iwamoto, Y., Kleinman, H. K., Martin, G. R., Aaronson, S. A., Kozlowski, J. M., & McEwan, R. N. (1987). A rapid in vitro assay for quantitating the invasive potential of tumor cells. *Cancer research*, *47*(12), 3239-3245.

[64] Duong, H. S., Le, A. D., Zhang, Q., & Messadi, D. V. (2005). A novel 3-dimensional culture system as an in vitro model for studying oral cancer cell invasion. *International journal of experimental pathology*, *86*(6), 365-374.

[65] Brekhman, V., & Neufeld, G. (2009). A novel asymmetric 3D in-vitro assay for the study of tumor cell invasion. *BMC cancer*, *9*(1), 415.

[66] Vinci, M., Gowan, S., Boxall, F., Patterson, L., Zimmermann, M., Lomas, C., ... & Eccles, S. A. (2012). Advances in establishment and analysis of three-dimensional tumor spheroid-based functional assays for target validation and drug evaluation. *BMC biology*, *10*(1), 29.

[67] Truong, H. H., de Sonneville, J., Ghotra, V. P., Xiong, J., Price, L., Hogendoorn, P. C., ... & Danen, E. H. (2012). Automated microinjection of cell-polymer suspensions in 3D ECM scaffolds for high-throughput quantitative cancer invasion screens. *Biomaterials*, *33*(1), 181-188.

[68] Wartenberg, M., Finkensieper, A., Hescheler, J., & Sauer, H. (2006). Confrontation cultures of embryonic stem cells with multicellular tumor spheroids to study tumor-induced angiogenesis. *Human Embryonic Stem Cell Protocols*, 313-328.

[69] Fjellbirkeland, L., Bjerkvig, R., & Laerum, O. D. (1998). Non-small-cell lung carcinoma cells invade human bronchial mucosa in vitro. *In Vitro Cellular & Developmental Biology-Animal*, *34*(4), 333-340.

[70] Hart, I. R., & Fidler, I. J. (1978). An in vitro quantitative assay for tumor cell invasion. *Cancer Research*, *38*(10), 3218-3224.

[71] Friedl, P., Noble, P. B., Walton, P. A., Laird, D. W., Chauvin, P. J., Tabah, R. J., ... & Zänker, K. S. (1995). Migration of coordinated cell clusters in mesenchymal and epithelial cancer explants in vitro. *Cancer research*, *55*(20), 4557-4560.

[72] Agudelo-Garcia, P. A., De Jesus, J. K., Williams, S. P., Nowicki, M. O., Chiocca, E. A., Liyanarachchi, S., ... & Viapiano, M. S. (2011). Glioma cell migration on three-dimensional nanofiber scaffolds is regulated by substrate topography and abolished by inhibition of STAT3 signaling. *Neoplasia*, *13*(9), 831IN15-840IN22.

[73] Saadi, W., Wang, S. J., Lin, F., & Jeon, N. L. (2006). A parallel-gradient microfluidic chamber for quantitative analysis of breast cancer cell chemotaxis. *Biomedical microdevices*, *8*(2), 109-118.

[74] Huang, Y., Agrawal, B., Sun, D., Kuo, J. S., & Williams, J. C. (2011). Microfluidics-based devices: New tools for studying cancer and cancer stem cell migration. *Biomicrofluidics*, *5*(1), 013412.

[75] Chung, S., Sudo, R., Mack, P. J., Wan, C. R., Vickerman, V., & Kamm, R. D. (2009). Cell migration into scaffolds under co-culture conditions in a microfluidic platform. *Lab on a Chip*, *9*(2), 269-275.

[76] Zervantonakis, I. K., Hughes-Alford, S. K., Charest, J. L., Condeelis, J. S., Gertler, F. B., & Kamm, R. D. (2012). Three-dimensional microfluidic model for tumor cell intravasation and endothelial barrier function. *Proceedings of the National Academy of Sciences*, *109*(34), 13515-13520.

[77] Liu, T., Lin, B., & Qin, J. (2010). Carcinoma-associated fibroblasts promoted tumor spheroid invasion on a microfluidic 3D co-culture device. *Lab on a Chip*, *10*(13), 1671-1677.

[78] Van der Meer, A. D., Poot, A. A., Duits, M. H. G., Feijen, J., & Vermes, I. (2009). Microfluidic technology in vascular research. *BioMed Research International*, *2009*.

[79] Chen, M. B., Whisler, J. A., Jeon, J. S., & Kamm, R. D. (2013). Mechanisms of tumor cell extravasation in an in vitro microvascular network platform. *Integrative Biology*, *5*(10), 1262-1271.

Chapter 2

Modeling of the liver microvasculature in static conditions by physiologically-relevant coculture

The work introduced in this chapter has been adapted from the manuscript that was published during this PhD thesis: "Alteration of pancreatic carcinoma and promyeloblastic cell adhesion in liver microvasculature by coculture of hepatocytes, hepatic stellate cells and endothelial cells in a physiologically-relevant model, Danoy *et al.*, Integrative Biology (2017)".

2.1 Introduction

The past decades have seen the development of many drug-screening model reproducing on cancer extravasation. They have enabled a better grasp of cancer metastasis [1] and of the role of inflammation in the adhesion of cancer cells and leukocytes to the endothelium [2-4]. Yet, *in-vivo* models remain the gold standard in terms a metastasis-related studies [5,6]. Nonetheless, the use of those model remains ethically criticizable and poses many problems such as species specificity and motivates the development of an alternative [7]. As a solution, *in-vitro* models have been developed with the objective to reproduce the cellular microenvironment of cancer cells extravasation as close as possible.

To study extravasation in *in-vitro* models, it is necessary to bring the metastatic cancer cells with the targeted tissue's endothelial cells [8,9,10]. As the cellular and physical environment of the cells is important, it has been tried to reproduce it by coculture and by using extracellular matrix or culture in inserts [11]. Still, published models often represent simpler situations and do not include all the surrounding cells.

In this chapter, we focused our work on the extravasation of cancer cells in the liver as it is a frequent target for metastasis. As it is a complex organ, the liver can be divided in three distinct main networks: lymphatic, biliary and vascular. The lymphatic network is a route for part of the filtered plasma and has a role in the immune defense. It is composed of lymphatic cells, white blood cells and lymphocytes. The biliary network, composed of biliary cells, is responsible for the retrieval of the bile produced by the hepatocytes. In our case, as pancreatic

cancer is known to migrate to the liver by the vascular network, we chose to focus on the vascular network. The liver microvasculature, responsible for transporting blood and oxygen, is composed of several cell types. Amongst these cells types, the crosstalk between hepatocytes, forming most of the liver mass, the endothelial cells, forming the vascular walls and the pericytes, acting as a scaffold for the latter, has been extensively studied [12.13] and those three types of cells have been shown to exhibit a high level of cross-talking. However, most of the established coculture models focusing on the cross-talk between the different types of cells, have for objective the improvement of the function of hepatocytes [14,15,16] and do not focus on the influence of those specific supportive cells on the endothelial cells and their interaction with the adhesion and migration of cancer cells. Human Umbilical Vein Endothelial Cells (HUVECs), which are vascular endothelial cells, have been widely used in models for the endothelial barrier and its interactions with cancer cells [17,18]. In addition, HUVECs are considered by the vascular research domain to be the golden standard [19]. Although those cells are not mature and not specific to the liver, they show a remarkable phenotype flexibility which allow to use them in many models. In addition, HUVECs can also be stimulated to reproduce inflammatory events in the endothelial barrier [20] which are known to be strongly involved in the adhesion and migration of cancer cells through the endothelial barrier and can be of use in our model.

The liver is composed of many different types of cells and its in-vivo structure is known to be hierarchical [21]. In the vascular network, the layers of hepatocytes and endothelial cells are separated by the space of Disse, composed of extracellular matrix and cells such as the pericytes. The reproduction of this structure is difficult in *in-vitro* models mainly because of the thickness of the stacked cell multilayers that would cause a shortage of oxygen as the compound can only be brought from the top of the culture by diffusion in the culture [22]. Previous studies have shown that the culture on polydimethylsiloxane (PDMS) as an alternative

to conventional plates, could be a solution as oxygenation from the bottom, through the membrane was possible [23,24]. It is then possible to embed the pericytes in extracellular matrix to reproduce the space of Disse. While hepatocytes are easily accessible, human primary hepatocytes are costly. Primary rat hepatocytes can be easily isolated from animals and are relatively low cost. Their analog behavior to the human counterpart make them a recognized choice for *in-vitro* models. However, the obtention of pericyte by isolation is still difficult [25]. A pericytes cells line, the LX-2 has been established as an alternative. They show close expression to those of *in-vivo*'s as well as high viability and high transfectability, making them suitable for our model.

2.2 Objectives

As previous research made in our group including hepatocytes cultured on PDMS membranes were focused on the improvement of the hepatic function [23.24], we had this time for objective, to establish a hierarchical coculture model composed of primary rat hepatocytes (Hep), LX-2 and HUVECs cultured on PDMS and to study the influence of coculture on PDMS on the adhesion of pancreatic cancer cells and on the endothelial phenotype. To achieve that, we studied the influence of the different cells in 4 different structures, HUVEC & gel, HUVEC & LX-2, HUVEC & Hep and HUVEC, LX-2 & Hep. The preservation of the hepatocytes' function and their interactions with the other cells were shown by measuring the concentration of two known protein and factor produced by hepatocytes, the albumin and VEGF (Vascular Endothelial Growth Factor) in culture. The expression of the HUVECs was assessed with several common liver endothelial markers. ICAM-1 (InterCellular Adhesion Molecule) and VAP-1 (Vascular Adhesion Protein), normally expressed by endothelial cells in the liver, were used to monitor the level of inflammation of the endothelial layer [27.28,29,30], Stabilin-1 was

used as a liver vascular specific endothelial marker [31] and LYVE-1 (LYmphatic VEssel endothelial hyaluronan receptor) as a liver lymphatic endothelial marker [32]. The adhesion of the pancreatic carcinoma cells line MiaPaCa-2 and of the promyeloblastic cells line HL60 was quantified in the different structure and the response of the model to inflammatory events was assessed by stimulation with TNF- α (Tumor Necrosis Factor).

2.3 Materials and methods

2.3.1 Routine cell culture

The HUVEC were purchased from Lonza, Inc. (Japan) and the LX-2 cells line was purchased from EMD Millipore (Temecula, CA, USA). For the pancreatic cancer cells adhesion assay, the MiaPaCa-2 cells line was used. It was purchased from AntiCancer, Inc. (Japan). The HL60 cells line was purchased from ATCC (USA). All cells were routinely cultured in 100mm TCPS (Tissue Culture PolyStyrene) dishes. Inoculation densities were 3×10^5 cells/dish for LX-2, 1×10^5 cells/dish for the HUVEC, 1×10^6 cells/dish for the MiaPaCa-2 and the HL60. The LX-2, MiaPaCa-2 and the HL60 were passaged every 3 and 4 days and were systematically used for experiments when subcultured 4 days before. The HUVEC were passaged 4 days before use and were used on passage number 3 and 4. Culture medium for the LX-2 and the MiaPaCa-2 cells was high glucose DMEM (Dulbecco's Modified Eagle Medium) (Gibco, Japan) supplemented with 10% Fetal Bovine Serum (Gibco, Japan), 1% MEM (Modified Eagle Medium) nonessential amino acids (Gibco, Japan), 100 U/mL penicillin, 100 U/mL streptomycin and 25 mM HEPES. The culture medium for the HUVEC was EGM-2 (Endothelial Cell Growth Medium) BulletKit (Lonza, Inc., Japan) and the culture medium for the HL60 was IMDM (Iscove's Modified Dulbecco's Medium) (Gibco, Japan) supplemented

with 20% Fetal Bovine Serum (Gibco, Japan) and 100 U/mL penicillin, 100 U/mL streptomycin.

Rat Hepatocytes were isolated from 7-8 weeks old, 200-300g, male Wistar rats (Sankyo Laboratory, Japan) using the previously described two-step collagenase perfusion method [33]. Rats were treated following the guidelines of the University of Tokyo for animal experiments in accord with the guidelines of the Japanese Ministry of Education. The rat hepatocytes used for the experiments were always issued from isolation in which the viability was superior to 80%. The culture medium for the rat hepatocytes was based on William's E medium (Gibco, Japan) supplemented with 1% nonessential amino acids (Gibco, Japan), 0,1µM insulin (Takara, Japan), 0,1µM dexamethasone (Wako, Japan), 10ng/mL mouse epidermal growth factor (Takara, Japan), 0.5 mM ascorbic acid 2-phosphate (from magnesium salt n-hydrate, Wako, Japan), 0,1µM $CuS0_4$, 0,01µM H_2SeO_3 and 1µM $ZnSO_4$.

2.3.2 Establishment of the hierarchical coculture

Custom culture plates with a 1mm - 1,5 mm thick PDMS membrane in the bottom were used. As demonstrated in previous research [26], the PDMS membrane is necessary to keep both a good viability and function of hepatocytes, especially in thick culture such as ours. Notably, custom 96 well plates with a step-wise structure were used, allowing us to avoid the formation of a meniscus when plating collagen gel. Those plates were made of polycarbonate, and the PDMS membrane was sandwiched between the plate and a stainless-steel bottom support. Cells were then cultured in a hierarchical structure mimicking the *in-vivo* situation (Fig. 2-1). On day 0, the PDMS bottom layer was prepared to allow for the cells to attach. It was treated using an oxygen plasma machine for 60 s (YHS-GZA 200, Sakigake-Semiconductor, Japan) after plate assembling. Then, 3-Mercaptopropyltrimethoxysilane (TCI, Japan) was attached to the PDMS layer and made to react with the cross linker GMBS (N-γ-maleimidobutyryl-

oxysuccinimide ester) (Dojindo, Japan) and activated by WSC (Dojindo, Japan) mixed with Sulfo-NHS (TCI, Japan). Finally, the plate was coated with collagen type 1-P (Nitta Gelatin, Japan). After coating and washing, the plate was incubated overnight with the culture medium of the cells added on the next day.

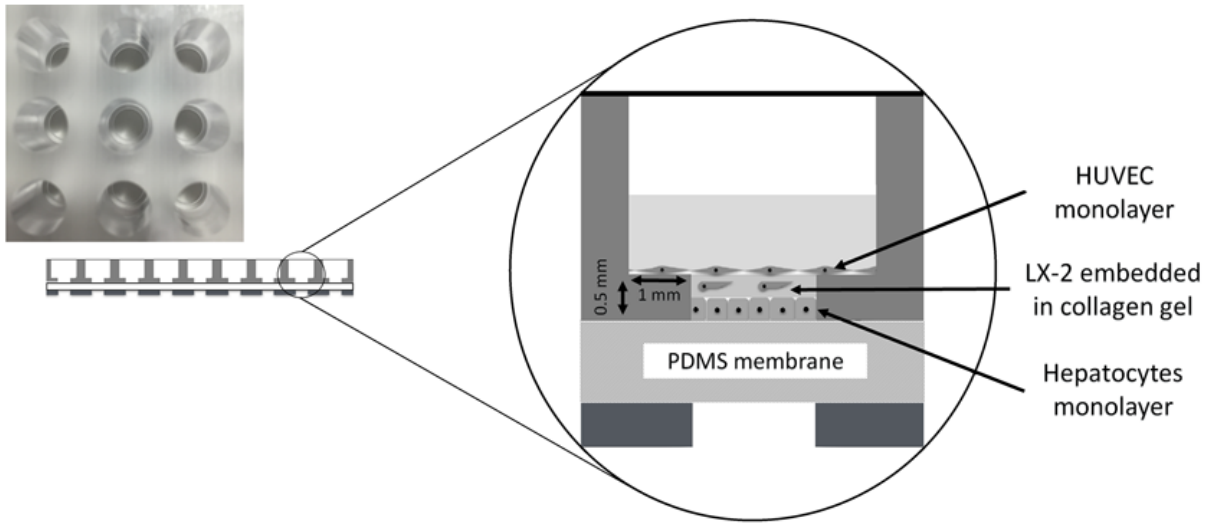

Fig. 2-1: Custom-designed culture well-plate, inspired from the 96 well-plate format. The PDMS membrane was clamped between the bottom frame (metal) and the main frame (polycarbonate). The described hierarchical coculture model was established in the plate as shown.

On day 1, isolated rat hepatocytes were seeded on the collagen coated PDMS surface in their culture medium, previously described, at a 1 x 10^5 / cm^2 density, which allows the obtainment of a monolayer after one day of culture. On day 2, LX-2 cells embedded in 16 µL of collagen gel at 8 x 10^4 / mL were added. The ratio of LX-2 in the well was kept the same as the ratio of hepatic stellate cells to hepatocytes in the liver [34]. From day 2, the culture medium used for the coculture was a 50/50 mix of HUVEC and rat hepatocytes culture media. HUVEC were added on day 3 to the well at a 1,5 x 10^5 / cm^2 density which led to the formation of a

monolayer. Culture medium was changed on day 4 and 5. On day 6, samples for ELISA (enzyme-linked immunosorbent assay) were taken, cells were either observed using a confocal microscope (Olympus, Japan) by live immunostaining or a pancreatic cancer cells adhesion assay was performed. The effects of the different cell types on the HUVECs were checked in all assays by varying the co-culture into four different conditions: Rat Hepatocytes + LX-2 in gel + HUVEC, Rat Hepatocytes + gel + HUVEC, LX-2 in gel + HUVEC and monoculture of HUVEC. For the ELISA samples, monoculture of rat hepatocytes, grown in the same conditions as the other conditions was also performed. To investigate the necessity of the use of PDMS in our thick hierarchical coculture model, controls with TCPS plate were performed for every previously cited condition.

2.3.3 Cytoplasmic fluorescent staining

To observe the live morphology of the LX-2 and HUVEC cells, the live cells were stained with Celltracker Green and Orange (Molecular probes by Life Technologies, Japan) as per the manufacturer's instructions on the day before addition to the coculture. The cells were finally observed by confocal microscopy (IX-81, Olympus, Japan) and not used for further experiments.

2.3.4 Measurement of the production of Albumin and VEGF

The levels of rat Albumin and rat VEGF secreted in the culture medium of the previously described conditions were measured by performing a sandwich ELISA. For the rat Albumin ELISA, the capture antibody used was a goat anti-rat albumin antibody (Cappel, CA) and the detection antibody was a horseradish peroxidase-conjugated sheep anti-rat albumin antibody (Cappel, CA). For the VEGF ELISA, a Rat VEGF kit (DuoSet Elisa, R&D Systems, USA) was used. Measurements were made using a microplate reader iMark (BioRAD, Japan)

at a 450nm wavelength with an optical correction of a 630nm wavelength and 570nm wavelength for the Albumin and VEGF respectively.

2.3.5 Cells adhesion assay

The adhesion assay was performed using the MiaPaCa-2 pancreatic cancer cells line and the HL60 promyeloblastic cells line. The cancer cells line choice for a liver microvasculature model was made by considering that pancreatic cancer mainly uses the blood stream as a route of spreading [35] and the HL60 were chosen as their adhesion mechanism is already well-known as described later. On day 5, MiaPaCa-2 and HL60 were stained using Celltracker Green (Molecular probes by Life Technologies, Japan). Cells were incubated in serum free culture medium with 5 µM of solution following the manufacturer instructions. On day 6 of the coculture, the cancer cells (5e4 cells / well) were added in each condition in serum-free culture medium and left to adhere for 90 minutes. The duration for the attachment assay was determined as per the necessary time for the adhesion of MiaPaCa-2 to collagen gel [36] and kept the same for HL60 to allow comparison. Each well was then manually washed 3 times with serum-free culture medium to prevent unspecific or weak attachment. Finally, each well was filled with 0,5% Triton X-100 (PlusOne, Pharmacia Biotech, Japan) diluted in deionized water for 30 minutes to lyse the cells present and release the cytoplasmic dye in solution. Samples were then taken and the fluorescence measured using a Fluorescence plate reader (ARVO X2, PerkinElmer). To determine the cell number from the fluorescence, a calibration curve was prepared for each experiment with a known number of lysed cells.

2.3.6 Live Immunostaining

Immunostaining for several markers was performed on live cells without PFA fixation and permeabilization. Especially, inflammation markers were chosen to confirm the role of

inflammation in cancer adhesion to the endothelium [2-4]. Live immunostaining was chosen over the usual staining on fixated cells considering the relative shrinking of tissues and damages caused by PFA [37] and the autofluorescent background from the hepatocytes [38], not negligible when the two cell layers come closer by the shrinking. For each staining, the first and the second antibodies were incubated for each corresponding well for 2 hours and DAPI (4',6-diamidino-2-phénylindole) staining was added 30 minutes before the end of the incubation as per the previously reported protocol for live immunostaining [39]. Then, each well was washed with supplements-free William's E medium (Gibco, Japan) 3 times and immediately taken for imaging on a confocal microscope (Olympus, Japan). The cells were stained with following markers: anti-ICAM-1 (Genetex, USA, GTX11359), anti-VAP-1 (Abnova, Taiwan, H00008639-M06), anti-Stabilin-1 (Abnova, Taiwan, H00023166-M05), anti-LYVE-1 (Genetex, USA, GTX44915). Those markers were coupled with an Alexa Fluor 647 secondary antibody (abcam, Japan, ab150107). DAPI was purchased from Dojindo (Japan).

2.3.7 TNF-α induced cell activation

The possibility to activate the endothelial cells in monoculture and in the coculture model was tested using TNF-α induced cell activation, a cytokine known as an initiator of inflammatory events [40,41]. TNF-α stimulation was performed by supplementing 10ng/mL for 10h in the culture medium of the desired conditions to optimize the inflammatory response [41]. After stimulation, the previously described MiaPaCa-2 and HL60 adhesion assay and ICAM-1 immunostaining were performed in both monoculture of HUVEC and in the coculture model.

2.3.8 Statistical Analysis

To perform a statistical comparison of two groups, Student's t-test was used. Differences with $P < 0.05$ (*), $P < 0.01$ (**) and $P < 0.001$ (***) were highlighted and considered to be significantly different. All data are presented as the mean with the standard error of the different replicates and repeats of the experiments. All experimental data are issued from 3 independents experiments.

2.4 Results

2.4.1 Cellular morphology in the different culture conditions

To allow comparison of the different culture conditions, the morphology of the different cell layers was observed (Fig. 2-2). In particular, in the coculture of HUVECs (Fig. 2-2A), hepatocytes and LX-2, the HUVECs formed a complete cell monolayer and covered the whole culture. The LX-2 cells were seen to be proliferating and to adopt a "star-like" morphology as they are cultured in collagen gel (Fig. 2-2H). The other culture conditions exhibited similar characteristics and not significant differences were found (Fig. 2-2 B, C, D, H). Those results indicate that in all culture conditions, the cells were grown with very low stress levels and that the comparison of adhesion of cancer and immune cells between conditions is relevant.

2.4.2 Hepatocytes function and cross-talk with other cells in coculture

To evaluate the maintenance of the function of the hepatocytes, measurement of the concentration of albumin, specific to the liver [42,43] and VEGF, in the culture were made. To assess the effect of the culture in the PDMS bottom plates, measurements of albumin were made both in those plates and in conventional tissue culture polystyrene (TCPS) (96 well plates (Fig.2-3). The culture in PDMS bottom plate exhibited significant higher production of

albumin compared to the TCPS plates'. In coculture with others cells on TCPS, the production of albumin was found to be reduced compared to the monoculture. However, in cocultures on PDMS, the production of albumin increased with the complexity of the coculture. The addition of LX-2 and HUVECs, in a hierarchical structure extremely significantly increased the maintenance of the function of the hepatocytes and are in accord with the previous results in our group [18].

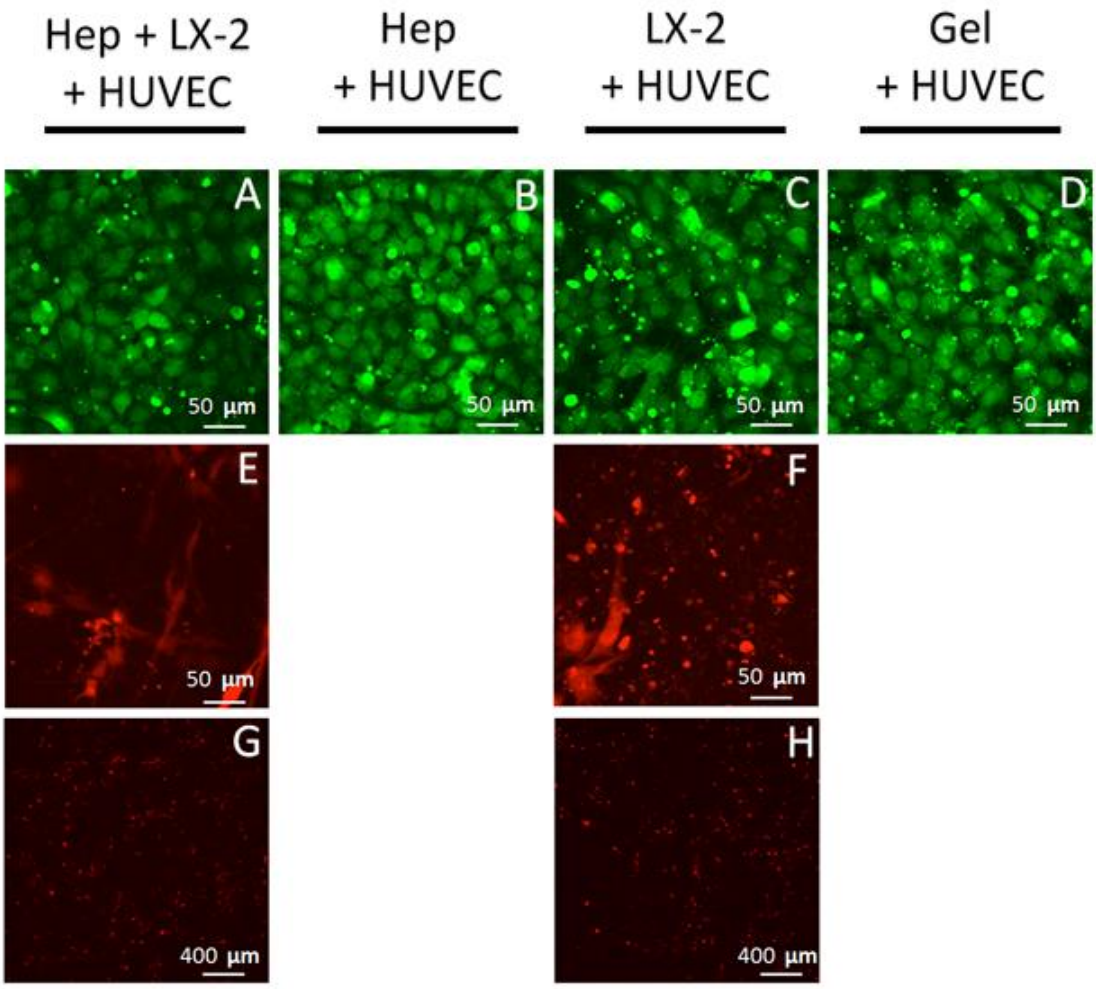

Fig. 2-2: Confocal imaging of the cell layers (HUVECs in green and LX-2 in red) on Day6 in the culture conditions at different magnification: 40X(A-F) and 5X(G-H).

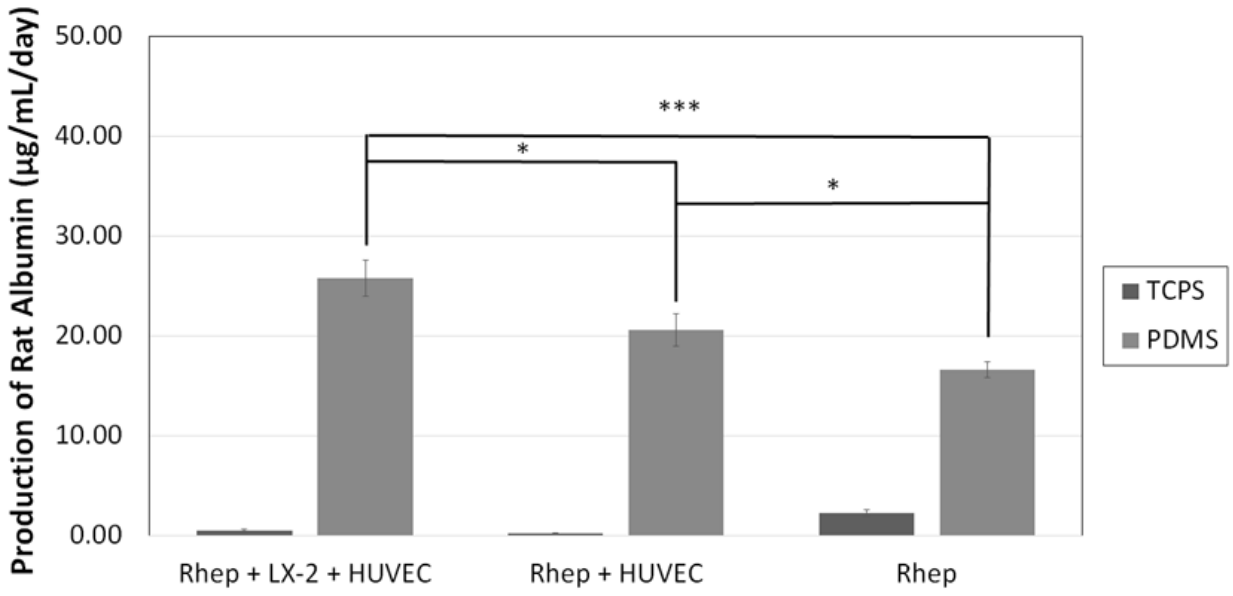

Fig. 2-3: Production of albumin in the different cultures conditions. Data represents the mean ± SE, Differences with $P < 0.05$ (*), $P < 0.01$ (**) and $P < 0.001$ (***) were considered to be significantly, highly or extremely different. Data are issued from 3 independents experiments.

To highlight the interactions between the hepatocytes and the HUVECs, the concentration of VEGF in culture was measured in all conditions as well as in the simple monoculture of hepatocytes and in the culture medium (Fig. 2-4). Human VEGF was cross-detected in the culture medium as it is used as a supplement. In the monoculture of hepatocytes, a significantly higher concentration of produced VEGF was detected. The coculture conditions where no hepatocytes were added exhibited a residual concentration of VEGF and the condition with hepatocytes displayed the same profile. Those results indicate that the supplemented and the produced VEGF are both consumed by the HUVECs and are not in excess. The improvement of the production of albumin and the consumption of VEGF in coculture illustrate very well the different interactions and the crosstalk between the different cell types of the liver model.

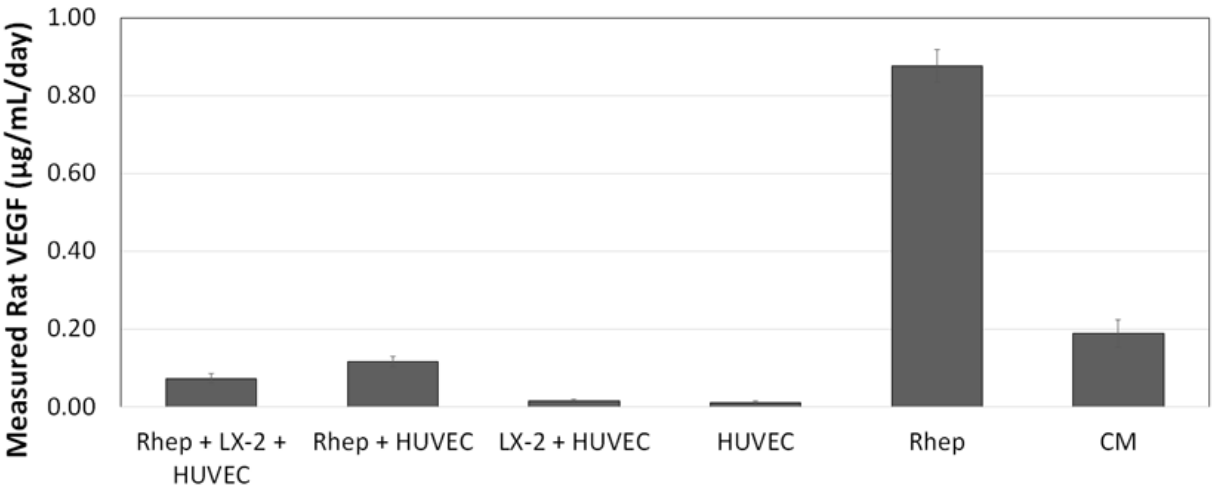

Fig. 2-4: Detected concentrations of VEGF in the different cultures conditions, in rat hepatocytes and culture medium control. Data represents the mean ± SE. Data are issued from 3 independents experiments.

2.4.3 Quantification of the adhesion of pancreatic cancer cells in the different conditions

The impact of the coculture with hepatocytes and pericytes on the adhesion propensity of MiaPaCa-2 on HUVECs was quantified by assaying the different conditions (Fig. 2-5). While the inclusion of the LX-2 did not cause substantial change in the adhesion, the addition of hepatocytes in the model significantly decreased the adhesion of MiaPaCa-2. Generally, when comparing the monoculture of HUVECs to the coculture of hepatocytes, LX-2 and HUVECs, the coculture exhibited highly significant lower adhesion of MiaPaCa-2 than the monoculture condition. Those results alone do not allow to make any conclusion on the state of the endothelial layer but, completed with the results of the immunostaining, the inflammatory state of the cells and the higher adhesion propensity of cancer cells could be linked as it was the case in previous work [2,3,4].

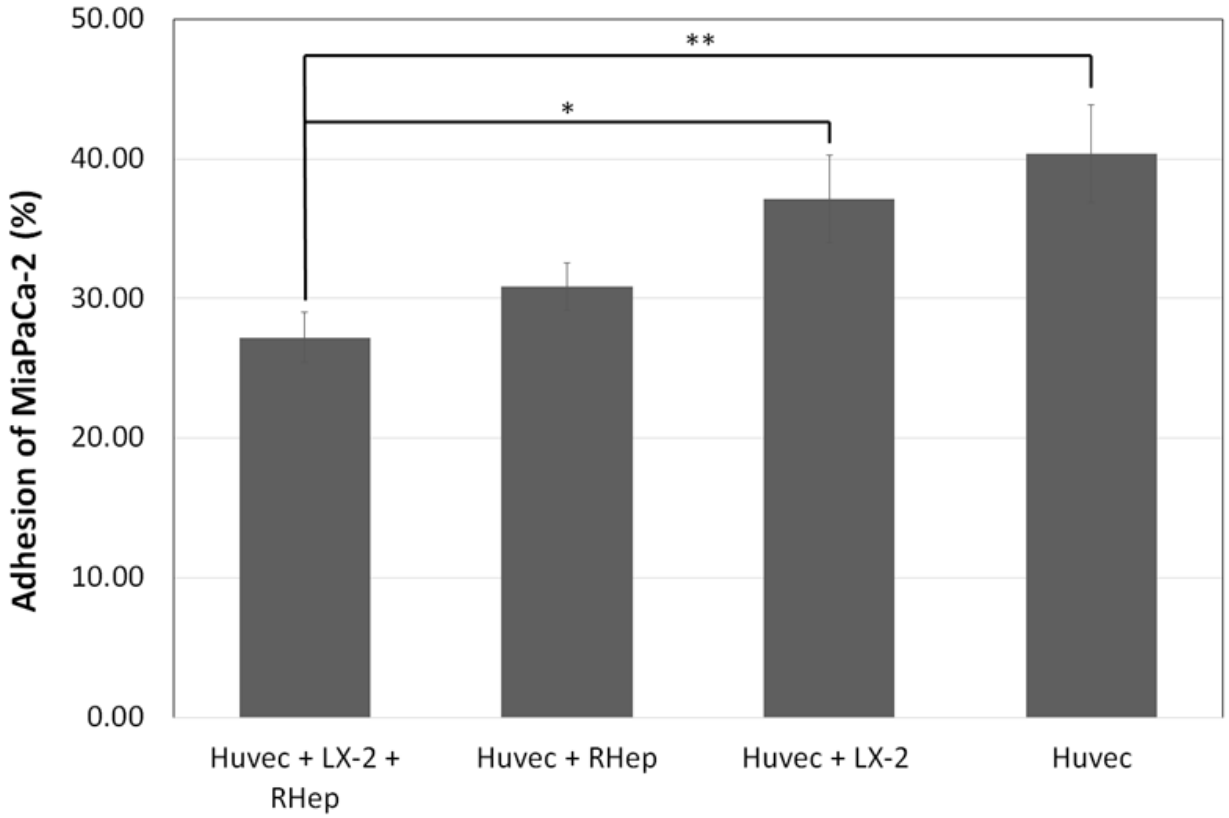

Fig. 2-5: Adhesion of MiaPaCa-2 in the different culture conditions. Data represents the mean ± SE, Differences with $P < 0.05$ (*), $P < 0.01$ (**) and $P < 0.001$ (***) were considered to be significantly, highly or extremely different. Data are issued from 3 independents experiments.

2.4.4 Influence of coculture on common liver endothelial markers

The inflammation markers ICAM-1 and VAP-1 (Fig. 2-6) were found to be overexpressed in all conditions, except for the condition of coculture of LX-2, hepatocytes and HUVECs (Fig. 2-6A, I). Especially, the condition of monoculture of HUVECs (Fig. 2-6D, L) exhibited the highest expression of those markers. The expression of the liver vascular endothelial marker Stabilin-1 followed an inverse tendency (Fig. 2-7). In all conditions except the condition of coculture of LX-2, hepatocytes and HUVECs, only clusters of expression could be observed (Fig. 2-7 B, C, D). In the most complete coculture condition, a clear

expression of Stabilin-1 could be observed on the membrane of the cells (Fig. 2-7 A). The lymphatic endothelial marker LYVE-1 was weakly or simply not detected in all conditions of culture (Fig. 2-8). To summarize, the complete coculture model exhibited a more mature liver vascular endothelial phenotype, which was found to be less inflamed compared to monoculture of HUVECs. In addition, in all conditions, the HUVECs did not derive toward a lymphatic endothelial phenotype.

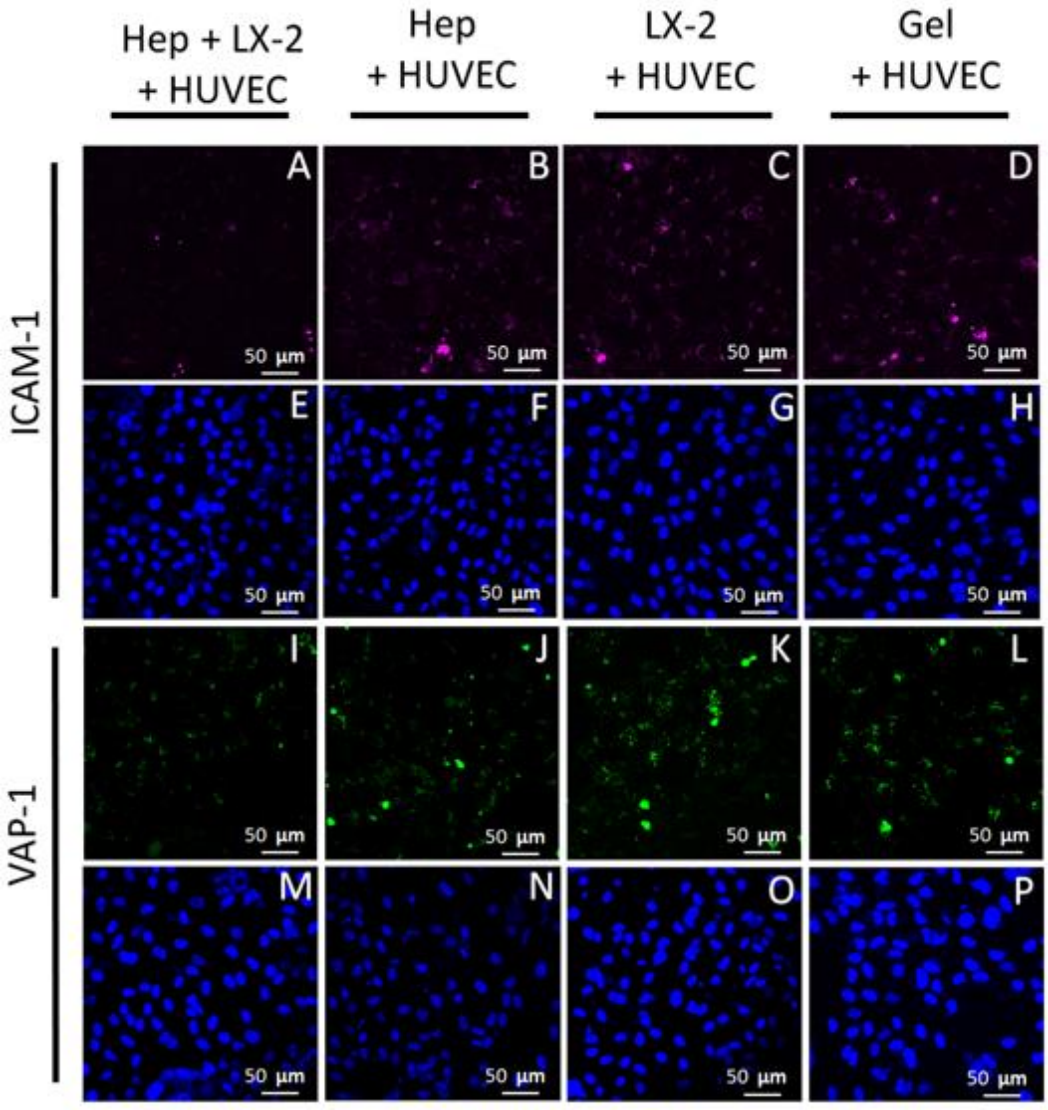

Fig. 2-6: Immunostaining of ICAM-1 (Magenta, A-D), DAPI (Blue, E-H) (Day 6) and of VAP-1 (Green, I-L), DAPI (Blue, M-P) (Day 6) obtained by confocal imaging.

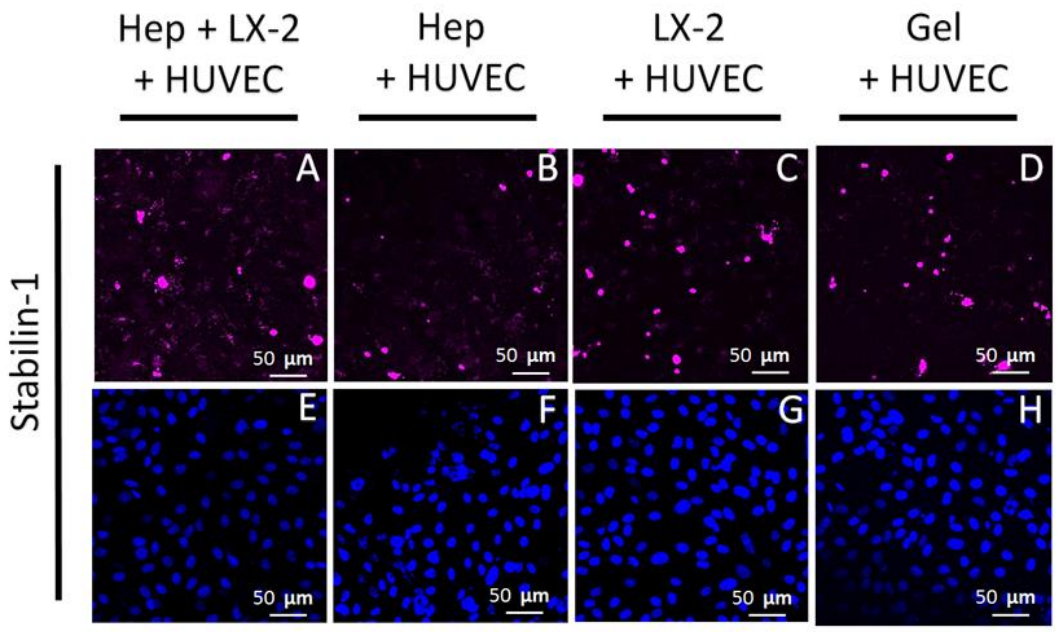

Fig. 2-7: Immunostaining of Stabilin-1 (Magenta, A-D) and DAPI (Blue, E-H) (Day 6) obtained by confocal imaging.

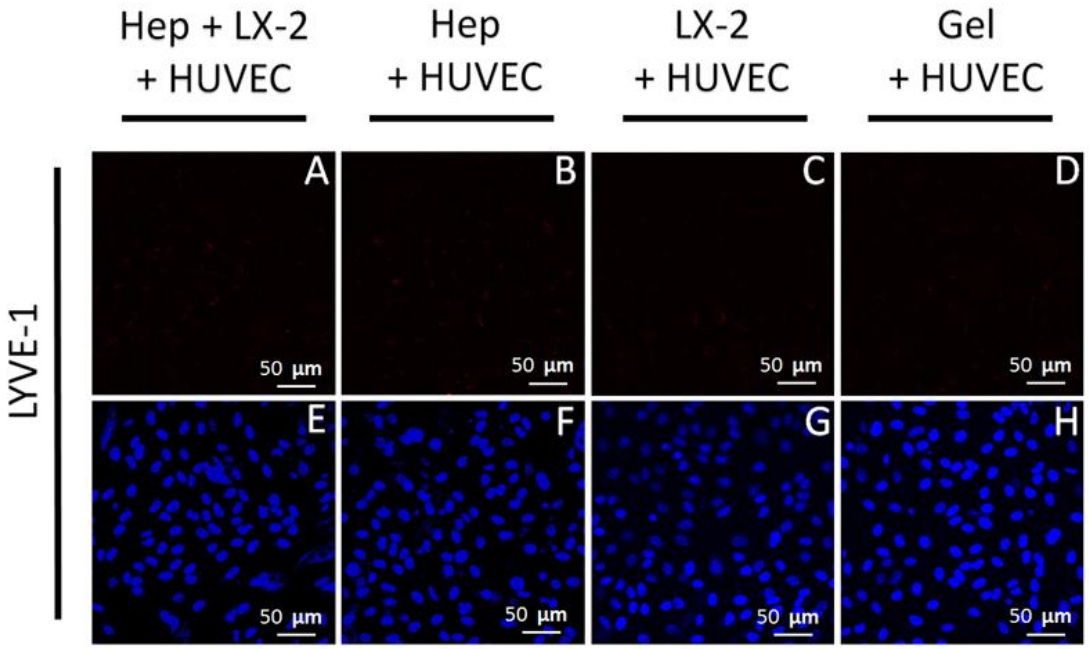

Fig. 2-8: Immunostaining of LYVE-1 (Red, A-D) and DAPI (Blue, E-H) (Day 6) obtained by confocal imaging.

2.4.5 Inflammatory stimulation with TNF-α

To simulate inflammatory events, the cytokine TNF-α was added to the culture as its effect on HUVECs, has been demonstrated [40,41]. To monitor the inflammatory response, the expression of ICAM-1 was observed in the monoculture of HUVEC and the coculture of HUVEC, LX-2 and hepatocytes. Both conditions exhibited a strong upregulation of ICAM-1 expression compared to the non-stimulated conditions (Fig. 2-9B, D). Yet, the inflammatory response was found to be significantly higher in monoculture (Fig. 2-9D) compared to the coculture condition (Fig. 2-9B). Regarding the MiaPaCa-2 cell adhesion, no change of adhesion percentage was observed in the coculture condition. In the monoculture of HUVECs, the adhesion percentage drastically raised after stimulation with TNF-α (Fig. 2-10). Those results emphasize that in coculture, the inflammation was either downregulated or countered and that the system was kept in a normal state with the help of the supportive cells.

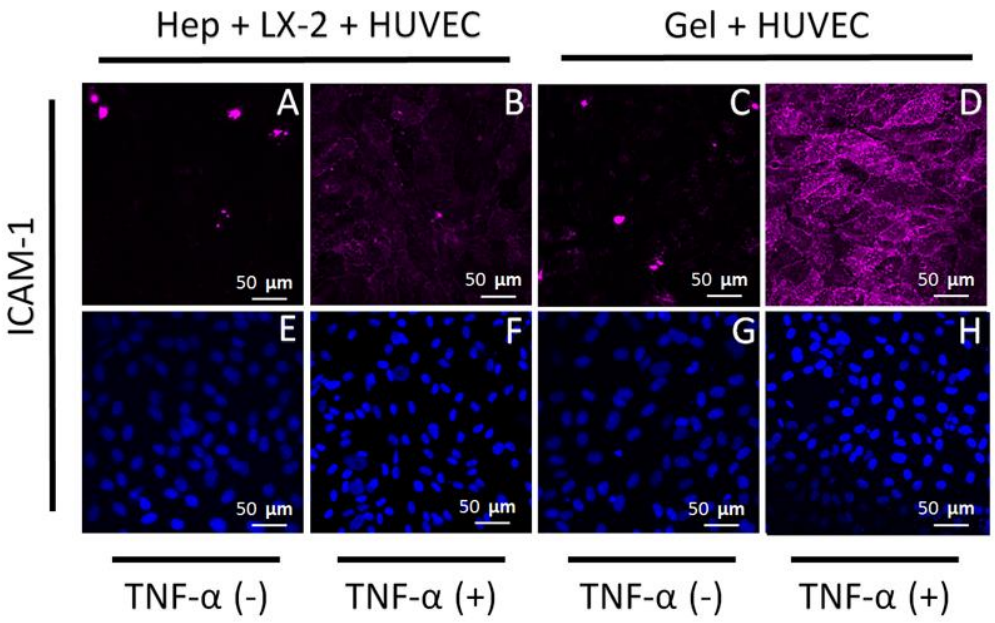

Fig. 2-9: Immunostaining of ICAM-1 (Magenta, A-D) and DAPI (Blue, E-H) (Day 6) obtained by confocal imaging after TNF-α stimulation.

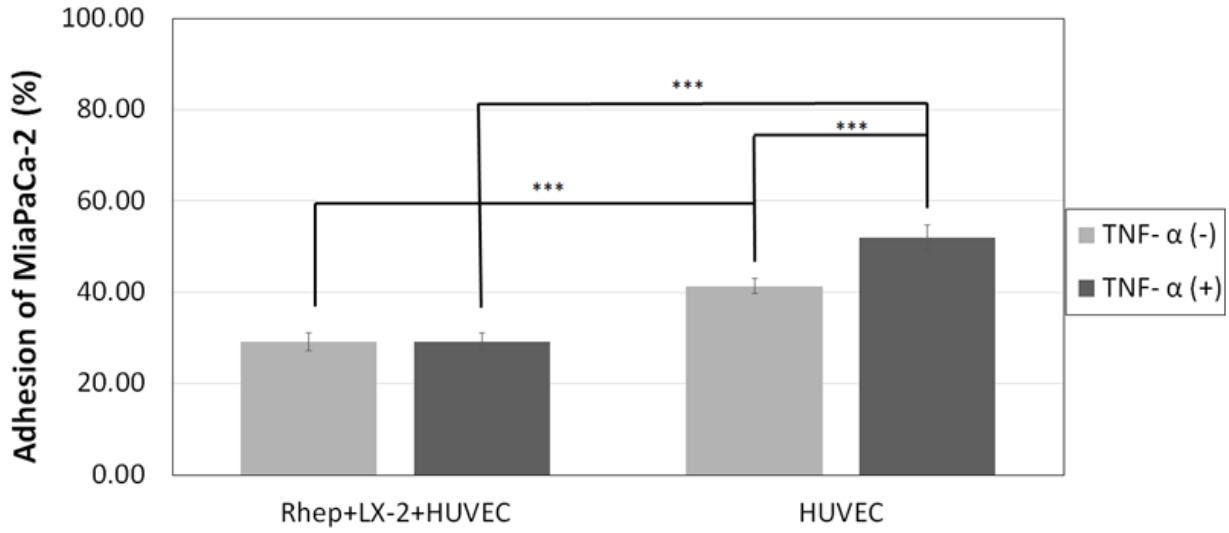

Fig. 2-10: Adhesion of MiaPaCa-2 in the different culture conditions with or without TNF-α stimulation. Data represents the mean ± SE, Differences with $P < 0.05$ (*), $P < 0.01$ (**) and $P < 0.001$ (***) were considered to be significantly, highly or extremely different. Data are issued from 3 independents experiments.

2.4.6 Immune status of the culture

The immune status of the culture was assessed by quantifying the adhesion of the promyeloblastic cells line HL60 in all the different previous conditions (Fig. 2-11A) and, in addition, under simulation with TNF-α in monoculture of HUVECs and in coculture of HUVECs, LX-2 and hepatocytes (Fig. 2-11B). The adhesion percentage was found to be the highest in the condition of monoculture of HUVECS and to decrease with the increase of the complexity of the culture, to finally be the lowest in the HUVECs, LX-2 and hepatocytes coculture condition. The addition of hepatocytes was found to have a strong influence on the adhesion of HL60. LX-2 had a significant influence on the adhesion only when also cocultured with hepatocytes. The stimulation with TNF-α increased the adhesion of HL-60 in both the HUVECs monoculture condition and in the HUVECs, LX-2 and hepatocytes coculture

condition. However, the inflammatory response was still higher in monoculture compared to the coculture condition, indicating a difference in the immune status of the model in both conditions.

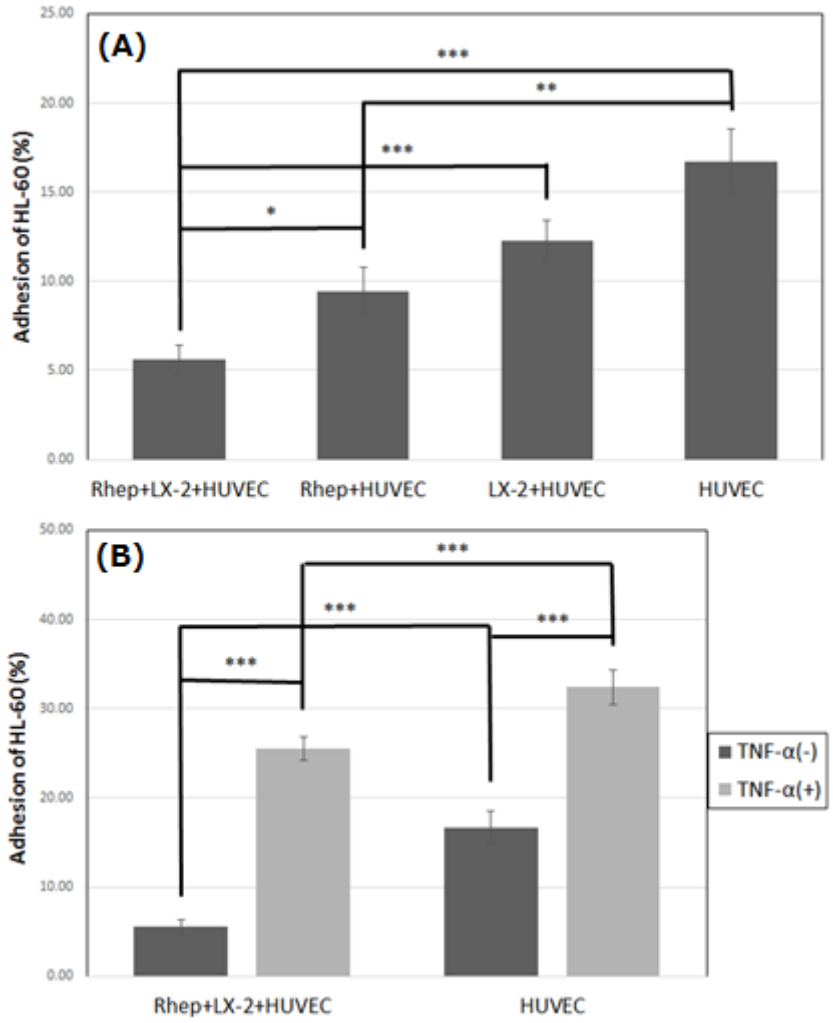

Fig. 2-11: Adhesion of HL-60 in the different culture conditions with or without TNF-α stimulation. Data represents the mean ± SE, Differences with $P < 0.05$ (*), $P < 0.01$ (**) and $P < 0.001$ (***) were considered to be significantly, highly or extremely different. Data are issued from 3 independents experiments.

2.5 Discussion

Motivated by the demand from industrials and clinicians, continued efforts have been made in order to develop a reliable *in-vitro* model for cancer cells extravasation. The established models are yet to be a reliable representation of the *in-vivo* situation as they lack in terms of complexity and depiction of the physical and cellular microenvironment of extravasation [6,7,8]. Still, those features are closely related to the maintenance of the endothelial barrier's phenotype [44] and its interactions during cancer cells extravasation [45]. Our model took into account both of those by coculturing the endothelial cells with both LX-2 and hepatocytes and by reproducing the *in-vivo* hierarchical structure of the liver microvasculature. In this thick coculture model, the oxygenation on the bottom layers was possible by culturing on a PDMS oxygen permeable membrane. Indeed, direct oxygenation has been showed to be of importance for the maintenance of the hepatic phenotype [18] as well as the reproduction of the cellular microenvironment [46]. Direct oxygenation is further necessary in our model as the hepatocytes bottom cell layer is separated from the culture medium by a thick collagen gel layer with LX-2 embedded and a HUVECs monolayer. The production of albumin (Fig. 2-3), a good marker of hepatic function, supported this hypothesis as it could be maintained only the conditions of culture of the PDMS membrane, indicating that the function of the hepatocytes was maintained [42,43].

While culturing on PDMS, it was also possible to observe that the production of albumin was increased in coculture with LX-2 and hepatocytes. Previous studies [18,23] gave similar results and showed that the coculture with non-parenchymal cells on PDMS improved the maintenance of the function of freshly harvested hepatocytes over long periods. Furthermore, the VEGF produced by the hepatocytes was found to be consumed by HUVECs in coculture, highlighting interactions between the two types of cells. Especially, VEGF is known to have important effect on the endothelium in terms of permeability [47,48] and in its

interactions with cancer cells [49,50]. Those measurements especially highlight the complicated interactions and relations between endothelial cells and hepatocytes and motivate furthermore their coculture in our model.

The benefits of coculture of hepatic cells in 3D on the phenotype of both hepatocytes and endothelial cells has been proved [51]. The immunostaining performed on our model indicated that the HUVECs tended toward a mature vascular endothelial phenotype in coculture with hepatocytes and LX-2 (Fig. 2-7, 2-8). Especially, cross-talk between pericytes and hepatocytes has been highlighted [52] but the need of the coculture of at least three different types of cells and the cross-talking between them was emphasized by the fact that the different markers of inflammation were notably downregulated only in the coculture of hepatocytes, LX-2 and HUVECs (Fig.2-6). The inflammation markers that were used, ICAM-1 and VAP-1, are both involved in either the adhesion or the migration of cancer cells [39,53,54]. ICAM-1 is specially known to be expressed as a response to TNF-α stimulation of HUVECs. In our model, the expression of ICAM-1 after stimulation was found to be drastically lower in coculture compared to the monoculture of HUVECs which preliminary indicates that the inflammation could be reduced after stimulation by the coculture of different cells with HUVECs.

In coculture of hepatocytes, LX-2 and HUVECs, it was also found that the adhesion of both the pancreatic carcinoma cells MiaPaCa-2 and the promyeloblastic cells line HL-60 were lowered compared to the condition of monoculture of HUVECs (Fig.2-5, 2-11A). Those results are well correlated with the ones obtained from the immunostaining as both of those cells adhere less on a mature and less inflamed endothelium [2,3,4]. Indeed, it was found in our model that the HUVECS, which are by definition, immature and not originated from the liver, matured toward a liver vascular endothelial phenotype, less inflamed, contrasting with previous research in our lab with liver sinusoids endothelial cells lines [55] which stayed in an inflamed state. Moreover, after stimulation with TNF-α, the results of the adhesion of both MiaPaCa-2 and

HL-60 were well associated with the immunostaining for ICAM-1 especially as the adhesion pathway of HL-60 is known to be using ICAM-1. Our model indeed exhibited an *in-vivo* like autoregulation of the inflammation after stimulation while still being able to go from a healthy condition to a disease condition. Those characteristics, both reflected in terms of surface markers and cellular adhesion allow it to be a model of choice in the study of the adhesion of cancer cells and its regulation mechanism.

While the coculture model of the three cell types exhibited several advantages such as the preservation and enhancement of the function of both hepatocytes and HUVECs, the inflammation auto-regulation mechanism observed, only when the three types of cells were cocultured is previously unpublished. Previous models did not feature this function and did not represent completely the *in-vivo* situation [9,10,11,12,13,18,19]. This mechanism could be explained by the fact that, in coculture, the interaction between pericytes and hepatocytes lead to the production of hepatocytes growth factor [52]. This molecule is known to have an anti-inflammatory effect, especially on HUVECs [56,57] and could be the reason why the co-culture condition was capable to limit the inflammatory response to TNF-α.

2.6 Conclusion

In this chapter, we established a hierarchical coculture model of the liver microvasculature including hepatocytes, pericytes and endothelial cells. The needs of the model in term of oxygenation could be reach by using custom-designed PDMS well-plate. Both the immunostaining for several markers and the adhesion of different types of cells indicated that the endothelial layer tended toward a less inflamed and more mature liver vascular endothelial phenotype. Such a complete model was yet to be described in the literature and its characterization, including immune status could be confirmed with the quantification of the

adhesion of HL60. Moreover, the model could be activated by using the inflammatory cytokine TNF-α and a new inflammation auto-regulation mechanism could be observed.

The present model exhibited new characteristics that had not been illustrated in the literature yet. It is relatively simple to use and is compatible with the current format of high-throughput screening used in the industry. The present results demonstrate the advantages and the necessity of the coculture of different cell types in a mimicking cellular microenvironment to study truthfully the adhesion of cancer cells and their extravasation. While it can be considered to be one of the closest reproduction of the physical and physiological situation of the liver microvasculature, some points of improvement yet remain. The model still lacks many function of the liver that are necessary for a complete representation. It does not include immune cells which are directly involved in the regulation of inflammation of the endothelial layer and thus, in the adhesion of cancer cells. The biliary network, necessary for the transport of the bile produce by the hepatocytes is not represented either while being an important challenge of liver tissue engineering. Finally, the blood flow and shear stress to which the endothelial and cancer cells are submitted during the adhesion and extravasation process are also not reproduced. We will discuss the reproduction of this phenomenon in the next chapter by using a microfluidic biochip.

References

[1] Jeon, J. S., Bersini, S., Gilardi, M., Dubini, G., Charest, J. L., Moretti, M., & Kamm, R. D. (2015). Human 3D vascularized organotypic microfluidic assays to study breast cancer cell extravasation. *Proceedings of the National Academy of Sciences*, *112*(1), 214-219.

[2] Ley, K., Laudanna, C., Cybulsky, M. I., & Nourshargh, S. (2007). Getting to the site of inflammation: the leukocyte adhesion cascade updated. *Nature Reviews Immunology*, *7*(9), 678-689.

[3] Carlos, T. M., & Harlan, J. M. (1994). Leukocyte-endothelial adhesion molecules. *Blood*, *84*(7), 2068-2101.

[4] Coussens, L. M., & Werb, Z. (2002). Inflammation and cancer. *Nature*,*420*(6917), 860-867.

[5] Ebos, J. M., Lee, C. R., Cruz-Munoz, W., Bjarnason, G. A., Christensen, J. G., & Kerbel, R. S. (2009). Accelerated metastasis after short-term treatment with a potent inhibitor of tumor angiogenesis. *Cancer cell*, *15*(3), 232-239.

[6] Olive, K. P., Jacobetz, M. A., Davidson, C. J., Gopinathan, A., McIntyre, D., Honess, D., ... & Frese, K. K. (2009). Inhibition of Hedgehog signaling enhances delivery of chemotherapy in a mouse model of pancreatic cancer.*Science*, *324*(5933), 1457-1461.

[7] White, R. E. (2000). High-throughput screening in drug metabolism and pharmacokinetic support of drug discovery. *Annual review of pharmacology and toxicology*, *40*(1), 133-157.

[8] Bersini, S., Jeon, J. S., Dubini, G., Arrigoni, C., Chung, S., Charest, J. L., ... & Kamm, R. D. (2014). A microfluidic 3D in vitro model for specificity of breast cancer metastasis to bone. *Biomaterials*, *35*(8), 2454-2461.

[9] Jeon, J. S., Zervantonakis, I. K., Chung, S., Kamm, R. D., & Charest, J. L. (2013). In vitro model of tumor cell extravasation. *PloS one*, *8*(2), e56910.

[10] Xu, X., Farach-Carson, M. C., & Jia, X. (2014). Three-dimensional in vitro tumor models for cancer research and drug evaluation. *Biotechnology advances*,*32*(7), 1256-1268.

[11] Kimlin, L. C., Casagrande, G., & Virador, V. M. (2013). In vitro three-dimensional (3D) models in cancer research: An update. *Molecular carcinogenesis*, *52*(3), 167-182.

[12] Kim, Y., Larkin, A. L., Davis, R. M., & Rajagopalan, P. (2010). The design of in vitro liver sinusoid mimics using chitosan–hyaluronic acid polyelectrolyte multilayers. *Tissue Engineering Part A*, *16*(9), 2731-2741.

[13] Rajagopalan, P., Shen, C. J., Berthiaume, F., Tilles, A. W., Toner, M., & Yarmush, M. L. (2006). Polyelectrolyte nano-scaffolds for the design of layered cellular architectures. *Tissue engineering*, *12*(6), 1553-1563.

[14] Cooley, L. S., Handsley, M. M., Zhou, Z., Lafleur, M. A., Pennington, C. J., Thompson, E. W., ... & Edwards, D. R. (2010). Reversible transdifferentiation of blood vascular endothelial cells to a lymphatic-like phenotype in vitro. *Journal of cell science*, *123*(21), 3808-3816.

[15] Chen, M. B., Whisler, J. A., Jeon, J. S., & Kamm, R. D. (2013). Mechanisms of tumor cell extravasation in an in vitro microvascular network platform.*Integrative Biology*, *5*(10), 1262-1271.

[16] Shimaoka, S., Nakamura, T., & Ichihara, A. (1987). Stimulation of growth of primary cultured adult rat hepatocytes without growth factors by coculture with nonparenchymal liver cells. *Experimental cell research*, *172*(1), 228-242.

[17] Seo, S. J., Kim, I. Y., Choi, Y. J., Akaike, T., & Cho, C. S. (2006). Enhanced liver functions of hepatocytes cocultured with NIH 3T3 in the alginate/galactosylated chitosan scaffold. *Biomaterials*, *27*(8), 1487-1495.

[18] Xiao, W., Perry, G., Komori, K., & Sakai, Y. (2015). New physiologically-relevant liver tissue model based on hierarchically cocultured primary rat hepatocytes with liver endothelial cells. *Integrative Biology*, *7*(11), 1412-1422.

[19] Armulik, A., Abramsson, A., & Betsholtz, C. (2005). Endothelial/pericyte interactions. *Circulation research*, *97*(6), 512-523.

[20] Bussolino, F., Di Renzo, M. F., Ziche, M., Bocchietto, E., Olivero, M., Naldini, L., ... & Comoglio, P. M. (1992). Hepatocyte growth factor is a potent angiogenic factor which stimulates endothelial cell motility and growth. *The Journal of cell biology*, *119*(3), 629-641.

[21] Clayton, D. F., Harrelson, A. L., & Darnell, J. E. (1985). Dependence of liver-specific transcription on tissue organization. *Molecular and cellular biology*,*5*(10), 2623-2632.

[22] Stevens, K. M. (1965). Oxygen requirements for liver cells in vitro.

[23] Xiao, W., Kodama, M., Komori, K., & Sakai, Y. (2014). Oxygen-permeable membrane-based direct oxygenation remarkably enhances functions and gene expressions of rat hepatocytes in both 3D and sandwich cultures. *Biochemical Engineering Journal*, *91*, 99-109.

[24] Xiao, W., Shinohara, M., Komori, K., Sakai, Y., Matsui, H., & Osada, T. (2014). The importance of physiological oxygen concentrations in the sandwich cultures of rat hepatocytes on gas-permeable membranes. *Biotechnology progress*,30(6), 1401-1410.

[25] Yamada, M., Blaner, W. S., Soprano, D. R., Dixon, J. L., Kjeldbye, H. M., & Goodman, D. S. (1987). Biochemical characteristics of isolated rat liver stellate cells. *Hepatology*, *7*(6), 1224-1229.

[26] Xu, L., Hui, A. Y., Albanis, E., Arthur, M. J., O'Byrne, S. M., Blaner, W. S., ... & Eng, F. J. (2005). Human hepatic stellate cell lines, LX-1 and LX-2: new tools for analysis of hepatic fibrosis. *Gut*, 54(1), 142-151.

[27] Lalor, P. F., Lai, W. K., Curbishley, S. M., Shetty, S., & Adams, D. H. (2006). Human hepatic sinusoidal endothelial cells can be distinguished by expression of phenotypic markers related to their specialised functions in vivo. *World Journal of Gastroenterology*, 12(34), 5429.

[28] Kurkijärvi, R., Adams, D. H., Leino, R., Möttönen, T., Jalkanen, S., & Salmi, M. (1998). Circulating form of human vascular adhesion protein-1 (VAP-1): increased serum levels in inflammatory liver diseases. *The Journal of Immunology*, 161(3), 1549-1557.

[29] Daneker, G. W., Lund, S. A., Caughman, S. W., Swerlick, R. A., Fischer, A. H., Staley, C. A., & Ades, E. W. (1998). Culture and characterization of sinusoidal endothelial cells isolated from human liver. *In Vitro Cellular & Developmental Biology-Animal*, 34(5), 370-377.

[30] Auguste, P., Fallavollita, L., Wang, N., Burnier, J., Bikfalvi, A., & Brodt, P. (2007). The host inflammatory response promotes liver metastasis by increasing tumor cell arrest and extravasation. *The American journal of pathology*, 170(5), 1781-1792.

[31] Géraud, C., Schledzewski, K., Demory, A., Klein, D., Kaus, M., Peyre, F., ... & Goerdt, S. (2010). Liver sinusoidal endothelium: A microenvironment-dependent

differentiation program in rat including the novel junctional protein liver endothelial differentiation-associated protein-1. *Hepatology, 52(1), 313-326.*

[32] Arimoto, J., Ikura, Y., Suekane, T., Nakagawa, M., Kitabayashi, C., Iwasa, Y., ... & Ueda, M. (2010). Expression of LYVE-1 in sinusoidal endothelium is reduced in chronically inflamed human livers. *Journal of gastroenterology*, *45*(3), 317-325.

[33] Seglen PO. Preparation of isolated rat liver cells. In: Prescott DM, editor. *Methods in Cell Biology. London: Elsevier Inc*.; 1976:29–83.

[34] H.T.Atmaca,A.N.Gazyagcı,S.Canpolat,andO.Kul, Hepatic stellate cells increase in Toxoplasma gondii infection in mice, *Parasites & Vectors*, vol. 6, no. 1, p. 135, 2013.

[35] Douglass, H. O., & Penetrante, R. B. (1990). Pancreatic cancer why patients die. *International Journal of* confirmed *Gastrointestinal Cancer*, 7(1), 135-140.

[36] McIntyre, L. J., Kleinman, H. K., Martin, G. R., & Kim, Y. S. (1981). Attachment of human pancreatic tumor cell lines to collagen in vitro. *Cancer research*, 41(9 Part 1), 3296-3299.

[37] Fox, C. H., Johnson, F. B., Whiting, J., & Roller, P. P. (1985). Formaldehyde fixation. *J histochem Cytochem*, 33(8), 845-853.

[38] Croce, A. C., Ferrigno, A., Vairetti, M., Bertone, R., Freitas, I., & Bottiroli, G. (2004). Autofluorescence properties of isolated rat hepatocytes under different metabolic conditions. *Photochemical & Photobiological Sciences*, 3(10), 920-926.

[39] Manos, P. D., Ratanasirintrawoot, S., Loewer, S., Daley, G. Q., & Schlaeger, T. M. (2011). Live-Cell Immunofluorescence Staining of Human Pluripotent Stem Cells. *Current protocols in stem cell biology*, 1C-12.

[40] Modur, V., Zimmerman, G. A., Prescott, S. M., & McIntyre, T. M. (1996). Endothelial Cell Inflammatory Responses to Tumor Necrosis Factor α CERAMIDE-DEPENDENT AND-INDEPENDENT MITOGEN-ACTIVATED PROTEIN KINASE CASCADES. *Journal of Biological Chemistry*, 271(22), 13094-13102.

[41] Mackay, F., Loetscher, H., Stueber, D., Gehr, G., & Lesslauer, W. (1993). Tumor necrosis factor α (TNF-α)-induced cell adhesion to human endothelial cells is under dominant control of one TNF receptor type, TNF-R55. *The Journal of experimental medicine*, 177(5), 1277-1286.

[42] Selden, C., Khalil, M., & Hodgson, H. J. F. (1999). What keeps hepatocytes on the straight and narrow? Maintaining differentiated function in the liver. *Gut*, 44(4), 443-446.

[43] Miller, L. L., Bly, C. G., Watson, M. L., & Bale, W. F. (1951). THE DOMINANT ROLE OF THE LIVER IN PLASMA PROTEIN SYNTHESIS A DIRECT STUDY OF THE ISOLATED PERFUSED RAT LIVER WITH THE AID OF LYSINE-ϵ-C14. *The Journal of experimental medicine*, 94(5), 431-453.

[44] DeLeve, L. D., Wang, X., Hu, L., McCuskey, M. K., & McCuskey, R. S. (2004). Rat liver sinusoidal endothelial cell phenotype is maintained by paracrine and autocrine regulation. *American Journal of Physiology-Gastrointestinal and Liver Physiology*, *287*(4), G757-G763.

[45] Wirtz, D., Konstantopoulos, K., & Searson, P. C. (2011). The physics of cancer: the role of physical interactions and mechanical forces in metastasis. *Nature Reviews Cancer*, *11*(7), 512-522.

[46] Bale, S. S., Golberg, I., Jindal, R., McCarty, W. J., Luitje, M., Hegde, M., ... & Yarmush, M. L. (2014). Long-term coculture strategies for primary hepatocytes and liver sinusoidal endothelial cells. *Tissue Engineering Part C: Methods*,*21*(4), 413-422.

[47] Hippenstiel, S., Krüll, M., Ikemann, A., Risau, W., Clauss, M., & Suttorp, N. (1998). VEGF induces hyperpermeability by a direct action on endothelial cells. *American Journal of Physiology-Lung Cellular and Molecular Physiology*, 274(5), L678-L684.

[48] Esser, S., Lampugnani, M. G., Corada, M., Dejana, E., & Risau, W. (1998). Vascular endothelial growth factor induces VE-cadherin tyrosine phosphorylation in endothelial cells. *Journal of cell science*, 111(13), 1853-1865.

[49] Weis, S., Cui, J., Barnes, L., & Cheresh, D. (2004). Endothelial barrier disruption by VEGF-mediated Src activity potentiates tumor cell extravasation and metastasis. *The Journal of cell biology*, *167*(2), 223-229.

[50] JuanYin, J., Tracy, K., Zhang, L., Munasinghe, J., Shapiro, E., Koretsky, A., & Kelly, K. (2009). Noninvasive imaging of the functional effects of anti-VEGF therapy on tumor cell extravasation and regional blood volume in an experimental brain metastasis model. *Clinical & experimental metastasis*, *26*(5), 403-414.

[51] Kim, Y., & Rajagopalan, P. (2010). 3D hepatic cultures simultaneously maintain primary hepatocyte and liver sinusoidal endothelial cell phenotypes. *PloS one*,*5*(11), e15456.

[52] Skrtic, S., Wallenius, V., Ekberg, S., Brenzel, A., Gressner, A. M., & Jansson, J. O. (1999). Hepatocyte-stimulated expression of hepatocyte growth factor (HGF) in cultured rat hepatic stellate cells. *Journal of hepatology*, 30(1), 115-124.

[53] Irjala, H., Alanen, K., Grénman, R., Heikkilä, P., Joensuu, H., & Jalkanen, S. (2003). Mannose receptor (MR) and common lymphatic endothelial and vascular endothelial receptor (CLEVER)-1 direct the binding of cancer cells to the lymph vessel endothelium. *Cancer research*, 63(15), 4671-4676.

[54] Maula, S. M., Luukkaa, M., Grénman, R., Jackson, D., Jalkanen, S., & Ristamäki, R. (2003). Intratumoral lymphatics are essential for the metastatic spread and prognosis in

squamous cell carcinomas of the head and neck region. *Cancer research*, 63(8), 1920-1926.

[55] Chowdhury, M. M., Danoy, M., Rahman, F., Shinohara, M., Kaneda, S., Shiba, K., ... & Sakai, Y. (2014). Adhesion of Pancreatic Cancer Cells in a Liver-Microvasculature Mimicking Coculture Correlates with Their Propensity to Form Liver-Specific Metastasis In Vivo. *BioMed research international*, *2014*.

[56] Van Buul, J. D., Allingham, M. J., Samson, T., Meller, J., Boulter, E., García-Mata, R., & Burridge, K. (2007). RhoG regulates endothelial apical cup assembly downstream from ICAM1 engagement and is involved in leukocyte trans-endothelial migration. *The Journal of cell biology*, *178*(7), 1279-1293.

[57] Gong, R., Rifai, A., & Dworkin, L. D. (2006). Anti-inflammatory effect of hepatocyte growth factor in chronic kidney disease: targeting the inflamed vascular endothelium. *Journal of the American Society of Nephrology*, 17(9), 2464-2473.

[58] Gong, R., Rifai, A., & Dworkin, L. D. (2006). Hepatocyte growth factor suppresses acute renal inflammation by inhibition of endothelial E-selectin. *Kidney international*, 69(7), 1166-1174.

Supplementary Information

Preliminary trials performed with other cells types

Before the establishment of the definitive model, different types of cells have been tested in coculture with LX-2. In our experiments, both experiments with models including HepG2 cells and TMNK-1 cells have been performed. The HepG2 cells line is a hepatocellular carcinoma and is widely used in drug screening in replacement of hepatocytes. The TMNK-1 cells line is an immortalized liver sinusoids endothelial cells line which present *in-vivo*-like features such as fenestration.

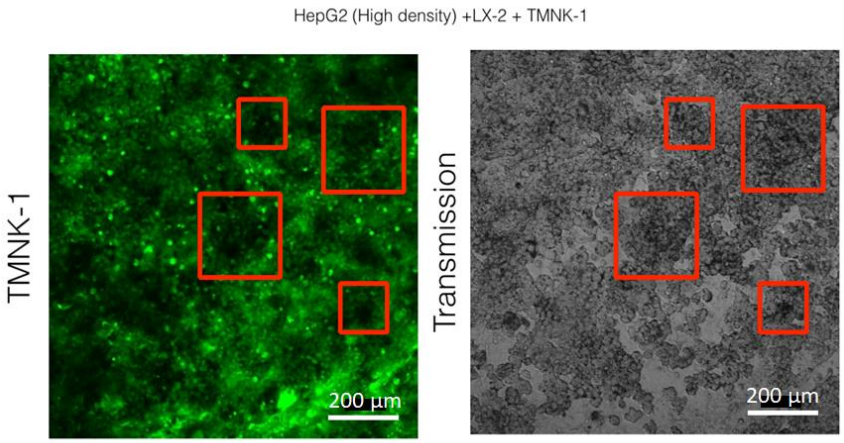

Fig. 2-12: Confocal imaging of Celltracker stained TMNK-1 on Day6 in coculture with HepG2 and LX-2. Highlighted in red are zones in which the green stained TMNK-1 could not be detected while darker cells (HepG2) in the transmission image were observed at the same position.

In the case of coculture of HepG2 with LX-2 and TMNK-1, the HepG2 were found to be migrating toward the top of the culture and by consequence, to breach through the endothelial cells layer (Fig. 2-12). As a direct consequence, the quantification of the

interactions of the adhering cancer cells with the endothelial layer would not be possible as the later would be a mix of endothelial cells and HepG2. Those results motivated the change toward rat hepatocytes which were suitable as previously explained. In the resulting experiment, the TMNK-1 failed to form a complete monolayer over collagen gel in coculture with both or either LX-2 and rat hepatocytes and in monoculture over collagen gel (Fig. 2-13). Additionally, when compared to HUVECs, which are considered to be the golden standard in vascular research, TMNK-1 exhibited a very uneven and leaky structure in monoculture over collagen gel as shown by staining of actin (Fig. 2-14). While HUVECs are actually not liver sinusoids endothelial cells, their usage was deemed preferable as they were able to form a complete monolayer over collagen gel, and thus, making them compatible with an inclusion in our model.

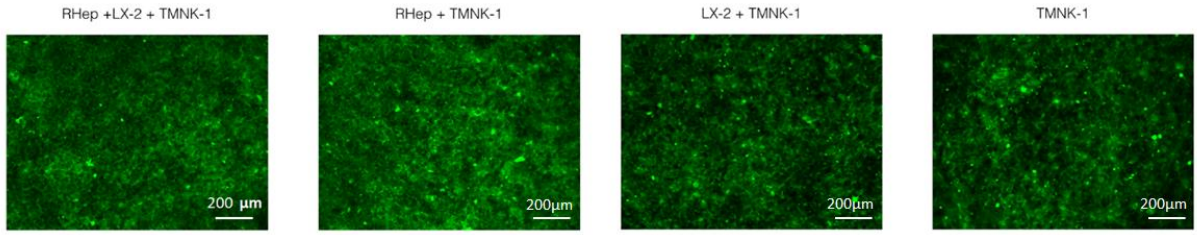

Fig. 2-13: Confocal imaging of Celltracker stained TMNK-1 on Day6 in different coculture conditions with HepG2, LX-2 or none.

Adhesion of different cell types in the model

In addition to the MiaPaCa-2 cells, the adhesion assay with different types of cells was performed in the coculture model. While the MiaPaCa-2, a carcinoma cells line is expected to be migrating to the liver, the migration of pancreatic cancer cells to the liver do not habitually use the lymphatic pathway. As a control, we performed the adhesion assay of BxPc-3, a pancreatic adenocarcinoma cells line in different conditions of the model (Fig. 2-15). Those cells are known to migrate to the liver using specifically the lymphatic pathway and not the

vascular one. Both the conditions of monoculture of HUVECs over collagen gel and of coculture of HUVECs, LX-2 and rat hepatocytes, did exhibit a lower adhesion (Around 17%) than the MiaPaCa-2 cells in all conditions (30% at the lowest). Moreover, no specific tendency of adhesion was observed in the conditions, confirming that the cells did not possibly differ to a lymphatic phenotype in those conditions.

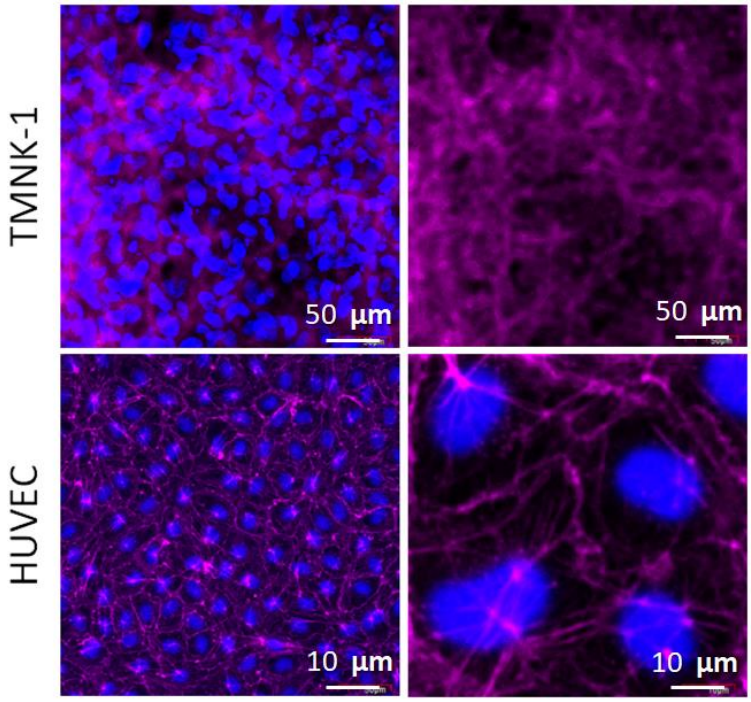

Fig. 2-14: Confocal imaging of actin stained TMNK-1 and HUVECs on Day6 in monoculture over collagen gel. While HUVECs formed an even monolayer, the TMNK-1 layer exhibited dense 3D aggregates and zone with fewer cells.

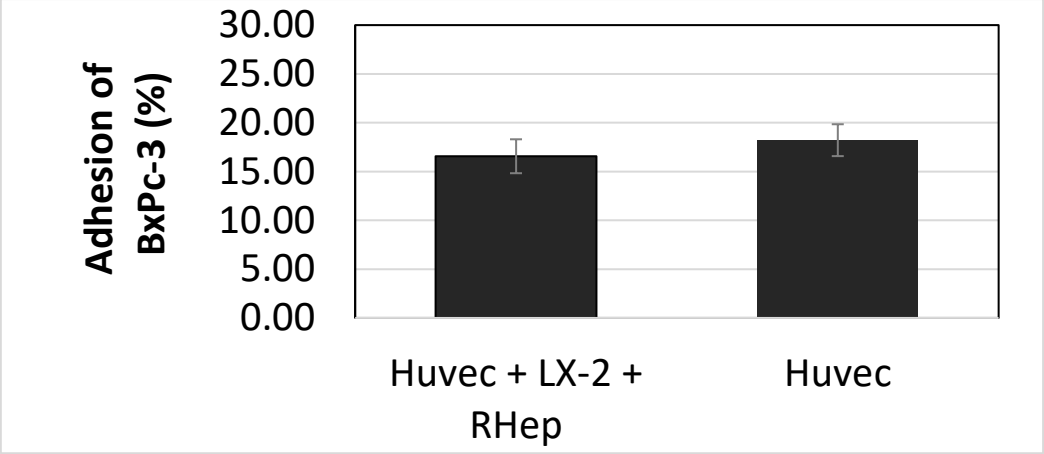

Fig. 2-15: Adhesion of BxPc-3 in the different culture conditions. Data represents the mean ± SE.

The quantification of the adhesion of THP-1 monocytic cells line, a type of leukocytes has also been performed. It was found that the addition of rat hepatocytes strongly reduced the adhesion of THP-1 while the effect of the addition of the LX-2 were neglectable. After stimulation with TNF-α, the adhesion of THP-1 was found to be strongly upregulated in both the condition of monoculture of HUVECs over collagen gel and in coculture of HUVECs, LX-2 and rat hepatocytes. Though, no significant difference in adhesion was found between the two conditions. The adhesion pathway of THP-1 is however quite unknown and the involvement of FAK (Focal adhesion kinase) still undefined. As the adhesion pathway of THP-1 could be not be linked to any of the markers that we had previously studied, no further investigations were made.

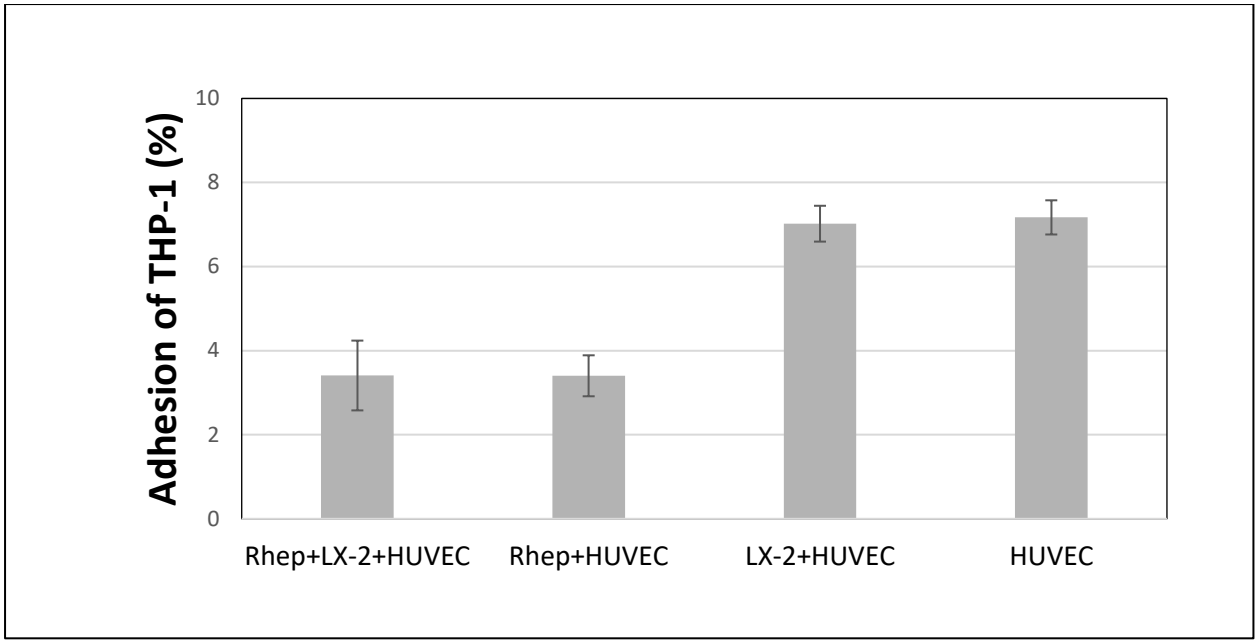

Fig. 2-16: Adhesion of THP-1 in the different culture conditions. Data represents the mean ± SE.

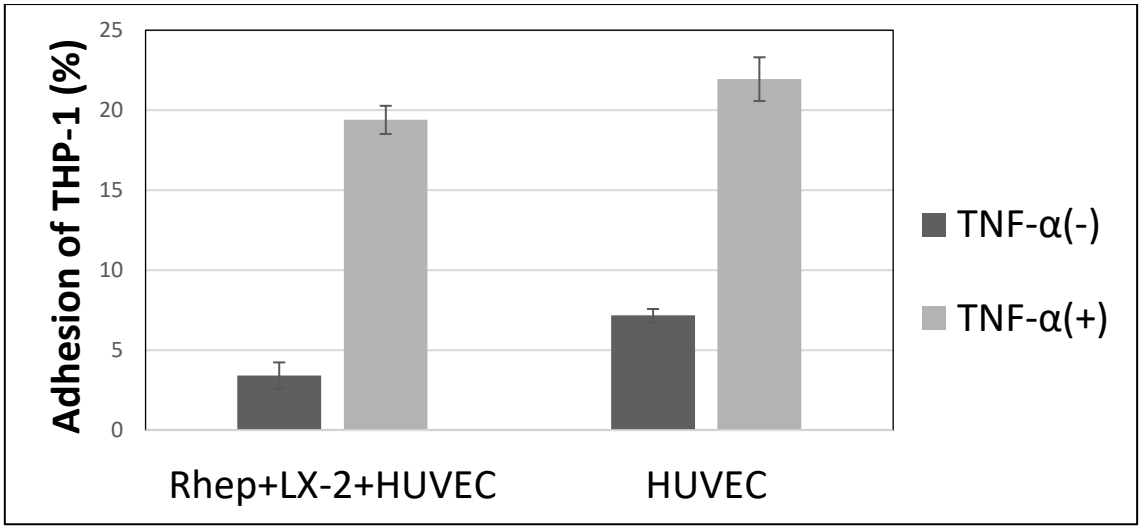

Fig. 2-17: Adhesion of THP-1 in the different culture conditions with or without TNF-α stimulation. Data represents the mean ± SE.

Cross-section and HE staining in the different culture conditions

HE (Hematoxylin and eosin) staining of cross-section samples is a widely used technique. Briefly, by using this technic, the cytoplasm of cells if stained pink and the nucleus dark purple. In our coculture model, cross-section and staining have been performed in the four previously described culture conditions. The observation by optical microscopy of the samples allowed to identify the notable shrinking of the collagen layer that motivated live immunostaining over immunostaining of paraformaldehyde-fixated samples. The staining also confirmed that complete monolayers of both hepatocytes and HUVECs were formed in all conditions. However, because of the relative weakness of the collagen layer when no hepatocytes are seeded as a bottom layer, no images with both the cell types in the LX-2 and HUVECs coculture conditions could be obtained.

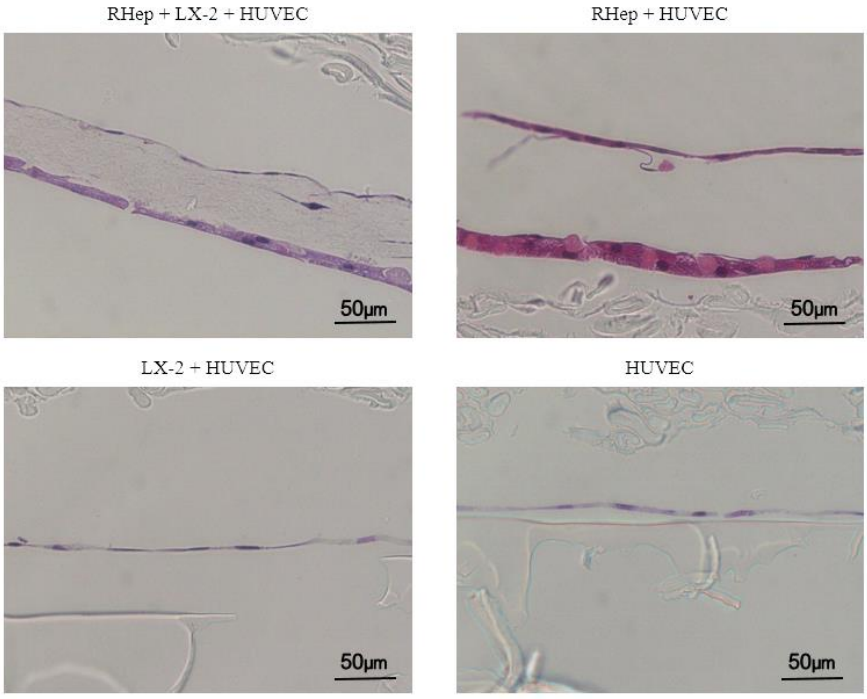

Fig. 2-18: Optical microscopy images of the cross-section of the indicated cultures conditions after HE staining.

Chapter 3

Modeling of the liver microvasculature in dynamic conditions by physiologically & physically-relevant coculture

3.1 Introduction

Despite significant medical advances, cancer is still an important topic of research for many researchers in the biology and the medical field. Indeed, cancer is the second leading cause of death in the United States and is likely to become the first in the near future [1]. Especially, cancer metastasis was found to be the cause in 90% of cancer-related deaths [2]. The metastatic process, which involves the migration of cancer cells from their original location, the primary site to a secondary site which can anatomically close or distant has been explained by several theories. However, the Soil & Seed theory described by Paget [3] over a century ago is the most admitted to explain the distribution pattern of metastatic cancer cells in different secondary sites [4]. The theory, hypothesized from clinical observations, describes the fact that cancer cells for a certain origin will have a higher tendency to migrate to specific organs and not to other. The cancer cells are then pictured as seeds that will be attracted to certain metastasis sites, the soil.

In the metastatic process, the step in which the cancer cells pass from the blood vessels to the secondary site is called extravasation. In many *in-vivo* models, the migration of injected or transplanted cancer cells into tissues could be observed [5-8]. Though, although the migration of the cancer cells can be easily studied by observation of animals after sacrifices [9-11] or by *in-vivo* fluorescence techniques [6-8], direct observation of the phenomenon is usually difficult. In addition to the difference between cancer in humans and in rodents and to the increasing regulations regarding animal experiments, the past decades have seen a strong development of *in-vitro* models. While those models are often incomplete compared to their *in-vivo* counterpart, they usually offer information on specific mechanisms that could not be completely elucidated in *in-vivo* models such as the interactions between blood vessels and tissues [12] and act as a complementary source of study regarding cancer metastasis.

A wide range of *in-vitro* models have been developed to study the migration of cancer cells. Popular models such as Boyden chamber assays [13-15] and the scratch assays [16] remain simple but have been improved over the years. To improve the physiological relevance of models, coculture of different cell types in one model has been done. Supportive cells have been used to influence the phenotype of endothelial cells notably in terms of inflammation [17] but most of the time, have been used to act as a chemoattractant to trigger the migration of cancer cells [18-19]. In the latter, microfluidic devices have been extensively developed and the migration of cells seeded in different channels toward each others could be observed. Microfluidic devices have also been used in vascular research to reproduce the *in-vivo* flow and shear stress to which endothelial cells are subjected [20]. More complex models have also been established in order to mimic a more complex vasculature and to observe cancer cells extravasation from vessels to extracellular matrix [21].

In chapter 2, we established a physiologically-relevant coculture model composed of hepatocytes, pericytes and endothelial cells which allowed to study the adhesion of pancreatic cancer cells and the response of the culture to inflammatory events. The model partially solved the lack of complexity of the previous *in-vitro* models by reproducing the hierarchical structure of the *in-vivo* liver microvasculature, composed of many different types of cells that interact with each other and especially with the space of Disse, containing hepatic stellate cells and acting as a scaffold for the vessels [22]. The model introduced in the chapter 2 is however still lacking compared to the *in-vivo* situation. It indeed does not include the physiological blood flow and shear stress to which the cells are subjected to. Moreover, direct observations of the pancreatic cancer cells interactions with the liver cells could not be observed and their adhesion could only be quantified. Those issues could be solved by the use of microfluidic devices, reproducing those phenomenon as well as other important characteristics of the liver such as the physiologically-relevant dimensions of the vasculature and chemical gradients.

3.2 Objectives

In this regard, we have reproduced the hierarchical structure of the liver microvasculature by coculturing hepatocytes, hepatic stellate cells and endothelial cells in a multichannel device including extracellular matrix to reproduce the space of Disse. To do so, a biochip where three parallel channels, separated by micropillars could be filled independently one from another was produced. Pericytes embedded in a hydrogel, hepatocytes and endothelial cells were successively injected in the middle, bottom and top channels respectively. Pancreatic cancer cells were then added in contact with endothelial cells in the top channel and let to adhere. Calcein staining in the different channels was performed after 10 days of culture to ensure the viability of all cells. Albumin measurements were made to monitor the function of the hepatocytes during the whole experiment. The movements of pancreatic cancer cells in the top channel were monitored in both the complete coculture model and in conditions with no pericyte and hepatocyte to evaluate their influence. In those conditions, the phenotype of hepatocytes and endothelial cells was also examined by immunodetection of albumin, intercellular adhesion molecule (ICAM-1) and vascular adhesion protein (VAP-1).

3.3 Material & Methods

3.3.1 Design and fabrication of the biochip for hierarchical coculture of the liver microvasculature

The microfluidic biochips were fabricated by molding polydimethylsiloxane (PDMS; Toray, Japan) onto micro-structured silicon. The molds were prepared using the conventional photolithography and plasma dry etching methods. The molded PDMS was then bound to a non-treated glass (Matsunami Glass Ind., Ltd, Osaka, Japan) slide by plasma treatment (YHS-GZA 200; Sakigake-Semiconductor, Japan). The design of the device was based on the principle of independent channels separated by micropillars previously illustrated [23]. Each of the three channels (3700 x 250 x 100 µm) were separated from each other by hexagonal micropillars of 100 µm width and spaced by 100 µm. Each of the channels was linked by an 850 µm long access channel to an inlet or an outlet to which PFTE tubing were attached (Fig. 3-1).

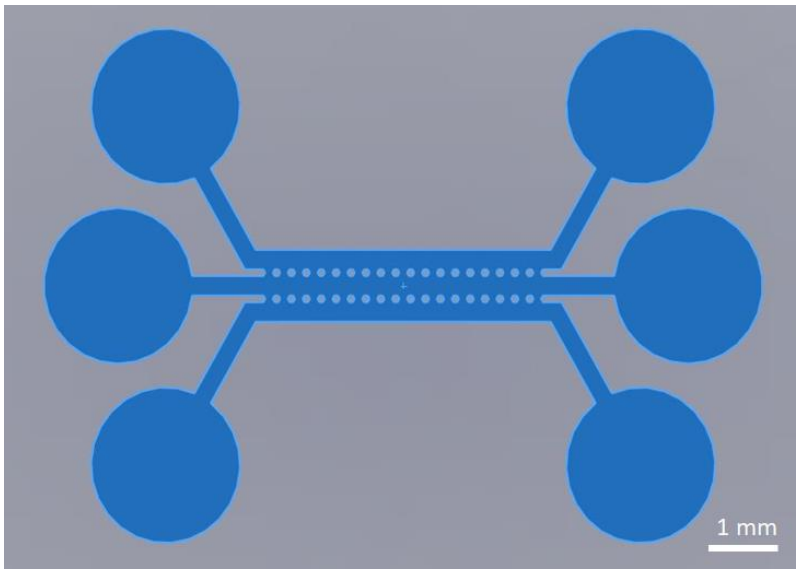

Fig. 3-1: Geometry of the microfluidic device with three channels: bottom for hepatocyte culture, center for pericytes in gel and top for endothelial cell culture and perfusion.

To determine the perfusion rate that would be necessary to mimic the physiological shear stress in the liver microvasculature, fluidic simulations were performed using Comsol Multiphysics (Comsol Inc., Stockholm, Sweden). It was found that at a 10 µL/min perfusion rate, the shear stress at the walls would be evaluated to 0.1 Pa (Fig. 3.-2) which correspond to the values in the literature for the liver microvasculature [24].

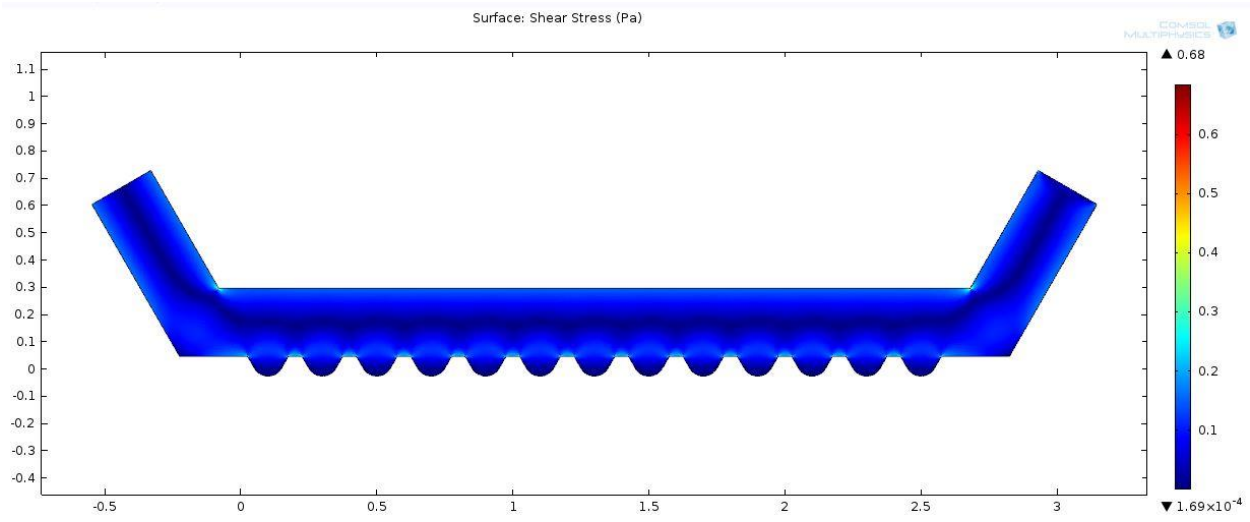

Fig. 3-2: Shear stress in the top channel of the device for a perfusion rate of 10 µL/min.

3.3.2 Cell culture

LX-2 were obtained from EMD Millipore (Temecula, CA, USA), HUVECs from Lonza (Tokyo, Japan) and Red Fluorescent Protein (RFP)-modified MiaPaCa-2 from AntiCancer (Tomisato, Japan). Cells were routinely cultured in 100-mm tissue culture polystyrene dishes. Seeding densities were 3×10^5/dish, 1×10^5/dish and 5×10^5/dish respectively. LX-2 and MiaPaCa-2 were passaged every 3 or 4 days and were added in the biochip 4 days after passaging. HUVECs were thawed from passage number 4 and added in the biochip at passage number 5 after 5 days of culture. LX-2 cells were cultured in high-glucose Dulbecco's Modified Eagle's Medium (Invitrogen Japan, Toyo, Japan) supplemented with 10% Fetal

Bovine Serum (Invitrogen Japan, Tokyo. Japan), 1% minimal essential medium nonessential amino acids (Invitrogen Japan, Tokyo, Japan), 100 U/ml penicillin, 100 U/ml streptomycin, and 25 mM HEPES. RFP-modified MiaPaCa-2 cells were cultured in RPMI-1640 culture medium (Wako Pure Chemical Industries, Osaka, Japan) supplemented with 10% Fetal Bovine Serum (Invitrogen Japan, Tokyo. Japan), 100 U/ml penicillin and 100 U/ml streptomycin. HUVECs were cultured with EGM-2 BulletKit (Lonza, Basel, Switzerland).

3.3.3 Isolation of primary rat hepatocytes

Isolation of primary rat hepatocytes was performed on male Wistar rats (Sankyo Laboratory, Tokyo, Japan) aged from 7 to 8 weeks and weighting from 200 to 300g using the two-step collagenase protocol previously described [25]. All the rats used in the experiments were treated in agreement with the guidelines for animal experiments of the University of Tokyo and the Japanese Ministry of Education. A threshold of 80% viability was set to decide if the isolated hepatocytes were suitable for the experiment. Primary rat hepatocytes were cultured in William's E medium (Invitrogen Japan) supplemented with 1% non-essential amino acids (Invitrogen Japan), 0.1 μM insulin (Takara Bio, Otsu, Japan), 0.1 μM dexamethasone (Wako Pure Chemical Industries, Osaka, Japan), 10 ng/ml mouse epidermal growth factor (Takara Bio), 0.5 mM ascorbic acid 2-phosphate (from magnesium salt n-hydrate; Wako Pure Chemical Industries, Osaka, Japan).

3.3.4 Establishment of the co-culture in the biochip

The device was filled layer by layer using the previously described method [23] adapted to our device. In details, the middle channel was first filled with pericytes embedded in gel at an 8×10^5cells/mL density. In the device, the gel used differs from the one used in chapter 2 as the later was found to be too soft for withstanding the addition of the other cells in the adjacent channels. Thus, we used Hystem-C Hydrogel supplied by ESI-BIO (Alameda, CA, USA). The hydrogel was found to be hard enough and only relies on a chemical crosslinker for gelation. The hydrogel was reconstituted at the concentration recommended by the furnisher and supplemented with 0.2mg/mL Fibronectin (Sigma, Japan) to provide a matrix suitable for cell growth. The hydrogel was injected in the device using a syringe pump (sp210iw, World Precision Instruments, Sarasota, FL, USA) and was allowed to set at room temperature for 1h30min to avoid any leak that would be caused by changes in pressure and temperature if the gelation process was carried on in an incubator. Stopcocks were used to avoid any sudden change of pressure as the syringe were disconnected. After gelation, a 50/50 mix of rat hepatocytes culture medium and HUVECs culture medium was manually introduced in the top channel. The bottom channel was coated overnight with Matrigel (Corning, Corning, NY, USA), diluted in the same culture medium mix as the top channel according to the manufacturer's recommendations. On the next day, freshly isolated rat hepatocytes were added in the bottom channel at a 4×10^7cells/mL density using a syringe pump to allow a complete coverage of the channel. Once the cells were inserted, stopcocks and surgical clamps were used to shut the entrance and the exit of the channel. This was made to avoid a pressure driven flow due to the volume of culture medium present in the access tubes. The cells were then allowed to adhere for 4 hours and the culture medium in the top channel was then changed. The first day of culture of rat hepatocytes in the device was labelled as "Day 0". On the next day, the culture medium in the bottom channel was manually changed to wash out unadhered

hepatocytes. The top channel was then coated with 0.5mg/mL Fibronectin (Sigma, Japan) for 1h30min. After coating, HUVECs were added using a syringe pump at a 4×10^7cells/mL density in the top channel and let to adhere for 4 hours. For the same reason previously described, stopcocks and surgical clamps were also used. After preparation and filling of the perfusion circuit, perfusion of 1.5 mL/device of culture medium with a peristaltic pump (Ismatec, Wertheim-Mondfeld, Germany) was then performed. The perfusion circuit was composed of the peristaltic pump, a bubble trap and the device connected serially using Polytetrafluoroethylene (PTFE) tubing to limit the possible adsorption of growth factors (Fig. 3-3). The culture medium was then changed daily and microscopy images were taken from day 2 to day 5 with JuliFL (NanoEnTek, Seoul, Korea). To keep consistency between the results, MiaPaCa-2 were added on day 5 as it was the case in chapter 2. Cells were carefully injected using a syringe pump to the top channel at a 2×10^7cells/mL density and let to adhere for 4 hours. To observe the interactions of the cancer cells with the liver cells, perfusion culture was then resumed until day 9 as viability assays and live immunostaining were performed. As a control to highlight the influence of coculture with hepatocytes and pericytes, devices in which only the hydrogel and HUVECs are added were also prepared in the same conditions.

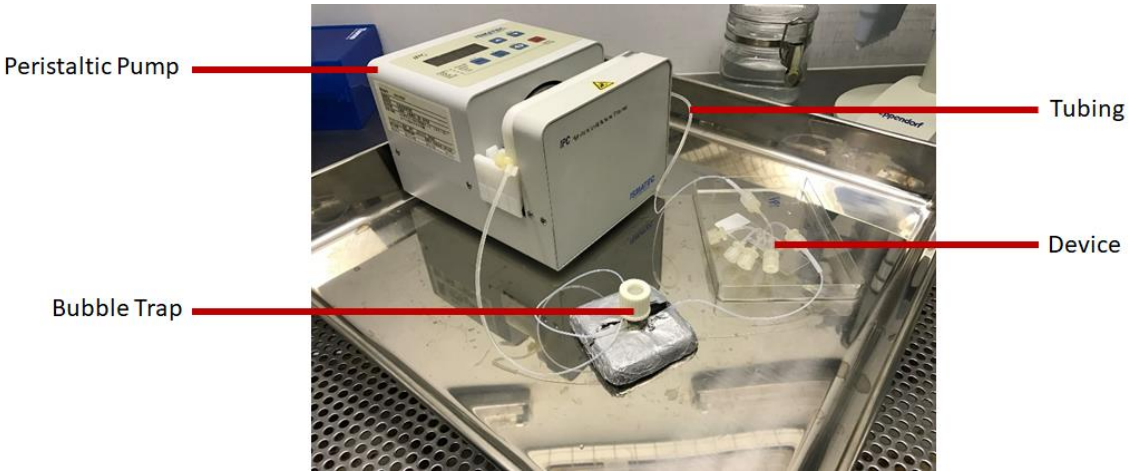

Fig. 3-3: Perfusion circuit including the peristaltic pump, the bubble trap, the biochip and the PTFE tubing.

3.3.5 Viability assay

To assess their viability in the device at the end of the culture, cells were stained on day 9 with Calcein (Dojindo Laboratories, Kumamoto, Japan) following the manufacturer's instructions. Stained samples were then immediately observed by confocal microscopy (IX-81; Olympus, Tokyo, Japan) and were not used any further.

3.3.6 Measurements of albumin levels

Albumin levels in the biochips were assessed by performing sandwich ELISA with samples taken from the perfused channel. For capture and detection, goat anti-rat albumin and horseradish peroxidase-conjugated sheep anti-rat albumin (both from *Cappel*/ICN Pharmaceuticals, Costa Mesa, CA, USA) antibodies were respectively used. Results were then measured on an iMark microplate reader (Bio-Rad, Osaka, Japan) set to a wavelength of 450nm an optically corrected at 630 nm.

3.3.7 Assessment of the influence of coculture on pancreatic cancer cells migration

In culture, cancer cells have a tendency to attract each other and to form aggregates. Their position, detected by red fluorescence, was extracted from the images taken daily with ImageJ [26]. The center of the aggregates was estimated using the software and the distance between the center of the aggregates and the gel interface was measured. Any change in this distance over the four last days of culture was noted in both complete coculture devices and in devices including only endothelial cells, gel and pancreatic cancer cells to evaluate the possible influence of the addition of pericytes and hepatocytes.

3.3.8 Live immunolabeling

Immunolabeling in the devices was performed without formaldehyde fixation and permeabilization. Live immunolabeling was chosen over typical methods on formaldehyde-fixated samples to avoid supplementary washes that were already found to damage the endothelial layer in the top channel. A constitutive liver vascular endothelial marker [27] and a marker related to inflammation were used in addition to a hepatic function marker to keep consistency with the work of chapter 2 [28]. A similar methodology, adapted to device experiment was used. Antibodies and washing steps were performed using a syringe pump. Antibodies against the following proteins were used: ICAM-1 (Genetex, Irvine, CA, USA), Stabilin-1 (Abnova, Taiwan) and Albumin (*Cappel*/ICN Pharmaceuticals, Costa Mesa, CA, USA). Detection of the immunoreactivity was performed with Alexa Fluor 647 & 488-conjugated secondary antibodies (Abcam, Tokyo, Japan) and with the appropriate controls.

3.4 Results

3.4.1 Viability of the cells in the biochip

The viability of the cells in the three channels was observed by Calcein staining (Fig. 3-4). The Propidium Iodide (PI) staining that is usually performed in tandem with the calcein staining to label dead cells was not performed due to the MiaPaCa-2 being modified to expressed RFP and the impossibility to distinguish the two red fluorescent emissions. During the staining procedure, the cells in the middle of the top channel were found to be detached and washed out by the numerous necessary washing steps (Fig. 3-4 A, B). This phenomenon was also observed in the live immunostaining performed simultaneously. Nonetheless, the hepatocytes in the bottom channel were found to be viable as they were labeled by calcein and were seen to be conserving their characteristic morphology (Fig. 3-4 C, D). In the top channel, both the adhered pancreatic cancer cells and the endothelial cells aggregates were stained with Calcein (Fig. 3-4 E, F). Pericytes embedded in the gel were also found to be stained, as the calcein could diffuse through the gel (Fig. 3-4 A, B).

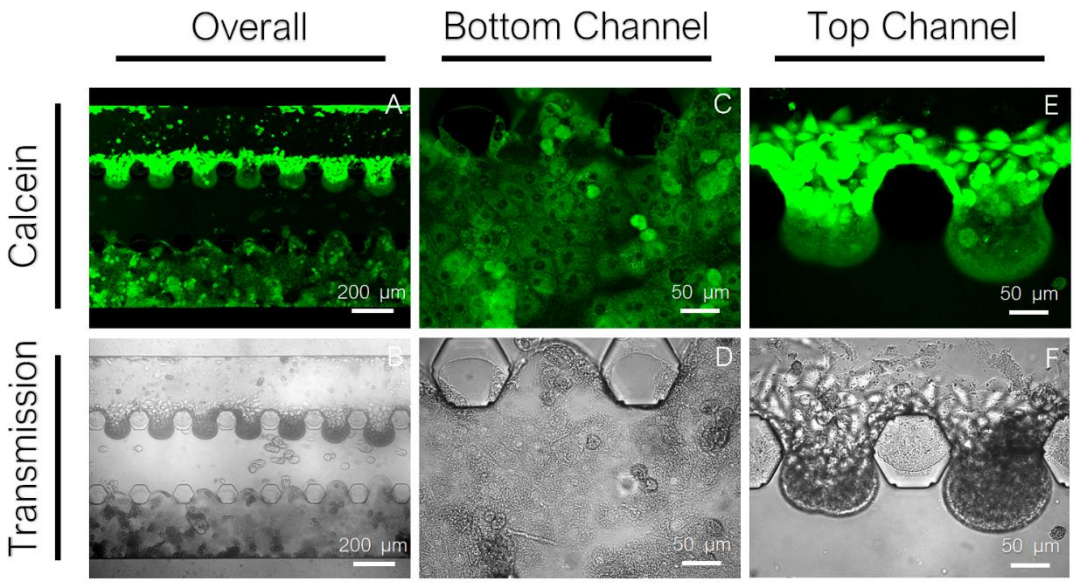

Fig. 3-4: Confocal imaging of the calcein labeled cells in the biochip channels.

The secretions of albumin, specific to the liver [29,30] in the perfused culture medium during the whole experiment were measured to ensure that the hepatocytes' function was maintained. While strong values of secretions could be observed in the beginning of the experiment, a decreasing trend was detected until day 5 and the addition of the pancreatic cancer cells. Afterwards, a strong increase over one day of the secretion was observed and the diminution then resumed. While an important device-to-device variability could be observed, the tendency remained the same in all the devices. The values of albumin secretions observed were in the same range as the ones previously observed in coculture models, confirming the physiological-relevancy of the biochip model [29,31]. In details, the albumin secretions in the microfluidic coculture model on day 5 were estimated at half those measured in chapter 2 (160 μg/1 × 10^6cells/day in the complete coculture condition). This difference can be attributed to the changes in cellular organization which were operated to include the hierarchical coculture in the biochip.

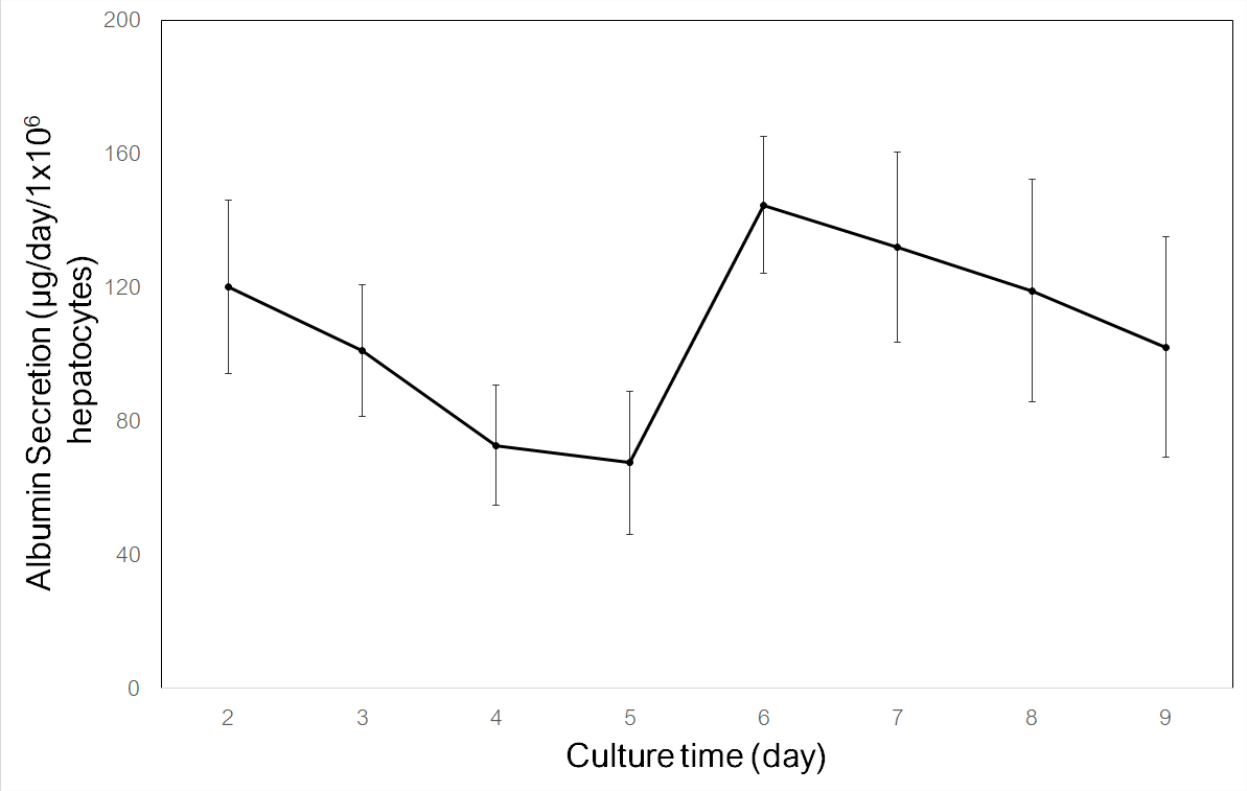

Fig. 3-5: Secretions of albumin in the perfused culture medium over the course of the experiment.

3.4.2 Effects of the coculture on the pancreatic cancer cells

Biochips with the complete coculture model and controls including only gel and endothelial cells were prepared. Before the addition of the pancreatic cancer cells, both the hepatocytes and the endothelial cells were seen to be forming a monolayer in the coculture model (Fig. 3-6). The pericytes aggregates in the gel were seen to be growing in size, indicating a potential cellular growth. In the monoculture of endothelial cells with gel, the endothelial cells also formed a monolayer and were confined in the top channel (Fig. 3-7). In both conditions, part of the endothelial cells were observed to relatively orient and elongate in zones of high shear stress.

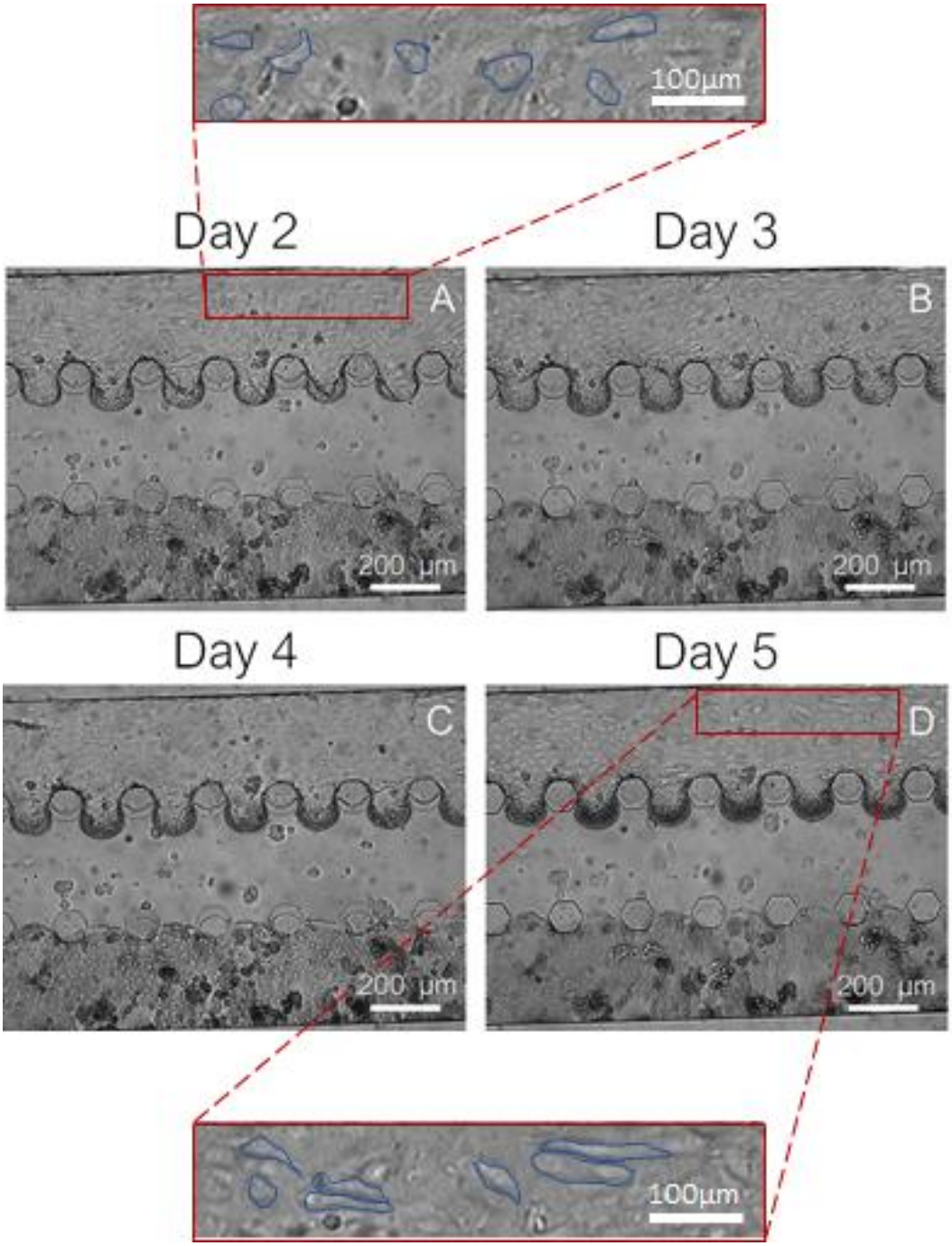

Fig. 3-6: Microscopy images of the coculture biochip including hepatocytes, pericytes embedded in gel and endothelial cells on Day 2 (A), 3 (B), 4 (C) and 5 (D). Details of the endothelial cells on Day 2 and 5. Morphology of some discernable cells are highlighted in blue.

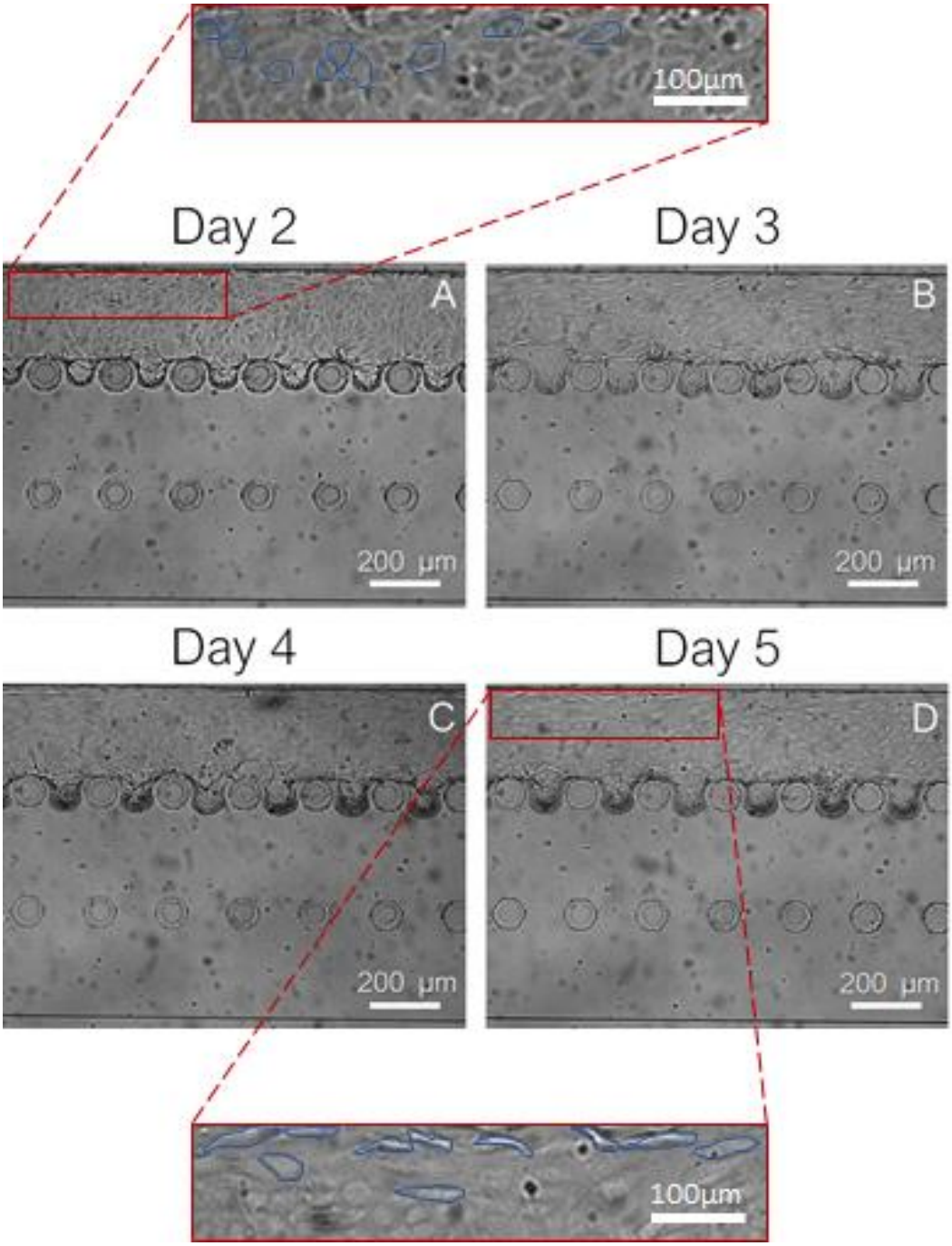

Fig. 3-7: Microscopy images of the monoculture biochip including endothelial cells on Day 2 (A), 3 (B), 4 (C) and 5 (D). Details of the endothelial cells on Day 2 and 5. Morphology of some discernable cells are highlighted in blue

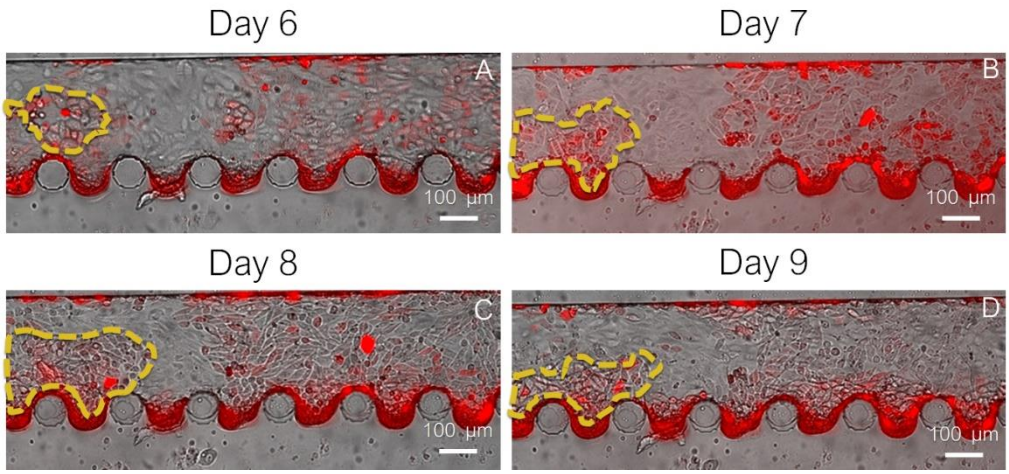

Fig. 3-8: Microscopy images of the coculture biochip including hepatocytes, pericytes embedded in gel, endothelial cells and pancreatic cancer cells on Day 6 (A), 7 (B), 8 (C) and 9 (D). The cancer cells can be observed in the red fluorescence channel in both the channel and at the interface. Aggregates that did not cover the whole channel were highlighted (in yellow here) to monitor their movement in the channel.

After the addition of the pancreatic cancer cells in the top channel, the culture was resumed for four additional days. While the well format introduced in chapter 2 allowed to quantify the adhesion of the cancer cells in physiologically-relevant conditions, the model in the biochip format allowed to observe the interactions between liver cells and cancer cells after their adhesion in the same physiologically-relevant conditions. In the coculture biochip, the endothelial cell layer was found to remain intact and the pancreatic cancer cells islets that adhered were found to be migrating toward the gel interface (Fig. 3-8). In the monoculture biochip, the endothelial layer was found to be damaged by the insertion of the pancreatic cancer cells but endothelial cells adhered on the gel interface remained attached (Fig. 3-9 A). The pancreatic cancer cells were found to be moving from day 2 toward the wall at the opposite of the interface and to settle there (Fig. 3-9 D). The measurement of the movement of the

pancreatic cancer cells in the different devices clearly confirmed that tendency as the cells tended to go toward opposite directions (Fig. 3-10).

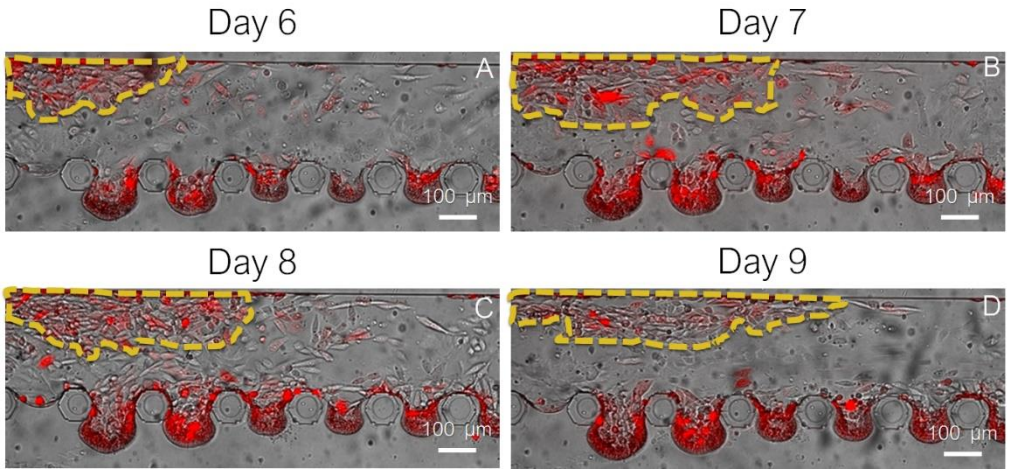

Fig. 3-9: Microscopy images of the coculture biochip including endothelial cells, gel and pancreatic cancer cells on Day 6 (A), 7 (B), 8 (C) and 9 (D). The cancer cells can be observed in the red fluorescence channel in both the channel and at the interface. Aggregates that did not cover the whole channel were highlighted (in yellow here) to monitor their movement in the channel.

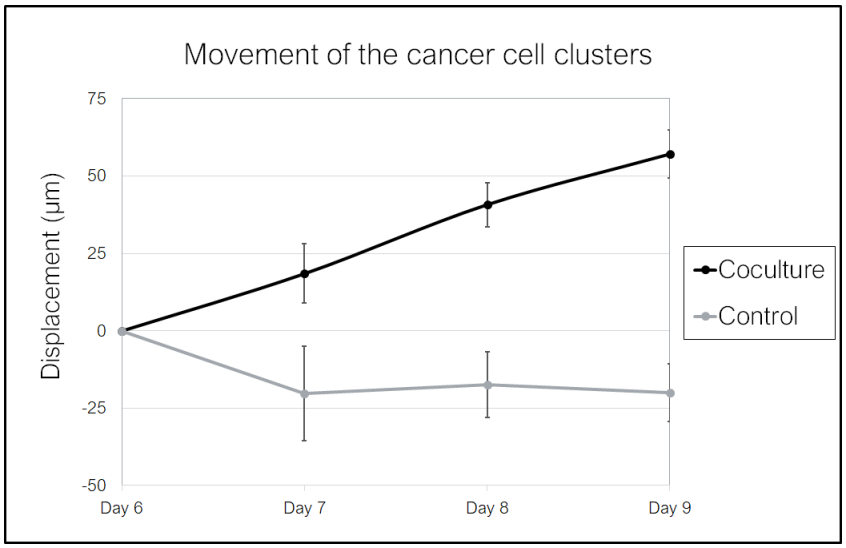

Fig. 3-10: Measurement of the movement of the pancreatic cancer cells in the top channel for both the coculture biochip and the control monoculture biochip.

3.4.3 Expression of hepatic and endothelial markers in the device

The hepatocytes in the bottom channel were found to express albumin uniformly (Fig. 3-11). In addition, gaps between the different cells in the monolayer could be observed. The microfluidic format of the model allowed to observe that the adhesion and inflammation-related marker ICAM-1 was expressed in the top channel in the zones of contact between endothelial cells and pancreatic cancer cells in both the coculture biochips (Fig. 3-12 A, B) and the monoculture biochips (Fig. 3-12 C, D). The marker was not found to be expressed by the pancreatic cancer cells but to be highly expressed in the endothelial cell aggregates at the gel interface. The liver-specific endothelial marker Stabilin-1 was also found to be expressed by the endothelial cells at the gel interface in the coculture biochips (Fig. 3-13). Those results are in conformity with the ones obtained in the model described in chapter 2.

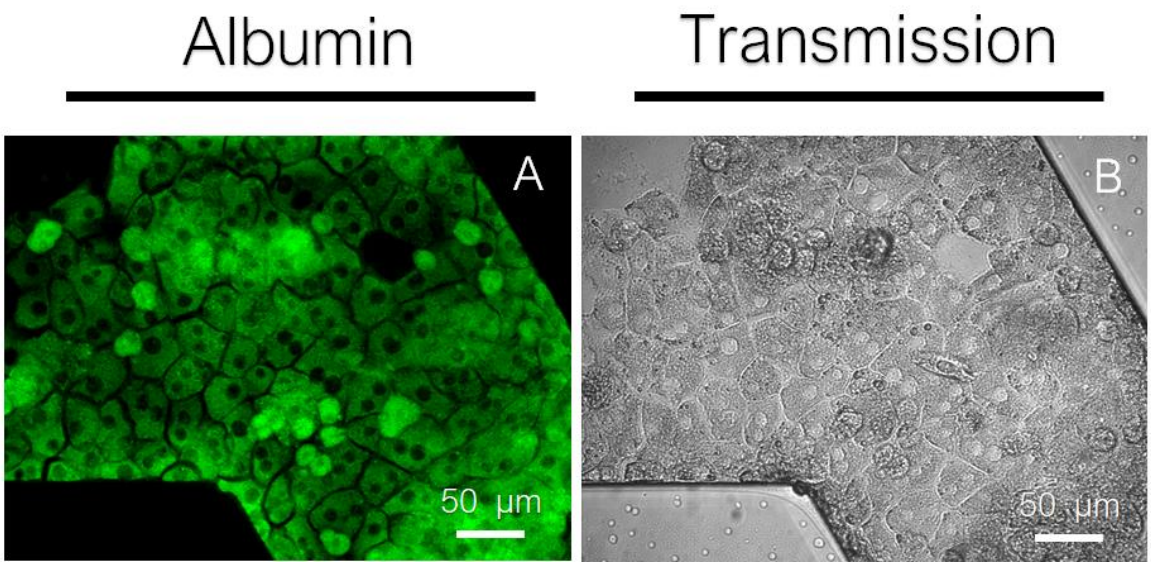

Fig. 3-11: Immunostaining of albumin (Green, A) and transmission image (B) obtained by confocal imaging.

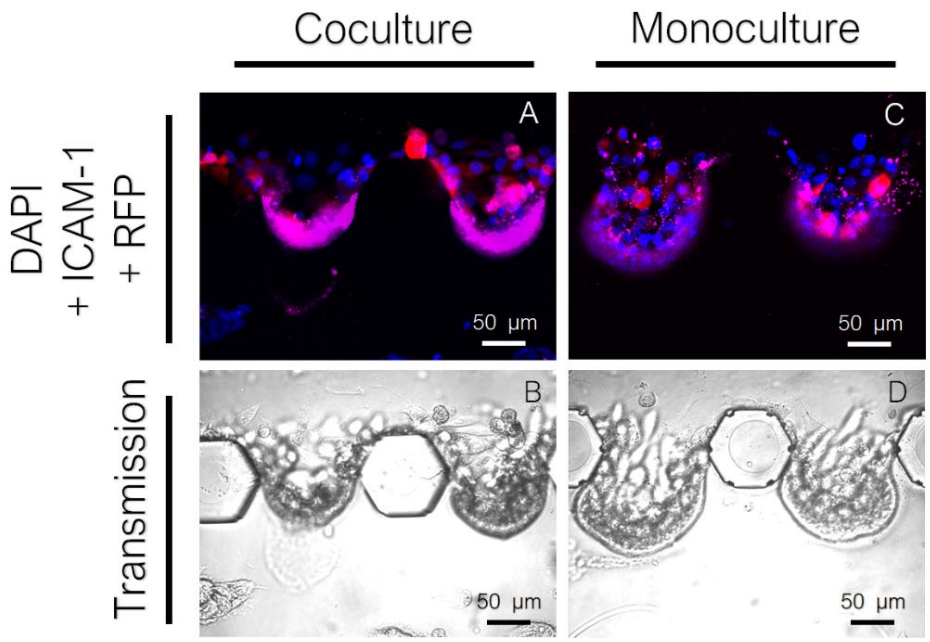

Fig. 3-12: Immunostaining of ICAM-1(Magenta) with DAPI (Blue) and labelled cancer cells (Red) in the coculture (A) and monoculture (C) biochips and corresponding transmission images (B, D) obtained by confocal imaging.

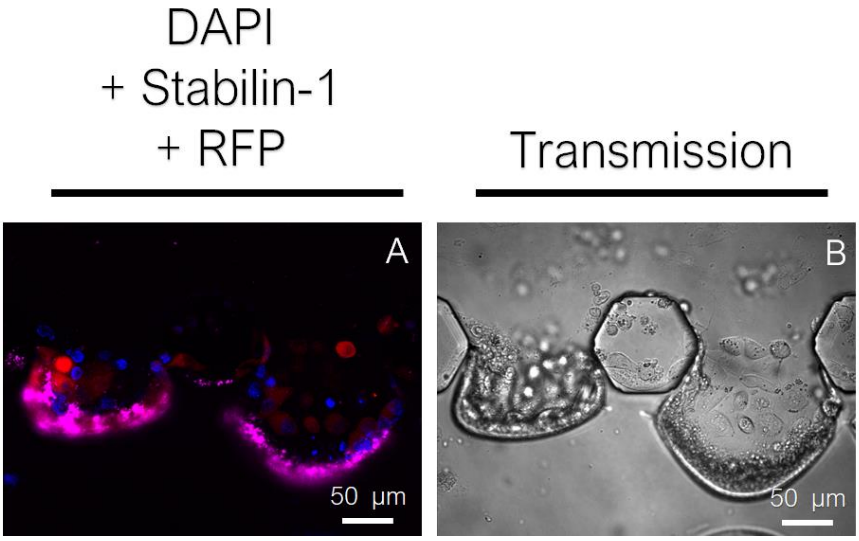

Fig. 3-13: Immunostaining of Stabilin-1(Magenta) with DAPI (Blue) and labelled cancer cells (Red) in the coculture biochips (A) and corresponding transmission image (B) obtained by confocal imaging.

3.5 Discussion

To provide to the demand of researchers and industrials for *in-vitro* models to achieve efficient drug screening [31-35], we established a complex coculture model in a microfluidic biochip that allows real-time monitoring of the behavior of adhering pancreatic cancer cells. This biochip combines the advantages of both the physically-relevancy of models developed in other groups [36-38] and the physiologically-relevancy of the model introduced in the chapter 2. We were able to establish a hierarchical coculture model of hepatocytes, pericytes embedded in gel and endothelial cells and to maintain the viability of the cells for 9 days (Fig. 3-4). Especially, while the gel was stiff enough to prevent the leaking of cells from one channel to another, it was observed to be suitable for cell culture as the pericytes were seen to be proliferating in aggregates (Fig. 3-12). Compared to the conventional hierarchical well format described in chapter 2, the observation of each cell layer separately was rendered trivial by the microfluidic biochip format. The physiological-relevancy of the model was confirmed by albumin measurement during the culture (Fig. 3-5). Those results and those of the viability assay proved the maintenance of the function of the hepatocytes as albumin was produced though the course of the experiment. Variability between devices can be explained by the fact that the filling procedure with cells is done manually, inducing slight differences in the number of cells in each device. However, a significant augmentation of the production of albumin was observed upon the addition of the pancreatic cancer cells in the top channel. The benefits of the coculture of pancreatic cells with liver cells is well-known, especially in terms of albumin [39-41]. Though, the phenomenon has yet to be shown with pancreatic cancer cells in the literature. The role of insulin and glucagon have been established in the increase of albumin secretion from hepatocytes in coculture [40]. In our biochip, the pancreatic cancer cells, MiaPaCa-2 are known to produce neither of these hormones. However, MiaPaCa-2 have still been observed to be rendered insulin producing in culture conditions without serum [42]. In

serum containing conditions, these cells are grown by supplementing from 10% to 12.5% serum in the media and do not produce insulin. In the biochip culture, the media is supplemented with only 1% serum which is significantly lower and could allow to hypothesize a behavior of the cells similar to serum-free cultures and thus, an insulin-producing behavior.

The inclusion of the coculture model in fluidic culture conditions, also allowed for the endothelial cells and the cancer cells to be subjected to a physiologically-relevant shear stress which is not represented in the static culture of chapter 2 (Fig. 3-2). As the reported wall shear stress in the liver microvasculature [24] is relatively low compared to previous work with HUVECs [43] mimicking larger vessels, the re-orientation of the endothelial cells with the flow was not as pronounced as those previous works (Fig. 3-6, 3-7). The microfluidic biochip format of the model also allowed to monitor the movement of the pancreatic cancer cells, which was not possible in the static model described in chapter 2. As it would have been expected according to the soil and seed theory [3], after their addition, the cancer cells, which formed aggregates in our model, were found to be drawn toward the interface with the other channels and liver cells. The reason behind this phenomenon could be the formation of a physiologically-relevant growth factor gradient. The observation and the measurement of such a gradient is another possibility enabled by microfluidic biochips as media samples can be taken in each channel and compared. In our case, we can hypothesize the formation of a gradient of hepatocytes growth factor (HGF) between the top and the bottom channels as in cancer, the importance of HGF was previously illustrated [44-46], stimulating growth, motility and invasiveness. Slight modifications to the experimental protocol would allow the verification of this hypothesis.

As it was the case in the physiologically-relevant model in the chapter 2, the cells in the biochip were also observed to express endothelial and liver specific markers. In agreement with the measurement of the albumin secretions, expression of albumin was detected in the

hepatocytes in the lower channel (Fig. 3-11). In addition, thin lines could be observed between the hepatocytes, indicating the possible formation of a biliary network as previously observed [47]. In the top channel, ICAM-1 was found to be expressed indifferently in both the coculture and the monoculture biochips (Fig. 3-12). The marker was expressed by the endothelial cells but not by the pancreatic cancer cells. Interestingly, the microfluidic format allowed to observe that the pancreatic cancer cells in contact with endothelial cells were found to be surrounded by a strong expression of ICAM-1. This observation, enabled by the biochip format, could be related to the previously described phenomenon [48], which can only be observed by time-consuming cross-sections or confocal images taken on numerous focal plans in conventional plate culture. Finally, Stabilin-1 was also found to be expressed by the endothelial cells, the marker, specific to the liver [49], was found to be only expressed by HUVECs in the same coculture conditions in our previous work [28].

3.6 Conclusion

In this chapter, we demonstrated the feasibility of a multi-channel microfluidic device for the study of the influence of liver cells on the pancreatic cancer cells. Culture in the device were maintained for 9 days as shown by the results of the viability assay, albumin production and immunostaining. The most significant advantage of the microfluidic biochip is to be able to follow the behavior of the cancer cells during the experiment in physiologically-relevant dynamic culture conditions. From the observations that we made, we were able to conclude that there are indeed chemoattracting interactions between the liver cells and the pancreatic cancer cells as the later are attracted by the former. In the soil and seed theory, it is hypothesized that the high probability of migration of one cancer type to a specific organ is due to the formation of chemical gradient. In the microfluidic format, the measurement of that gradient, once identified is possible due to the physical separation of the two culture channels. The microfluidic biochip format is also readily adaptable to many improvements which are yet to

be done in our model. To produce an even more physiologically-relevant model, modifications can be made toward a better 3D representation of the vessels, with a more complete culture model, including immune cells. The described microfluidic format is also readily compatible with the quantification of the attachability of circulating cancer cells which could arrest in the vessel and then migrate into the cellular matrix. While the device, in its present form, establish the basis for more complex in-vitro coculture models, many improvements are required in term of complexity and user-friendliness to allow its use in the drug-screening process by industries.

References

[1] Siegel, R. L., Miller, K. D., & Jemal, A. (2015). Cancer statistics, 2015. *CA: a cancer journal for clinicians*, 65(1), 5-29.

[2] Weigelt, B., Peterse, J. L., & Van't Veer, L. J. (2005). Breast cancer metastasis: markers and models. *Nature reviews cancer*, *5*(8), 591-602.

[3] Paget, S. (1889). The distribution of secondary growths in cancer of the breast. *The Lancet*, 133(3421), 571-573.

[4] Nicolson, G. L. (1988). Organ specificity of tumor metastasis: role of preferential adhesion, invasion and growth of malignant cells at specific secondary sites. *Cancer and Metastasis Reviews*, 7(2), 143-188.

[5] Khanna, C., & Hunter, K. (2005). Modeling metastasis in vivo. *Carcinogenesis*, *26*(3), 513-523.

[6] Jenkins, D. E., Oei, Y., Hornig, Y. S., Yu, S. F., Dusich, J., Purchio, T., & Contag, P. R. (2003). Bioluminescent imaging (BLI) to improve and refine traditional murine models of tumor growth and metastasis. *Clinical & experimental metastasis*, *20*(8), 733-744.

[7] Yang, M., Baranov, E., Jiang, P., Sun, F. X., Li, X. M., Li, L., ... & Shimada, H. (2000). Whole-body optical imaging of green fluorescent protein-expressing tumors and metastases. *Proceedings of the National Academy of Sciences*, *97*(3), 1206-1211.

[8] Hoffman, R. M. (2002). Green fluorescent protein imaging of tumour growth, metastasis, and angiogenesis in mouse models. *The lancet oncology*, *3*(9), 546-556.

[9] Nierodzik, M. L. R., Kajumo, F., & Karpatkin, S. (1992). Effect of thrombin treatment of tumor cells on adhesion of tumor cells to platelets in vitro and tumor metastasis in vivo. *Cancer Research*, *52*(12), 3267-3272.

[10] AN, Zili, WANG, Xiaoen, GELLER, Jack, *et al.* Surgical orthotopic implantation allows high lung and lymph node metastatic expression of human prostate carcinoma cell line PC-3 in nude mice. *The Prostate*, 1998, vol. 34, no 3, p. 169-174.

[11] Hoffman, R. M. (1999). Orthotopic metastatic mouse models for anticancer drug discovery and evaluation: a bridge to the clinic. *Investigational new drugs*, *17*(4), 343-360.

[12] Wartenberg, M., Finkensieper, A., Hescheler, J., & Sauer, H. (2006). Confrontation cultures of embryonic stem cells with multicellular tumor spheroids to study tumor-induced angiogenesis. *Human Embryonic Stem Cell Protocols*, 313-328.

[13] Lewalle, J. M., Cataldo, D., Bajou, K., Lambert, C. A., & Foidart, J. M. (1998). Endothelial cell intracellular Ca concentration is increased upon breast tumor cell contact and mediates tumor cell transendothelial migration. *Clinical & experimental metastasis*, *16*(1), 21-29.

[14] Albini, A., Iwamoto, Y., Kleinman, H. K., Martin, G. R., Aaronson, S. A., Kozlowski, J. M., & McEwan, R. N. (1987). A rapid in vitro assay for quantitating the invasive potential of tumor cells. *Cancer research*, *47*(12), 3239-3245.

[15] Li, Y. H., & Zhu, C. (1999). A modified Boyden chamber assay for tumor cell transendothelial migration in vitro. *Clinical & experimental metastasis*, *17*(5), 423-429.

[16] Yarrow, J. C., Perlman, Z. E., Westwood, N. J., & Mitchison, T. J. (2004). A high-throughput cell migration assay using scratch wound healing, a comparison of image-based readout methods. *BMC biotechnology*, *4*(1), 21.

[17] Coulouarn, C., Corlu, A., Glaise, D., Guénon, I., Thorgeirsson, S. S., & Clément, B. (2012). Hepatocyte–stellate cell cross-talk in the liver engenders a permissive inflammatory microenvironment that drives progression in hepatocellular carcinoma. *Cancer research*, *72*(10), 2533-2542.

[18] Chung, S., Sudo, R., Mack, P. J., Wan, C. R., Vickerman, V., & Kamm, R. D. (2009). Cell migration into scaffolds under co-culture conditions in a microfluidic platform. *Lab on a Chip*, *9*(2), 269-275.

[19] Zervantonakis, I. K., Hughes-Alford, S. K., Charest, J. L., Condeelis, J. S., Gertler, F. B., & Kamm, R. D. (2012). Three-dimensional microfluidic model for tumor cell intravasation and endothelial barrier function. *Proceedings of the National Academy of Sciences*, *109*(34), 13515-13520.

[20] Van der Meer, A. D., Poot, A. A., Duits, M. H. G., Feijen, J., & Vermes, I. (2009). Microfluidic technology in vascular research. *BioMed Research International*, *2009*.

[21] Chen, M. B., Whisler, J. A., Jeon, J. S., & Kamm, R. D. (2013). Mechanisms of tumor cell extravasation in an in vitro microvascular network platform. *Integrative Biology*, *5*(10), 1262-1271.

[22] Clayton, D. F., Harrelson, A. L., & Darnell, J. E. (1985). Dependence of liver-specific transcription on tissue organization. *Molecular and cellular biology*,*5*(10), 2623-2632.

[23] Huang, C. P., Lu, J., Seon, H., Lee, A. P., Flanagan, L. A., Kim, H. Y., ... & Jeon, N. L. (2009). Engineering microscale cellular niches for three-dimensional multicellular co-cultures. *Lab on a Chip*, *9*(12), 1740-1748.

[24] Lalor, P. F., Herbert, J., Bicknell, R., & Adams, D. H. (2013). Hepatic sinusoidal endothelium avidly binds platelets in an integrin-dependent manner, leading to platelet and endothelial activation and leukocyte recruitment. *American Journal of Physiology-Gastrointestinal and Liver Physiology*, *304*(5), G469-G478.

[25] Seglen PO. Preparation of isolated rat liver cells. In: Prescott DM, editor. *Methods in Cell Biology. London: Elsevier Inc*.; 1976:29–83.

[26] Schneider, C. A., Rasband, W. S., & Eliceiri, K. W. (2012). NIH Image to ImageJ: 25 years of image analysis. *Nature methods*, *9*(7), 671-675.

[27] C. Geraud, K. Schledzewski, A. Demory, D. Klein, M. Kaus, F. Peyre & S. Goerdt, Liver sinusoidal endothelium: A microenvironment-dependent differentiation program in rat including the novel junctional protein liver endothelial differentiation-associated protein-1, Hepatology, 2010, 52(1),313–326.

[28] Danoy, M., Shinohara, M., Rizki-Safitri, A., Collard, D., Senez, V., & Sakai, Y. (2017). Alteration of pancreatic carcinoma and promyeloblastic cell adhesion in liver microvasculature by co-culture of hepatocytes, hepatic stellate cells and endothelial cells in a physiologically-relevant model. *Integrative Biology*, *9*(4), 350-361.

[29] Selden, C., Khalil, M., & Hodgson, H. J. F. (1999). What keeps hepatocytes on the straight and narrow? Maintaining differentiated function in the liver. *Gut*, 44(4), 443-446.

[30] Miller, L. L., Bly, C. G., Watson, M. L., & Bale, W. F. (1951). The dominant role of the liver in plasma protein synthesis a direct study of the isolated perfused rat liver with the aid of lysine-ϵ-C14. *The Journal of experimental medicine*, 94(5), 431-453.

[31] Xiao, W., Perry, G., Komori, K., & Sakai, Y. (2015). New physiologically-relevant liver tissue model based on hierarchically cocultured primary rat hepatocytes with liver endothelial cells. *Integrative Biology*, *7*(11), 1412-1422.

[32] DiMasi, J. A., Feldman, L., Seckler, A., & Wilson, A. (2010). Trends in risks associated with new drug development: success rates for investigational drugs. *Clinical Pharmacology & Therapeutics*, *87*(3), 272-277.

[33] Macarron, R. (2006). Critical review of the role of HTS in drug discovery. *Drug discovery today*, *11*(7), 277-279.

[34] Fox, S., Farr-Jones, S., Sopchak, L., Boggs, A., Nicely, H. W., Khoury, R., & Biros, M. (2006). High-throughput screening: update on practices and success. *Journal of biomolecular screening*, *11*(7), 864-869.

[35] Butcher, E. C. (2005). Can cell systems biology rescue drug discovery?. *Nature reviews. Drug discovery*, *4*(6), 461.

[36] Chen, M. B., Whisler, J. A., Fröse, J., Yu, C., Shin, Y., & Kamm, R. D. (2017). On-chip human microvasculature assay for visualization and quantitation of tumor cell extravasation dynamics. *Nature protocols*, *12*(5), 865.

[37] Jeon, J. S., Zervantonakis, I. K., Chung, S., Kamm, R. D., & Charest, J. L. (2013). In vitro model of tumor cell extravasation. *PloS one*, *8*(2), e56910.

[38] Pavesi, A., Tan, A. T., Chen, M. B., Adriani, G., Bertoletti, A., & Kamm, R. D. (2015, August). Using microfluidics to investigate tumor cell extravasation and T-cell

immunotherapies. In *Engineering in Medicine and Biology Society (EMBC), 2015 37th Annual International Conference of the IEEE* (pp. 1853-1856). IEEE.

[39] Lee, K. W., Lee, S. K., Joh, J. W., Kim, S. J., Lee, B. B., Kim, K. W., & Lee, K. U. (2004). Influence of Pancreatic Islets on Spheroid Formation and Functions of Hepatocytes in Hepatocyte—Pancreatic Islet Spheroid Culture. *Tissue engineering*, *10*(7-8), 965-977.

[40] Kaufmann, P. M., Fiegel, H. C., Kneser, U., Pollok, J. M., Kluth, D., & Rogiers, X. (1999). Influence of pancreatic islets on growth and differentiation of hepatocytes in co-culture. *Tissue engineering*, *5*(6), 583-596.

[41] Jun, Y., Kang, A. R., Lee, J. S., Jeong, G. S., Ju, J., Lee, D. Y., & Lee, S. H. (2013). 3D co-culturing model of primary pancreatic islets and hepatocytes in hybrid spheroid to overcome pancreatic cell shortage. *Biomaterials*, *34*(15), 3784-3794.

[42] Bose, B., & Shenoy, P. (2013). Non insulin producing cell line, MIA PaCa-2 is rendered insulin producing in vitro via mesenchymal epithelial transition. *Journal of cellular biochemistry*, *114*(7), 1642-1652.

[43] Abaci, H. E., Shen, Y. I., Tan, S., & Gerecht, S. (2014). Recapitulating physiological and pathological shear stress and oxygen to model vasculature in health and disease. *Scientific reports*, *4*.

[44] To, C. T., & Tsao, M. S. (1998). The roles of hepatocyte growth factor/scatter factor and met receptor in human cancers. *Oncology reports*, *5*(5), 1013-1037.

[45] Klominek, J., Baskin, B., Liu, Z., & Hauzenberger, D. (1998). Hepatocyte growth factor/scatter factor stimulates chemotaxis and growth of malignant mesothelioma cells through c-met receptor. *International journal of cancer*, *76*(2), 240-249.

[46] Corps, A. N., Sowter, H. M., & Smith, S. K. (1997). Hepatocyte growth factor stimulates motility, chemotaxis and mitogenesis in ovarian carcinoma cells expressing high levels of c-met. *International journal of cancer*, *73*(1), 151-155.

[47] Liu, X., LeCluyse, E. L., Brouwer, K. R., Gan, L. S. L., Lemasters, J. J., Stieger, B., ... & Brouwer, K. L. (1999). Biliary excretion in primary rat hepatocytes cultured in a collagen-sandwich configuration. *American Journal of Physiology-Gastrointestinal and Liver Physiology*, *277*(1), G12-G21.

[48] Van Buul, J. D., Allingham, M. J., Samson, T., Meller, J., Boulter, E., García-Mata, R., & Burridge, K. (2007). RhoG regulates endothelial apical cup assembly downstream from ICAM1 engagement and is involved in leukocyte trans-endothelial migration. *J Cell Biol*, *178*(7), 1279-1293.

[49] Géraud, C., Schledzewski, K., Demory, A., Klein, D., Kaus, M., Peyre, F., ... & Goerdt, S. (2010). Liver sinusoidal endothelium: A microenvironment-dependent differentiation program in rat including the novel junctional protein liver endothelial differentiation-associated protein-1. *Hepatology*, *52*(1), 313-326.

Supplementary Information

Filling of a single channel with gel

As theoretically described in the literature [23], the filling of a channel independently from the others was computed using Comsol Multiphysics in our specific structure. Those simulations were made in the first version of our device which comported only two channels instead of the three in the final version (Fig. 3-14). Those simulations allowed to set the different geometrical parameters of the device such as its length, the width of the channels, the pillars size and the space between the pillars. The filling of the bottom channel with collagen gel was set as pressure driven. The characteristics of the collagen gel (from Nitta Gelatin, used in chapter 1) were obtained from the manufacturer (Density: 1003kg/m^3, Dynamic viscosity: 0.034 Pa.s). The PDMS/liquid contact angle was approximated to 110 degrees, the same value as the PDMS/water contact angle as its exact value is unknown. It was found that for channels of 250 µm width, pillars of 100 µm spaced by 100 µm, the device could be easily filled up to 18 pillars. For longer devices, leakage to the other channel happened with the same device's parameters.

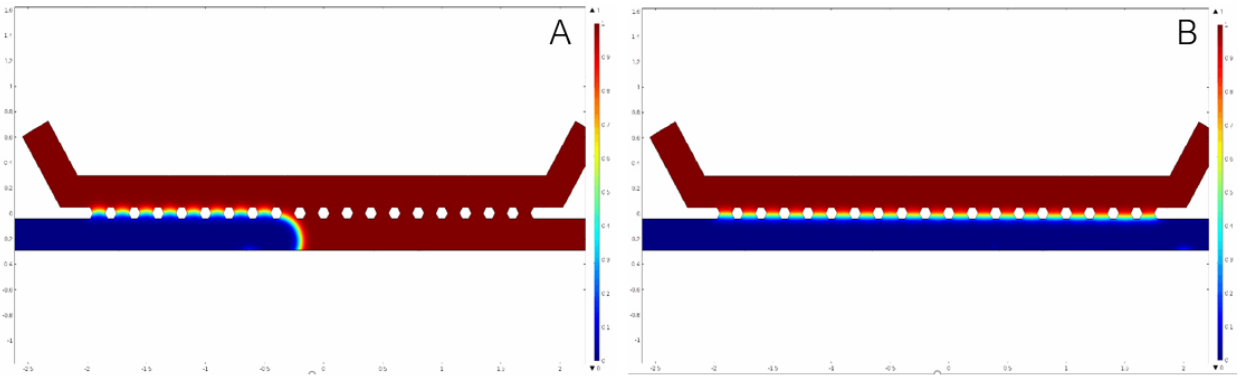

Fig. 3-14: Comsol Multiphysics simulations of channel gel filling with the previously described parameters. During the filing (A) and after the filling (B). The gel is represented in blue and the air in red.

Filling was then performed in the device with different gels. It was found to the collagen gel used in chapter 2 was not hard enough to withstand a flow in the adjacent channels. Filling with pure Matrigel was found to be difficult as a leak would occur during gelation. We then set our choice on the gel described on chapter 3 which could withstand flow and was more resistant to the environment. At that point, the device was updated to a three channels device to maximize the number of hepatocytes in the bottom channel to be more physiologically-relevant as hepatocytes compose most of the liver. In this new device, the middle channel was filled with the previously described gel and no specific problem was detected. After gelation, the gel was however found to retracted significantly, leading to the formation of cavities between the pillars (Fig. 3-15).

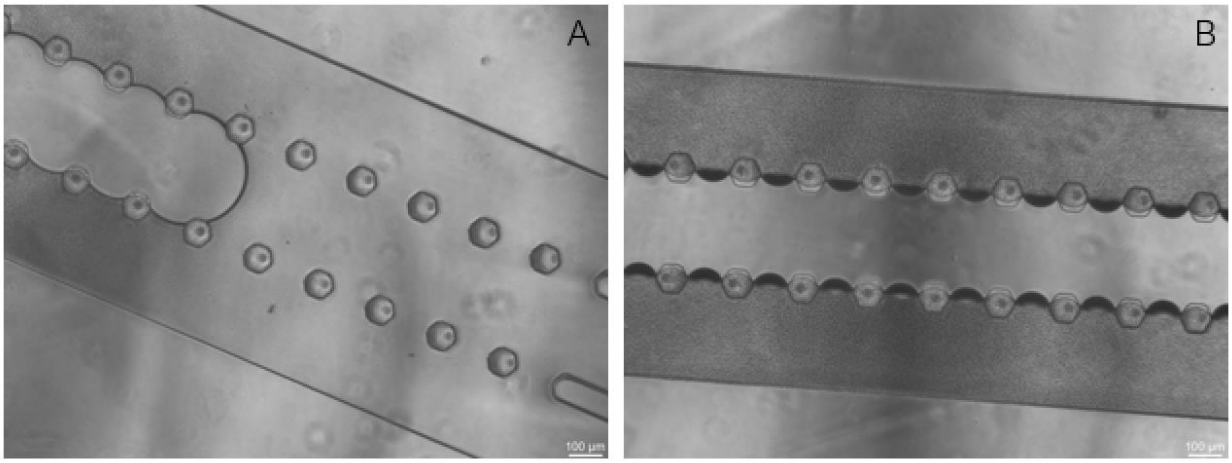

Fig. 3-15: Microscopy images of the device during the filling of the middle with gel (A) and after gelation for 1h30 at room temperature (B).

Trials for the establishment of the culture in the biochip

Regarding the addition of cells in the device, different organization of the cells were tested. At first, we confirmed the effects of gravity on the cells in the device and the possibility to seed cells on the interface between a channel and the gel by adding polystyrene beads in water in the device. Under a tilt of 30 degrees, it was found that the beads in the device tended to accumulate in the bottom of the device, confirming the effects of gravity during cell seeding (Fig. 3-16). Hopefully, beads were still found in the channels, indicating that the cells could be seeded on the gel interface and on the glass at the same time. This technic was used to seed the HUVECs and form a layer of endothelial cells on the gel interface and in the whole channel.

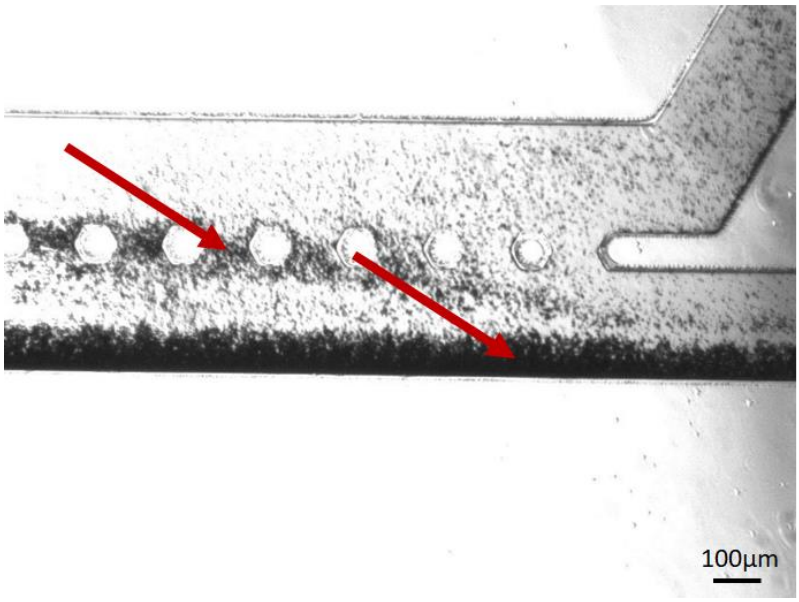

Fig. 3-16: Microscopy images of the device filled with beads (Accumulations of beads indicated by the red arrows).

After gelation of the gel in the middle channel, rat hepatocytes were added in the bottom channel. Following 4 hours of adhesion, it was found that few cells adhered in the device mostly at the interface with gel (Fig. 3-17). After observation under the transmission microscope, it was found that after seeding, the cells kept moving during the adhesion step. We hypothesized that the constant flow of liquid in the device was due to the large volume of media present in the tubing. Indeed, the tubing in both the accesses contains more media than the device itself. Thus, every single movement of the tubing or any change in the pressure due to incubation caused a strong flow in the channel which is not favorable to the adhesion of the cells in the device and to the formation of a complete layer of cells. We solved this problem by using stopcocks and surgical clamps on each of the channels. Those allowed to isolate the channel filled with cells from the tubing during the adhesion step as the media could not circulate anymore from the tubing to the inside of the device.

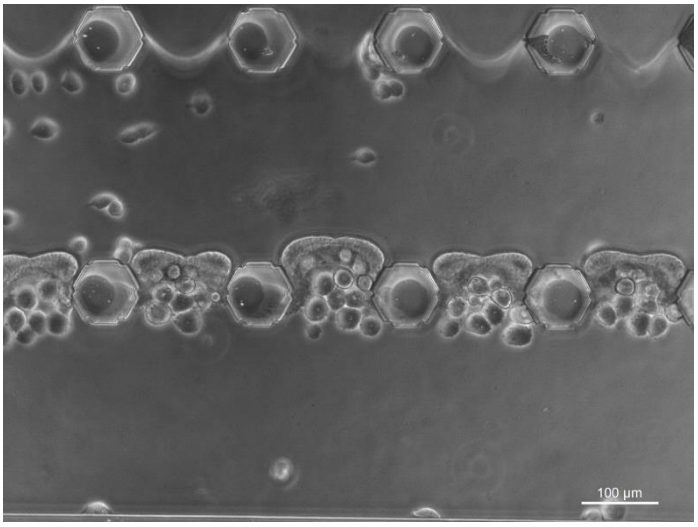

Fig. 3-17: Microscopy images of hepatocytes seeded in the bottom channel after 4 hours of adhesion. The middle channel is filled with pericytes embedded hydrogel.

Chapter 4

Conclusions & Prospects

4.1 Conclusions

This thesis work has contributed to both the liver tissue engineering and to the cancer-related communities. The different remaining problems of in-vitro models for the study of the interactions between cancer and the liver have been discussed in the introduction. Current models still lack in term of physiological-relevance to the cellular and physical microenvironment of cancer cells adhesion and migration. Indeed, the liver is a vital yet, complex organ, composed of numerous cell types with a specific organization. The complete hierarchical structure of the liver, including cells such as hepatocytes, pericytes, endothelial cells, Kupffer cells and others has yet to be reproduced in *in-vitro* models.

Establishing models which reproduce as close as possible those characteristics independently and even, trying to combine them in a single device is the main originality of this study. The main contributions of this thesis to the literature can be detailed as follows:

1) A physiologically-relevant model of the liver microvasculature was established. The model exhibited an *in-vivo* auto-regulation of the inflammation which was yet to be described in the literature.
2) The influence of coculture on pancreatic cancer cells and promyeloblastic cells was investigated. The relation between the inflammatory state of the model of the adhesion was also examined.
3) A model reproducing the physiological physical environment of the cancer adhesion in the liver microvasculature was established. The model also included the coculture model previously introduced.

In the chapter 2, we complexified the study of the adhesion of pancreatic cancer cells and promyeloblastic cells by including hepatocytes and pericytes in addition to endothelial cells in a hierarchical coculture. The feasibility of the model was established as the different cells were

confirmed to be viable and functional. The endothelial cells as well as the hepatocytes formed a monolayer and the pericytes exhibited a "star-like" morphology in the gel. Cross-talking between the cells was observed as the production of albumin was enhanced by coculture and VEGF was consumed in coculture. In the complete coculture condition, the adhesion of the pancreatic cancer was decreased, the inflammation-related markers were less expressed and the liver-specific marker was more expressed compared to the other conditions. Those results indicate that the coculture favored a more mature and less inflamed culture condition of the endothelial cells. The response of the model to an inflammatory cytokine was also monitored. In coculture, the condition was found to be significantly less inflamed than in monoculture of endothelial cells. In addition, the adhesion of both the pancreatic cancer cells and the promyeloblastic cells was lower in coculture after stimulation. Based on the results of this chapter, we could conclude on the necessity of an *in-vitro* mimicking hierarchical coculture to represent in a more physiologically-relevant manner the *in-vivo* interactions between the liver and adhering cells.

In the chapter 3, the developed coculture model was adapted to and introduced in a multi-channel microfluidic biochip reproducing the *in-vivo* physiological shear stress to which the endothelial cells and the adhering cells are subjected. The feasibility of the model was demonstrated as the cells in all the channels were found to be viable and the liver function to be expressed during the complete experiment. In the perfused channel of the device, the pancreatic cancer cells were found to be attracted toward the channels containing the hepatocytes and the pericytes whereas the cancer cells in the monoculture of endothelial cells devices migrated toward the opposite wall. Hepatic markers, inflammation and adhesion-related markers were also found to be expressed in the chip by both the hepatocytes and the endothelial cells. Those results gave a good overview of the numerous advantages of including biological systems in a microfluidic format. The proposed microfluidic format allowed for

direct observation of the interactions between the cancer cells and the liver cells in physiologically-relevant dynamic conditions which could not be reproduced in the well format. In addition, this format is compatible to assays for real-time monitoring of cancer cells migration, for quantification of the attachability of circulating cancer cells, and to the study of chemical gradient effects and their measurements.

In conclusion, we proposed in this thesis a novel methodology to study the interactions between the liver and cancer cells. In both the well format and the biochip format, the engineered approaches allowed to reproduce the hierarchical structure of the liver as a better physiologically-relevant representation of the *in-vivo* situation. The inclusion of the model in the biochip allowed further reproduction of the physical environment as well as direct observations of the interaction between the liver and the pancreatic cancer cells. The proposed models allowed a more profound understanding of the impact of coculture on the interactions between cancer cells and the liver. Improvements in term of design, cellular complexity and user-friendliness can be done to favorize a more systematic use of those models for drug-screening.

4.2 Prospects

4.2.1 Toward a more complete in-vitro representation of the liver

The introduced hierarchical coculture model is relatively more complete than other models presented in the literature so far. Usually, coculture models are designed step by step in order to understand as much as possible the role of each cells of the model. As other supportive cells are also involved in the interactions between the liver and the adhering cancer cells, the next stage is to include them in the model. In particular, the addition of immune cells and Kupffer cells in the model would be of great interest. Kupffer cells are macrophages specific to the liver and are located in the microvasculature, attached to the vascular wall. They

are known to play an important role in the host defense and especially in the inflammatory response of the tissues to external stimulations. As shown in chapter 2, the adhesion of pancreatic cancer cells in the microvasculature was strongly related to the inflammatory state of the endothelial layer. Thereby, Kupffer cells, which have been shown to interact with cancer cells and to protect the liver from cancer metastasis, are an important parameter to add to the model and should allow the obtention of a more physiologically-relevant model that the one presented in the chapter 2. In terms of improvements of the current model, a hierarchical coculture model, including Kupffer cells seeded on the top layer could be used for high-throughput screening of compounds against cancer cells adhesion in the well format (Fig. 4-1).

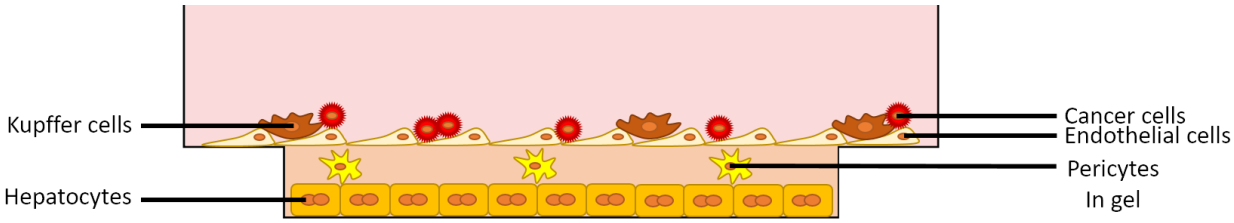

Fig.4-1: Proposed improved hierarchical coculture model in wells with Kupffer cells.

4.2.2 Toward a device for real-time observation of the cancer cells extravasation

The microfluidic device introduced in the chapter 3 allowed direct observations of the interactions of pancreatic cancer cells with the liver. However, observation of the cancer cells extravasation was not possible in its current form. Due to the current design of the device, a relatively hard hydrogel was used to fill the middle channel, rendering impossible the migration of cells from one channel to another. In addition to that issue, the small dimensions of the perfused top channel did not allow for complete simple analysis such as immunostaining as the cells in the top channel were found to be detached by the procedure. To solve these issues, the

design of the device must be refined. As cancer cells are relatively small and flexible, the size between the pillars can be significantly reduced to limit the leakage of the gel in the middle channel to the other channels while still allowing the migration of cancer cells. In addition, the dimensions of the device can be tuned to limit the flow rate at the cell layer to avoid cell detachment during the staining while keeping a physiologically-relevant shear stress. Indeed, while the width of the top channel is of 250 µm, its height is only of 100 µm. By increasing this size to 250 µm, the flood rate would be greatly reduced and the shear stress can still be tuned. Finally, as previously described, the physiological-relevancy of the microfluidic model can be, like in the well format, increased by the addition of other supportive cells such as the cells of the immune system. Such model, using of the microfluidic format, allows for a more complete study of the interactions of the cancer cells with the liver, by including a physiologically-relevant cellular structure in a dynamic physiologically-relevant environment. More complete analysis can be performed on top, notably with an easier and more precise visualization of the cells interactions as well as the measurement of the chemical gradient formed. This model could be of use in the more specific understanding of the effect of compounds during drug-screening, in condition of both cellular and physical physiological-relevancy but would not be compatible with high-throughput screening.

Acknowledgments

There were many people involved in this French-Japanese collaboration but I would first like to express all my gratitude to Pr. Yasuyuki Sakai for hosting me for those three years and for his guidance until graduation. I would also like to particularly thank my two PhD thesis co-directors, Pr. Vincent Senez and Pr. Dominique Collard who made my wish to work in Japan come true. Especially, Pr. Senez always followed thoroughly my work and results and kept much enthusiasm and interest during those three years despite the distance.

I thank the University of Lille 1 for granting me a MESR scholarship during my thesis. I also thank my thesis committee members: Prs. Yasuyuki Sakai, Vincent Senez, Dominique Collard, Atsushi Miyajima, Teruo Okitsu, C*é*cile Legallais and Fabrice Soncin.

I would like to thank the LIMMS staff, the LIMMS current and previous directors, Dominique Collard, Eric Leclerc, Hideki Kawakatsu and Beom Joon Kim who provided a structure of exchange with other researchers and helped a lot with administrative tasks. Thanks to all previous and current LIMMS members who always were of great help as well as a good source of inspiration. In particular, thanks to Yannick Tauran, Timothée Lévi, Bertrand-David Segard and Myriam Lereau-Bernier whom I hold dearly as friends.

Thanks to Anthony Treizebre for his precious help during the second part of the thesis, to Fabrice Soncin and Chann Lagadec for their precious advice in the first part.

A very special thanks to previous and current Sakai lab. members, whom I consider as a family: Naoko Yamamoto, Atsuko Shimizu, Yuan Pang, Marie Shinohara, Yusuke Urabe, Xiao Wenjin, Koudai Harano, Sapana Poudel, Tomokazu Ikoma, Kaketsu Kou, Benedikt Scheidecker, Keiichi Kimura, Shinya Shimoda, Nami Mizushima, Astia Rizki-Safitri, Han Bin

Kim, Xu Xinting, Ayaka Uemura, Kouhei Shimizu, Masaharu Nakane, Yuichi Oda, Yukimi Kobayashi, Ikki Horiguchi, Masato Ibuki, Kumiko Matsunaga, Fuad Gandhi Torizal, Seong Min Kim, Haruka Inose, Kohei Hatano, Daiki Miyazaki, Pierre Wuthrich, Kazuhiro Ohashi, Hyeon Jin Choi, Masataka Usui and Mamiko Ono. Reading those names only brings me good memories, thank you for supporting and for some of you in that list, for being some of my best friends.

At last, thank you to the three women of my life, my grandmother, my mother and my fiancée, Yuko. Thank you for making me the person I am and will be. I love you. A special though for Titus, my pet, who accompanied me from primary school to almost the end of this thesis. I already miss you a lot.

List of publications and presentations

Publications

Pang, Y., Horimoto, Y., Sutoko, S., Montagne, K., Shinohara, M., **Danoy, M.**, ... & Sakai, Y. (2016). Novel integrative methodology for engineering large liver tissue equivalents based on three-dimensional scaffold fabrication and cellular aggregate assembly. *Biofabrication*, *8*(3), 035016.

Leclerc, E., Kimura, K., Shinohara, M., **Danoy, M.**, Le Gall, M., Kido, T., ... & Sakai, Y. (2017). Comparison of the transcriptomic profile of hepatic human induced pluripotent stem like cells cultured in plates and in a 3D microscale dynamic environment. *Genomics*, *109*(1), 16-26.

Danoy, M., Shinohara, M., Rizki-Safitri, A., Collard, D., Senez, V., & Sakai, Y. (2017). Alteration of pancreatic carcinoma and promyeloblastic cell adhesion in liver microvasculature by co-culture of hepatocytes, hepatic stellate cells and endothelial cells in a physiologically-relevant model. *Integrative Biology*, *9*(4), 350-361.

International conferences

Danoy, M., Shinohara, M., Rizki-Safitri, A., Collard, D., Senez, V., & Sakai, Y., A novel hierarchical *in-vitro* coculture model of the liver microvasculature for pancreatic cancer cells adhesion monitoring, TERMIS-AP 2016, Tamsui, Taiwan, September 2016, **Best poster award.**

Domestic conferences

Danoy, M., Shinohara, M., Rizki-Safitri, A., Collard, D., Senez, V., & Sakai, Y., Adhesion of pancreatic cancer cells in a liver microvasculature model using an in-vitro coculture model, The 28th Annual Meeting of the Japanese Society for Alternatives to Animal Experiments, Workpia Yokohama, Yokohama, Japan, December 2015.